The Radio Science Bulletin

ISSN 1024-4530

INTERNATIONAL
UNION OF
RADIO SCIENCE

UNION
RADIO-SCIENTIFIQUE
INTERNATIONALE

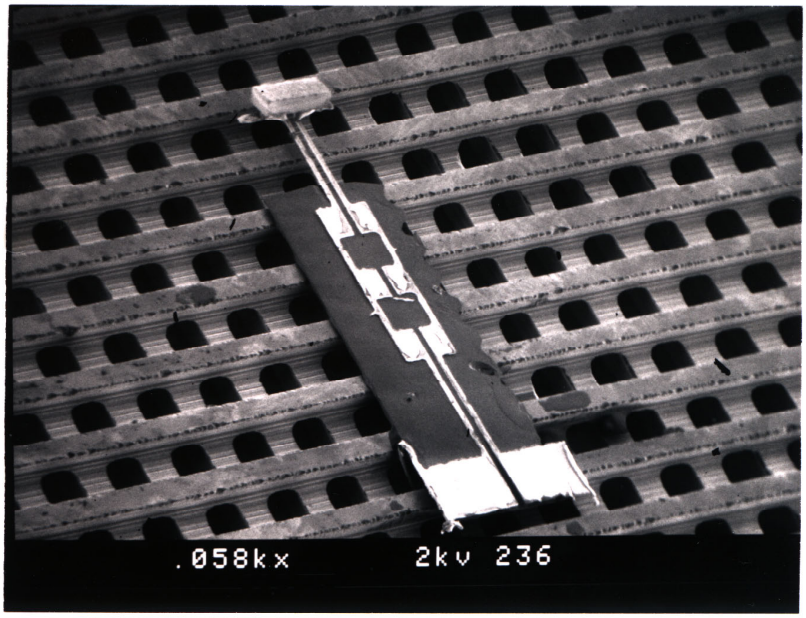

No 309
June 2004

Publié avec l'aide financière de l'ICSU
URSI, c/o Ghent University (INTEC)
St.-Pietersnieuwstraat 41, B-9000 Gent (Belgium)

Contents

Front cover: An electron-microscope photograph of 500 GHz dipole antenna on top of a "woodpile". See the paper by Peter de Maagt, Ramon Gonzalo, J. (Yiannis) Vardaxoglou and J-M Baracco.

For information, please contact :
The URSI Secretariat
c/o Ghent University (INTEC)
Sint-Pietersnieuwstraat 41, B-9000 Gent, Belgium
Tel.: (32) 9-264 33 20, Fax: (32) 9-264 42 88
E-mail: ursi@intec.rug.ac.be
http://www.ursi.org

Editorial

What's in this Issue

Electromagnetic bandgap (EBG) materials are materials that have the property that they permit propagation of electromagnetic waves at frequencies above and below a certain band of frequencies, and block propagation within the band. They were first developed about 15 years ago by drilling holes in a periodic pattern in an otherwise normal dielectric material. Since then, a variety of micro-fabrication techniques have been developed, usually involving two- and three-dimensional periodic structures. Peter de Maagt, Ramon Gonzalo, Yiannis Vardaxoglou, and Jean-Mark Baracco describe such materials in their invited Commission B *Review of Radio Science* paper in this issue. They explain several methods for modeling and thereby designing such materials. They then give examples of a number of applications at microwave and millimeter wavelengths, including antennas, absorbers, resonators, filters, and waveguiding structures. They describe how the properties of some of these materials can be tuned, and how use of such properties can permit miniaturization of a variety of antennas and components. This is a good review of a fascinating and rapidly developing field.

Lot Shafai is the Commission B Associate Editor for the *Reviews of Radio Science*, and his efforts are greatly appreciated.

Fiber-optic cables have found widespread use in telecommunications. One of the more interesting recent uses is to connect wireless-communication base stations to the central station. When the RF signals are generated at the central station and sent over the fiber optics to the base stations, what are referred to as chromatic dispersion effects can be a major limitation. These effects are due to the fact that different wavelengths of light propagate with different speeds in the fiber-optic cables. The result can be a cancellation of the RF power due to propagation through the cable. In their invited Commission D *Reviews of Radio Science* paper, D. Hervé, J. L. Corral, J. M. Fuster, J. Herrera, A. Martínez, V. Polo, F. Ramos, E. Vourc'h, and J. Martí describe a variety of techniques to compensate for such chromatic distortion. These include using various types of single-sideband transmission, applying different types of external modulation to the optical signals, techniques based on nonlinear effects, and the use of semiconductor optical amplifiers. One of the nice aspects of this review is that it makes some rather sophisticated communications principles readily understandable.

The efforts of Fréderique de Fornel, Commission D Associate Editor for the *Reviews of Radio Science*, are greatly appreciated.

The title of Martin Friedrich's invited *Reviews of Radio Science* paper from Commission G very cleverly makes an important point. For years, much of the research dealing with the lower portions of the ionosphere (e.g., the D region) was related to communications. However, recent work has shown that the lower regions of the ionosphere can yield information that is of substantial importance to more-general atmospheric science. This includes support for modeling chemical processes and constituents, transport of constituents, and information about temperature and energy input, among other possibilities. It may even be possible to use ionospheric parameters to trace changes in global climate. This is an interesting and thought-provoking review.

Paul Cannon's efforts as Associate Editor for Commission G for the *Reviews of Radio Science* are gratefully acknowledged, as are Phil Wilkinson's excellent overall efforts with the *Reviews*.

Start Planning for the General Assembly!

URSI's XXVIIIth General Assembly will be held in New Delhi, India, October 23 to 29, 2005. I just returned from the Coordinating Committee meeting, and I had the pleasure of visiting the conference venue last year. You need to start planning *now* to attend the General Assembly: it is going to be a great experience! The Commissions have a full program of oral and poster sessions planned, and the call for papers will be available around the first of September. The General Assembly Web site is under construction at http://www.ursiga2005.org, and the draft schedule can be found through the "GAIndia05" link on the URSI Web page, at http://www.ursi.org. Please encourage young scientists to apply for the URSI Young Scientist Awards for the General Assembly: the application appears in this issue, and can be downloaded from the URSI Web page. The deadline is November 15, 2004. There are many special events being planned by the Indian National and Local Organizing Committees in conjunction with the General Assembly. It is going to be a landmark event in radio science for the region, and a particularly memorable General Assembly. Do start planning to participate and attend right now!

Help Wanted

The *Radio Science Bulletin* is looking for someone to coordinate and solicit input for a regular column reviewing books, and abstracts of dissertations, of interest to radio scientists. If you would like to become involved in this way, please contact me.

New Delhi General Assembly

23 - 29 October 2005

The local Organising Committee takes great pleasure in inviting you to attend the XXVIIIth URSI General Assembly that will take place in the *Vigyan Bhawan Convention Center* in New Delhi, India, from 23 to 29 October 2005.

New Delhi, the capital of India, has always occupied a strategic position in the country's history, as Hindu and Islamic dynasties have ruled from here, leaving their imprint in the form of relics. Delhi, is today, one of the fastest growing cities of India, rich with culture, architecture and human diversity.

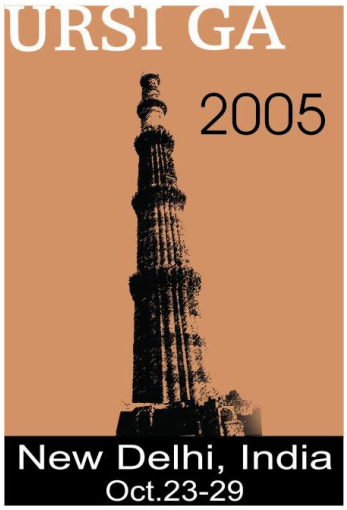

The National Physical Laboratory, also located in New Delhi, is the nodal Agency for the Organisation of this Assembly. Dr. A.P. Mitra, who was elected as URSI Honorary President at the Maastricht General Assembly in 2002, is Chairman of the National Organising Committee.

The local Organising Committee has been founded under the chairmanship of Dr. Vikram Kumar. As scientific Coordinator Council appointed Professor Gert Brussaard. As Associate Coordinator of the Scientific Programme Dr. Behari will serve. Convenor of the LOC is Dr. P. Banerjee.

The URSI GA2005 logo is finalised and the conference website is launched but still under construction. There's a direct link at the URSI website to the site of the India GA, i.e.:

http://www.ursiga2005.org

We sincerely hope that many radioscientists of the URSI community will get together in the fall of 2005 when temperatures in New Delhi are very agreeable. We also would like to mention that the LOC secured the accomodation by blocking rooms in a few hotels nearby the convention center which are of very good quality.

Please contact for further information:

Dr. P. Banerjee
Time & Frequency Section
National Physical Laboratory
New Delhi 110 012, INDIA
Tel: +91 11 2584 1506, +91 11 2874 4318
Fax: +91 11 2572 6952, +91 11 2572 6938
Email: pbanerjee@mail.nplindia.ernet.in

URSI Accounts 2003

Following a good tradition, we present in this June issue of the *Radio Science Bulletin* the audited accounts of URSI.

The URSI accounts are closely linked to the General Assemblies and follow therefore a 3 years cycle. After increased expenditure on the year of the General Assembly, on the following two years we accumulate funds to cover the expenses of the next GA. We received substantial income in 2003 because we received the revenues of the 2002 GA in Maastricht and because one national Member Committee paid its arrears. Unfortunately, both ICSU and UNESCO ceased to support our Young Scientists Programme and we were forced to ask the National Member Committees for the assistance, which will let young scientists, mainly from the developing countries, attend the 2005 GA in New Delhi, India.

We kept the expenditure low, at the level of the year 2000. The net URSI assets, after a decrease in 2002, in 2003 rose slightly. Overall, the finances of URSI are in good shape.

Paul Lagasse, Secretary General — Andrzej Wernik, Treasurer

BALANCE SHEET: 31 DECEMBER 2003

ASSETS	USD	USD	EURO	EURO
Dollars				
Merrill Lynch WCMA	10,107.02		8,510.11	
Fortis	10,909.26		9,185.60	
Smith Barney Shearson	(53.86)		(45.35)	
		20,962.42		17,650.36
Euros				
Banque Degroof	1,456.45		1,226.33	
Fortis	224,730.71		189,223.26	
		226,187.16		190,449.59
Investments				
Demeter Sicav Shares	22,794.75		19,193.18	
Rorento Units	111,969.73		94,278.51	
Aqua Sicav	64,103.22		53,974.91	
Merrill-Lynch Low Duration (305 units)	3,117.59		2,625.01	
Massachusetts Investor Fund	277,478.91		233,637.24	
	479,464.20		403,708.85	
684 Rorento units on behalf of van der Pol Fund	12,476.18		10,504.94	
		491,940.38		414,213.79
Short Term Deposito		59,579.62		50,166.04
Petty Cash		482.64		406.38
Total Assets		799,152.22		672,886.16
Less Creditors				
IUCAF	22,686.69		19,102.19	
ISES	8,847.26		7,449.39	
		(31,533.95)		(26,551.58)
Balthasar van der Pol Medal Fund		(12,476.18)		(10,504.94)
NET TOTAL OF URSI ASSETS		**755,142.09**		**635,829.64**

The net URSI Assets are represented by:	USD	USD	EURO	EURO
Closure of Secretariat				
Provision for Closure of Secretariat		90,000.00		75,780.00
Scientific Activities Fund				
Scientific Activities in 2004	32,000.00		26,944.00	
Publications in 2004	47,500.00		39,995.00	
Young Scientists in 2004	25,000.00		21,050.00	
Administration Fund in 2004	77,000.00		64,834.00	
I.C.S.U. Dues in 2004	9,000.00		7,578.00	
		190,500.00		160,401.00
XXVIII General Assembly 2005 Fund:				
During 2003-2004-2005		75,000.00		63,150.00
Total allocated URSI Assets		355,500.00		299,331.00
Unallocated Reserve Fund		399,642.09		336,498.64
		755,142.09		**635,829.64**

Statement of Income and expenditure for the year ended 31 December 2003

I. INCOME	USD	USD	EURO	EURO
Grant from ICSU Fund and US National				
Academy of Sciences	0.00		0.00	
Allocation from UNESCO to ISCU Grants Programme	0.00		0.00	
UNESCO Contracts	0.00		0.00	
Contributions from National Members	283,667.46		238,848.00	
Contributions from Other Members	0.00		0.00	
Special Contributions	0.00		0.00	
Contracts	0.00		0.00	
Sales of Publications, Royalties	0.00		0.00	
Sales of scientific materials	129.48		109.02	
Bank Interest	1,103.38		929.05	
Other Income	95,256.25		80,205.76	
Total Income		**380,156.57**		**320,091.83**

II. EXPENDITURE

A1) Scientific Activities		15,700.00		13,219.40
General Assembly 2002	260.57		219.40	
Scientific meetings: symposia/colloqiua	15,439.43		13,000.00	
Working groups/Training courses	0.00		0.00	
Representation at scientific meetings	0.00		0.00	
Data Gather/Processing	0.00		0.00	
Research Projects	0.00		0.00	
Grants to Individuals/Organisations	0.00		0.00	
Other	0.00		0.00	
Loss covered by UNESCO Contracts	0.00		0.00	

A2) Routine Meetings		14,176.20		11,936.36
Bureau/Executive committee	14,176.20		11,936.36	
Other	0.00		0.00	
A3) Publications		46,875.29		39,468.99
B) Other Activities		14,183.19		11,942.24
Contribution to ICSU	4,682.00		3,942.24	
Contribution to other ICSU bodies	9,501.19		8,000.00	
Activities covered by UNESCO Contracts	0.00		0.00	
C) Administrative Expenses		78,205.32		65,848.88
Salaries, Related Charges	60,699.35		51,108.85	
General Office Expenses	5,701.71		4,800.84	
Office Equipment	4,144.28		3,489.48	
Accountancy/Audit Fees	5,532.68		4,658.52	
Bank Charges	2,127.30		1,791.19	
Loss on Investments	0.00		0.00	
Total Expenditure:		**169,140.00**		**142,415.87**
Excess of Income over Expenditure		211,016.57		177,675.96
Currency translation difference (USD => EURO) - Bank Accounts		(5,136.07)		(4,324.57)
Currency translation difference (USD => EURO) - Investments		(117,474.44)		(98,913.48)
Currency translation difference (USD => EURO) - others		130,288.79		109,703.15
Accumulated Balance at 1 January 2003		536,447.24		451,688.58
		755,142.09		**635,829.64**

Rates of exchange:

January 1, 2003	$ 1 = 1.0483 EUR
December 31, 2003	$ 1 = 0.8420 EUR

	USD	EURO
Balthasar van der Pol Fund		
684 Rorento Shares: market value on December 31, 2003		
(Aquisition Value: USD 12.476,17)	31,535.49	26,552.88
Market Value of investments on December 31, 2003		
Demeter Sicav	63,708.03	53,642.16
Rorento Units (1)	599,358.67	504,660.00
Aqua-Sicav	92,310.67	77,725.58
M-L Low Duration	3,138.45	2,642.57
Massachusetts Investor Fund	199,121.68	167,660.45
	957,637.50	**806,330.77**

(1) Including the 684 Rorento Shares of the van der Pol Fund

APPENDIX: Detail of Income and Expenditure

	USD	USD	EURO	EURO
I. INCOME				
Other Income				
Income General Assembly - support YS Japan	0.00		0.00	
Income General Assembly 2002	95,011.88		80,000.00	
Fee Radioscientists	47.51		40.00	
Interest on M-L Short Term	196.86		165.76	
Interest on Massachusetts Investor Fund	0.00		0.00	
		95,256.25		80,205.76
II . EXPENDITURE				
General Assembly 2002				
Organisation	260.57		219.40	
Vanderpol Medal	0.00		0.00	
Expenses officials	0.00		0.00	
Young scientists	0.00		0.00	
		260.57		219.40
Symposia/Colloquia/Working Groups:				
Commission A	0.00		0.00	
Commission B	0.00		0.00	
Commission C	0.00		0.00	
Commission D	1,187.65		1,000.00	
Commission E	3,562.95		3,000.00	
Commission F	3,562.95		3,000.00	
Commission G	1,781.47		1,500.00	
Commission H	3,562.95		3,000.00	
Commission J	1,781.46		1,500.00	
Commission K	0.00		0.00	
		15,439.43		13,000.00
Contribution to other ICSU bodies				
FAGS 2002+2003	4,750.60		4,000.00	
IUCAF 2002+2003	4,750.60		4,000.00	
		9,501.20		8,000.00
Publications:				
Printing ‘The Radio Science Bulletin’	20,557.93		17,309.78	
Mailing ‘The Radio Science Bulletin’	26,317.36		22,159.21	
		46,875.29		39,468.99

UNION RADIO-SCIENTIFIQUE INTERNATIONALE

INTERNATIONAL UNION OF RADIO SCIENCE

URSI AWARDS FOR YOUNG SCIENTISTS

CONDITIONS

A limited number of awards are available to assist young scientists from both developed and developing countries to attend the General Assembly of URSI.

To qualify for an award the applicant :

1. must be less than 35 years old on September 1 of the year of the URSI General Assembly;

2. should have a paper, of which he or she is the principal author, submitted and accepted for oral or poster presentation at a regular session of the General Assembly;

Applicants should also be interested in promoting contacts between developed and developing countries.

All successful applicants are expected to participate fully in the scientific activities of the General Assembly. They will receive free registration, and financial support for board and lodging at the General Assembly. A basic accommodation is provided by the assembly organizers that permits the Young Scientists from around the world to collaborate and interact. Young scientists may arrange alternative accommodation, but such arrangements are entirely at their own expense. Limited funds will also be available as a contribution to the travel costs of young scientists from developing countries.

Apply before 15 November 2004 to the URSI Secretariat (address below). Please submit ***THREE COPIES*** *of each of the following: (1) a completed application form, (2) a CV and list of publications, (3) an abstract of proposed paper.*

Applications will be assessed by the URSI Young Scientist Committee taking account of the national ranking of the application and the technical evaluation of the abstract by the relevant URSI Commission. Awards will be announced on the URSI web-site in May 2005.

The URSI Secretariat
c/o Ghent University / INTEC
Sint-Pietersnieuwstraat 41
B-9000 GENT
BELGIUM
fax : (32) 9-264.42.88
e-mail : ursi@intec.rug.ac.be

For more information about URSI, the General Assembly and the activities of URSI Commissions, please look at the URSI web site at: http://www.ursi.org

APPLICATION FOR A YOUNG SCIENTISTS AWARD

I wish to apply for an award to attend the XXVIIIth General Assembly of the International Union of Radio Science in New Delhi, India, 23-29 October 2005.

Name : Prof./Dr./Mr./Mrs./Ms. .....

Sex : male / female Family Name First Name Middle Initials

Date of birth (day / month / year) : .... / .... / .... Nationality : .....

Studying/Employed at : .....

Institution .....

Department .....

Mailing address : Please send all correspondence to my ☐ business / ☐ home address, i.e.

Street .....

City and postal code .....

Province/State ..... Country .....

Fax ..... E-mail .....

Academic qualifications, with date(s) obtained : .....

.....

Title of abstract submitted : .....

.....

Type of session preferred: ☐ in an oral session ☐ in a poster session

The subject of the paper is relevant to URSI Commission …….session (leave blank if uncertain).

Date :..... Signed .....

For applicants from developing countries only :

I estimate the cheapest return fare to the URSI meeting is EURO .....

For graduate students only - Supervisor's endorsement :

I support the application for an award to enable this young scientist to attend the forthcoming General Assembly of URSI for the following reasons : .....

.....

.....

.....

Supervisor's Name and Title : .....

Address : .....

Date :..... Signed : .....

Review of Electromagnetic-Bandgap Technology and Applications

P. de Maagt
R. Gonzalo
J. Vardaxoglou
J-M Baracco

Abstract

This paper reviews the primary application areas of electromagnetic-bandgap (EBG) technology at microwave and (sub)millimeter-wave frequencies. Examples of EBG configurations in the microwave region are shown, including array antennas, high-precision GPS, mobile telephony, wearable antennas, and diplexing antennas. In the sub-millimeter-wave region, a 500 GHz dipole configuration and a novel heterodyne mixer are shown. Some emphasis is also placed on EBG waveguides, high-impedance planes (artificial magnetic conductors, AMCs), resonators, and filters.

As most fundamental components will be available in EBG technology, a fully integrated receiver could be developed in order to take full advantage of this technology. True integration of passive and active components can now begin to materialize using EBG technology.

1. Introduction

Microwave engineers are familiar with the concept of electromagnetic waves interacting with periodic structures. Periodic structures – in both closed metallic and open waveguides – have been used for many years, for example, in filters and traveling-wave tubes. Planar versions of these can be found in the form of frequency-selective surfaces (FSS) and phased-array antennas. In the late 1980s, a fully three-dimensional periodic structure, working at microwave frequencies, was realized by Yablonovitch [1] and his coworkers, by mechanically drilling holes into a block of dielectric material. This so-called "Yablonovite" material prevents the propagation of microwave radiation in any three-dimensional spatial direction, whereas the material is transparent in its solid form at these wavelengths.

These artificially engineered materials are generically known as photonic bandgap (PBG) materials, or photonic crystals. Although "photonic" refers to light, the principle of a "bandgap" applies to electromagnetic waves of all wavelengths. Consequently, there is a controversy in the microwave community about the use of the term "photonic," [2] and the names electromagnetic-bandgap (EBG) material or electromagnetic crystal are being proposed.

Electromagnetic-bandgap materials presently represent one of the most rapidly advancing sectors in the electromagnetic arena. They allow us to manipulate the propagation of electromagnetic waves to an extent that was previously not possible. The rapid advances in both theory and experiment, together with substantial technological potential, have driven the development of electromagnetic-bandgap technology. Emphasis is now placed on finding tangible applications, combined with detailed modeling. Owing to the tremendous potential of electromagnetic-bandgap (EBG) structures, there is a plethora of applications in which they can be used. New startup companies have been founded solely to exploit the commercial potential of this technology.

Communications services are one pertinent example of an increasingly important area. There has been a significant increase in demand for high-speed data services for voice and multimedia applications, particularly for accessing the Internet and the fixed and mobile services. As a result, broadband microwave wireless access has emerged. Ultimately, these applications will require new frequency allocations, with higher operational frequencies around 30 GHz, 40 GHz, and 60 GHz for point-to-point, point-to-multipoint, and high-density fixed services, respectively.

Furthermore, technology in the sub-millimeter-wave region of the electromagnetic spectrum is currently experiencing an explosive growth. The growth is fuelled in

Peter de Maagt is with the Electromagnetics Division, European Space Research and Technology Centre (ESTEC), European Space Agency (ESA), PO Box 299, 2200 AG Noordwijk, The Netherlands; e-mail:Peter.de.Maagt@esa.int.
Ramon Gonzalo is with the Electrical and Electronic Engineering Department, Universidad Publica de Navarra, Campus Arrosadia,E-31006, Pamplona, Navarra, Spain.
J. (Yiannis) Vardaxoglou is with the Department of Electronic and Electrical Engineering, Loughborough University,Loughborough,Leicestershire, LE11 3TU, United Kingdom.
Jean-Mark Baracco is with the MARDEL, 06140 Vence, France

Editors note: This is one of the invited *Reviews of Radio Science*, from Commission B

part by the need for faster signal processing and communications, high-resolution spectroscopy, atmospheric and astrophysical remote sensing, and medical imaging for cancer detection. The increased atmospheric absorption and specific molecular resonances observed over this range of frequencies gives rise to applications in secure ultra-high-bandwidth communication networks.

EBG technology offers promising alternatives for overcoming the limitations of current technology, and it is envisaged that many new structures will evolve. EBG technology represents a major breakthrough with respect to the current planar approaches, mainly due to their ability to guide and efficiently control electromagnetic waves. In order to get the most out of this technology, a fully integrated receiver or emitter system should be developed, in which all the components are designed using EBG technology. The first step in order to achieve this goal is the design of the individual components.

This paper starts with a discussion of basic EBG performance and computational tools for analysis and design. It subsequently shows some applications in the microwave and sub-millimeter-wave frequency range. Several existing EBG antennas, waveguide, and filter configurations are highlighted. Emphasis is also placed on the tuning capabilities of devices.

Owing to the newness of the subject area and the associated devices, novel modeling tools and testing procedures have been successfully developed. A large part of the research at microwave frequencies is already applications driven, while the developments for sub-millimeter-wave systems remain technologically more challenging. Simultaneous developments at these two frequency ranges provide verification of scalability in design, and provide essential insight into any possible optical applications of such devices.

Due to the large number of groups that have started working in this field, it is impossible to incorporate a complete list of original and pertinent research. There have been many books, special journal issues, and journal articles written in this area, and the interested reader should consult them for more details on the many novel configurations that exist.

The content of this paper is an update of a review article previously published in a special issue on metamaterials (*IEEE Transactions on Antennas and Propagation*, **AP-51**, 10, October 2003).

2. Numerical Modeling of Electromagnetic-Bandgap Crystals

As in any novel technological field, on occasion a cut-and-try method was initially applied because of a lack of reliable prediction methods. The theoretical description of electromagnetic waves in electromagnetic-bandgap crystals involves the exact solution of Maxwell's equations in a periodic medium. Over the past few years, several techniques have emerged that allow us to predict the performance of EBGs, providing useful prefabrication data.

The first models were based on scalar theory, but it was soon discovered that this did not provide the required accuracy; consequent models were based on the full vectorial Maxwell's equations. While other techniques exist (order *N* [3]), the following methods have been used very frequently:

2.1 Plane-Wave Expansion or Spherical-Wave Expansion

This method starts with Maxwell's equations in a generalized eigenvalue form. The plane-wave expansion allows this set of equations to be solved by converting them into a Hermitian eigenvalue problem [4], and many commercial packages exist to aid in their solution. The plane-wave method became the first method to find widespread use because it is easy to understand and is computationally very straightforward to implement. Because many plane waves are usually required in order to obtain good convergence, this can limit the use of the method for treatment of more complicated crystals. Several means have been proposed to improve the convergence of the plane-wave expansion [5]. Spherical waves may be used instead of plane waves as a basis set if the electromagnetic crystal is composed of spherical or cylindrical parts. This method is called the spherical-wave expansion method of the vector KRR (Koringa-Kohn-Rostker) method [6].

2.2 The Transfer Matrix Method

At a fixed frequency, the equations are solved in the plane perpendicular to the crystal-surface normal for a given propagation depth through the crystal (a boundary-value problem). The field is then transferred throughout the crystal by successively applying Maxwell's equations to obtain the scattering matrix for a single layer of crystal [7]. By cascading the scattering matrices for each layer, the transmission and reflection coefficients can be propagated down through layers by successive matrix multiplications.

2.3 The Finite-Difference Time-Domain Method

The Finite-Difference Time-Domain (FDTD) method is capable of characterizing the broadband frequency response of arbitrary and inhomogeneous EBG elements in a single run, and can be computational efficient. The application of the FDTD method in the modeling of EBG materials can be straightforward. The structure is meshed in a conventional Yee's Cartesian grid, with absorbing

boundaries such as the perfectly matched layer. To activate the structure, infinitesimal dipoles [8] or plane waves with a Gaussian-pulse waveform are usually used. EBG properties described in the scattering parameters can be extracted from the time-domain electric- and magnetic-field responses. Different approaches have been developed to further improve the efficiency in the simulation. These include FDTD with periodic boundary conditions/perfectly matched layer (PBC/PML) and the split-field method [9] for both normal and oblique wave incidence, the FDTD/Prony technique [10] for extraction of accurate bandgap parameters over short periods of time, and nonorthogonal FDTD approaches [11] for oblique wave incidence and potentially conformal FDTD modeling on curved EBG elements without "staircasing" approximations. These modified approaches generally only consider a "unit cell" of the EBG structure truncated with perfect boundary conditions, and are effective in modeling the bandgap properties of complex three-dimensional EBG structures. However, it has been found that spatial harmonic effects are often neglected by these approaches. Although it has been demonstrated that the results are valid for the prediction of the bandgap, such approaches do not seem sufficient for evaluating the pass-band behavior [12].

2.4 Commercial Packages

There exist a number of commercially available software packages that can readily deal with the analysis and simulation of EBG and associated structures, as well as with general periodic arrays. The following are but a few of these: Ansoft *HFSS* and Ansoft *Designer*, *Fidelity* and *IE3D* by Zeeland Software, *EMPIRE* by IMST, *Microstripes* by Flomerics, *Microwave Studio* by CST and Sonnet, and *Microwave Office* by Applied Wave Research. Whereas planar array performance can be assessed using a two-and-one-half-dimensional MoM (Method of Moments), for generalized three-dimensional structures one needs to use a three-dimensional FEM (Finite-Element Method), FDTD, or TLM (Transmission-Line Matrix) package. There is a varying degree of accuracy depending on the mesh resolution, which is normally traded off against the computational time.

The above methods are able to reproduce experimental results well, and allow the physics of some specific properties of electromagnetic crystals to be intuitively understood. The initial results from the plane-wave- or spherical-wave-expansion methods give the dispersion curves and allow modal visualization, while those of the Transfer Matrix Method give the transmission and reflection coefficients of the crystal. Most methods become computationally demanding as soon as three-dimensional EBGs are analyzed, but in some cases one can still play simple but effective computational tricks that allow treating some special three-dimensional structures [13].

3. Applications of Microwave Electromagnetic-Bandgap Antennas

A multitude of basic EBG applications exist, especially within the microwave and low millimeter-wave region, for example in electronically scanned phased arrays, high-precision GPS, Bluetooth, mobile telephony, wearable antennas, etc.

Electronically scanned phased arrays find uses in many applications. For example, constellations of low-Earth-orbit satellites can be used for high-data-rate transmission for multi-media applications. These applications require scanned multibeam antennas with relatively wide bandwidth. Each beam usually works in dual circular polarization. Most of these constellations work at frequencies up to 30 GHz. The use of active phased arrays made using microstrip technology is then an attractive solution. However, the need for bandwidth and scanning increases the undesirable effects caused by surface waves. A very promising way to eradicate the problems created by surface waves (e.g., scan blindness) while at the same time improving performance is to substitute electromagnetic-bandgap crystals for standard dielectric substrates [14, 15].

Another microwave application is high-precision GPS (Global Positioning Satellite). High precision GPS surveying can make measurements with sub-centimeter-accuracy levels. While software can greatly reduce multipath errors, extra precautions that can shield the antenna from unwanted multipath signals are needed to obtain these accuracies. Choke rings provide excellent electrical performance for GPS antennas, but they are usually very large, heavy, and costly. One can design EBG solutions in printed-circuit technology by making use of the fact that metallo-dielectric EBG antennas can behave as artificial magnetic conductors [16].

Data and voice transmission are bound to become even more common as the world goes wireless. Attention is now focused on Bluetooth [17], the first implementation of such systems in everyday life. Moreover, for other applications, such as mobile phones, more attention is being paid to the shielding offered by the antenna and to potential health hazards. EBG technology may prove useful in mobile-antenna handset designs [18], and may reduce the radiation (the Specific Absorption Rate, or SAR) into the operator's hand and head. Note that all new mobile phones will have to display the SAR value of the handset.

Shielding is not only important for reducing health concerns: It is also important in multi-point communications. For example, devices placed on the side of a laptop computer interact with the screen and the case, resulting in a lower bit rate between two computers. Again, electromagnetic-bandgap materials may play an important role in this area.

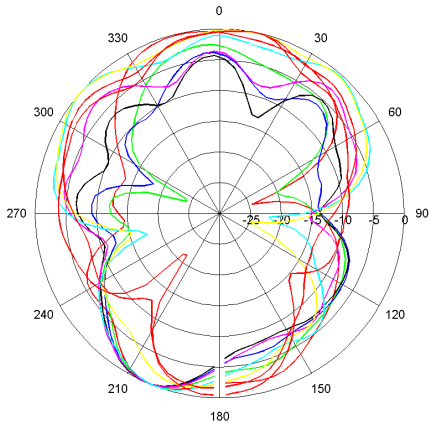

Figure 1a. The measured radiation patterns from 14 to 16 GHz, measured at each 0.25 GHz, for the H plane for the conventional patch antenna. Each color shows a different frequency value. Each division is 10 dB.

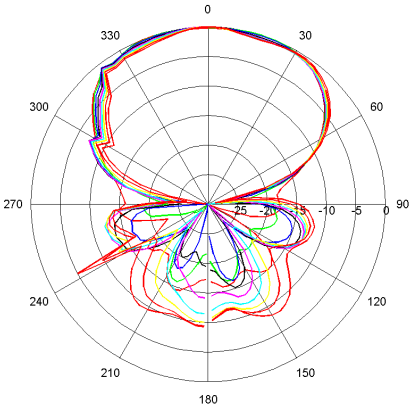

Figure 1b. The measured radiation patterns from 14 to 16 GHz, measured at each 0.25 GHz, for the H plane for the electromagnetic-crystal substrate. Each color shows a different frequency value. Each division is 10 dB.

Future clothing may have a variety of consumer electronics built into the garments. Wearable antennas have received much interest recently, due to the introduction of personal-communication technology. Several applications of wearable antennas can be found, such as radio tagging and miniature remote cameras. Eventually these may even help parents to pinpoint their child's position. Antennas play a paramount role in the optimal design of wearable or hand-held units used in these services. The electromagnetic interactions among the antenna, the wearable unit, and the human operator are clearly important factors to be considered in designing these antennas. EBG technology has been proposed as a design solution [19].

Microwave filtering has also turned out to be an important area where electromagnetic-bandgap materials play an important role [20]. The broad stop-band can be exploited to suppress spurious pass-bands that are always present in conventional microstrip filters. The sharp cutoff can also be used to improve the roll-off of a low-pass filter. Furthermore, combinations of conventional designs and electromagnetic-bandgap materials could lead to very compact structures.

The area of conventional waveguides is another field were hybrid solutions could play an important role. Rectangular waveguides with uniform field distributions are of great concern for applications in quasi-optical power combining. A standard waveguide can be modified by placing an electromagnetic crystal on the two sidewalls of a waveguide [21], potentially creating a very efficient waveguiding structure. Coupled-cavity waveguides (CCW) have recently attracted considerable attention. This concept is believed to enable bends in the waveguide with very low bend-reflection loss [22].

4. Microwave Electromagnetic-Bandgap Antennas and Components

Several antenna configurations using electromagnetic-bandgap crystals have already been studied, including the following, to mention but a few: dipole antennas [23-24], slot antennas, [25], patch antennas [14, 26-29], bow-tie antennas [30], spiral and curl antennas [31-33], superstrate antennas or resonant-cavity antennas [34-36], parabolic-reflector antennas [37], and combinations of the above [38].

The patch antenna is a popular configuration at microwave frequencies, as it is robust; conformable, if required; and inexpensive to manufacture. One limitation is the possible excitation of surface waves, which can result in poor efficiency, degradation of the radiation pattern, reduction in gain, and an increase in mutual coupling. Surface waves can become dominant if high-dielectric-constant substrates are used, such as those commonly used for MMIC RF circuitry, and also if the thickness of the substrate is increased in order to have a larger bandwidth. Furthermore, if patches are to be used in an array configuration, the isolation between separate patches is generally believed not to be sufficient. It has been demonstrated that EBG substrates for patch antennas significantly reduce the effect of surface waves as a function of frequency [39] (see Figure 1), and are able to provide relatively broadband frequency performance.

Superstrate and resonant-cavity antennas differ slightly from patch antennas, which work in the middle of the bandgap. Instead, they work at the edges of the bandgap (see Figure 2), making use of the fact that there is an angular dependence of the transmission curves. While full

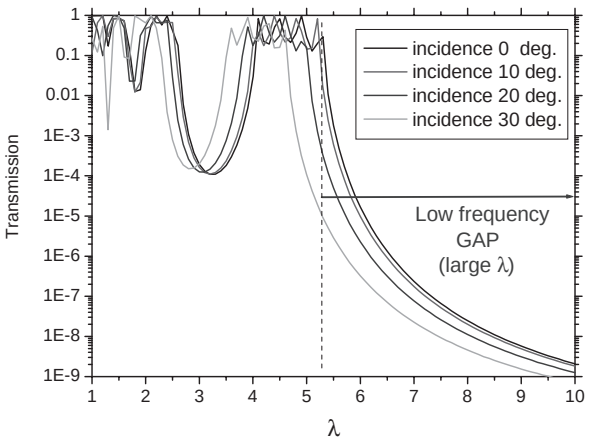

Figure 2a. The transmission of a plane wave through a stack of five metallic grids. The vertical dashed line indicates the operational frequency (reproduced with the kind permission of Gerard Tayeb).

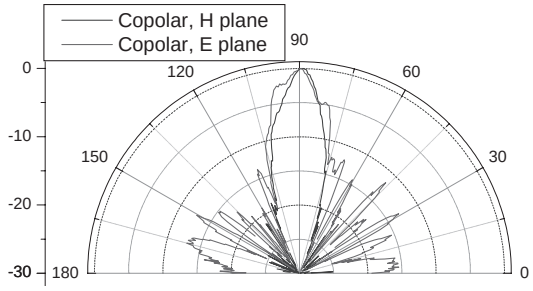

Figure 2b. The measured radiation pattern of a device consisting of six grids placed on a ground plane, fed by a monopole in the center (reproduced with the kind permission of Gerard

transmission is achieved at normal incidence, significant attenuation still occurs for other angles [40]. The result is a highly directive radiation pattern, with good rotational pattern symmetry, but a rather narrowband performance. In general, these are built using a ground plane underneath a feeding source (a patch, slot, or wire), while a resonator cavity is formed by using an EBG material as a superstrate ([35]; see Figure 3).

Metallo-dielectric EBG (MD-EBG) antennas seem to have two actions: they suppress surface currents, and they introduce in-phase image currents. The structure consists of a two-dimensional pattern of capacitive and inductive elements, facilitating compact EBGs that operate at relatively low microwave frequencies. Presently, there exist two main designs: the "high-impedance ground plane" [41], which uses grounding pins to connect the two-dimensional pattern with a ground plane; and the fully planar version, a "Uni-planar compact photonic bandgap (UC-PBG)" [28].

Some simple two-dimensional arrays of conducting elements have been used to improve the performance of patch antennas [42]. Figure 4 shows an example of a hexagonal array of tripole elements around a patch, and the resulting measured improvements in radiation pattern and return loss.

The "reflection phase diagram" of metallo-dielectric EBG structures (or of an artificial magnetic conductor, an AMC) gives information about how the structure reacts to a wave impinging on it. A characteristic feature of MD-EBGs is the existence of a frequency range over which an incident electromagnetic wave does not experience any phase reversal upon reflection. In this range, the structure behaves as a perfect magnetic conductor (PMC).

Multiband artificial magnetic conductors can be delivered by interlacing elements of variable dimensions. Defects can also be introduced by means of reducing the length of some of the array elements, and therefore altering their resonant frequency [43, 44]. The frequencies of zero-phase reflection can be altered by independently adjusting the element dimensions.

The angular stability of the multi-band artificial magnetic conductor surface is also important for enabling applications in communications antennas. With respect to the design of high-impedance ground planes, many practical aspects play important roles, such as the maximum-allowed thickness and the minimum-required operational bandwidth. One of the key requirements is that the structure behave as a perfect magnetic conductor for the whole spatial spectrum of the antenna's radiation. Many high-impedance surface

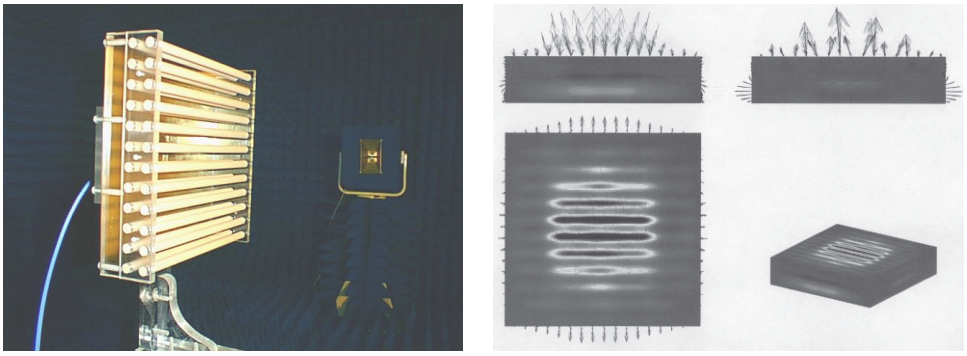

a) b)

Figure 3. (a) A resonant EBG antenna using a two-dimensional EBG as the superstrate. (b) The Poynting vector and electric-field distribution on the two-dimensional EBG structure (reproduced with the kind permission of Bernard Jecko).

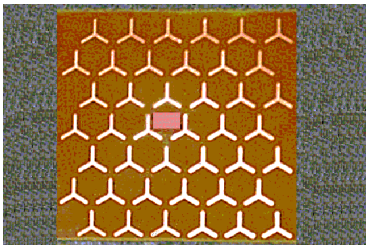

photo

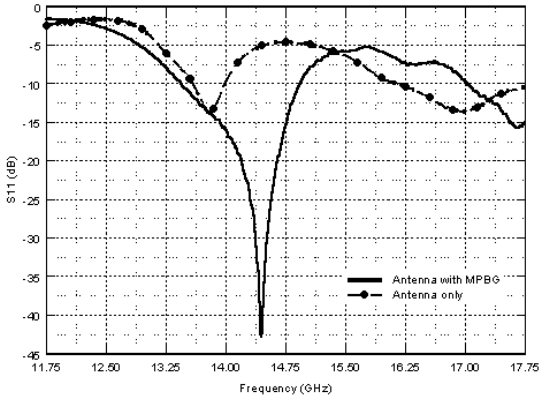

a)

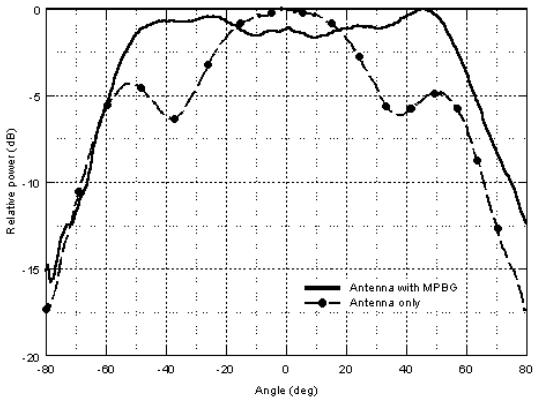

b)

Figure 4. The return loss of a patch antenna (see photo) with and without a tripole metallo-dielectric EBG array(a) and H-plane radiation-pattern measurements of a patch antenna with and without a tripole metallo-dielectric EBG array.).

designs used in the cited references do not comply with this requirement since they do not exhibit a uniform surface impedance with respect to different directions of the incident wave. The surface impedance calculated and measured in the cited references is a plane-wave surface impedance, which normally depends strongly on the angle of incidence. The structures also generally behave differently for the two different polarizations of the incident wave ([32]; see Figure 5). Currently, emphasis is being placed on the stabilization of the surface impedance and resonance frequency [45, 46].

A similar issue is at hand for the design of RF absorbers. The design of thin absorbing layers for radar cross section reduction is a challenging task, because a thickness reduction leads to a decrease of the bandwidth. Another problem is that obliquely incident waves are absorbed much less effectively than normally incident plane waves. High-impedance ground plane structures are being considered to address this problem [47]. The high-impedance ground plane has already been used for mobile-telephone applications and good results have been reported [18]. The uni-planar compact photonic-bandgap (UC-PBG) structure has already been applied in the design of microstrip diplexer patch antennas to enhance the isolation between the transmitter and receiver ports. It was demonstrated that some planar metallo-dielectric EBG lattices are inherently anisotropic, and when constructed with different periods along two orthogonal directions they exhibit different forbidden bandgap responses. The self-diplexing antenna on an anisotropic uni-planar compact photonic-bandgap ground plane has demonstrated improved isolation, and this concept can lead to the development of the direct integration of an RF transceiver with planar antennas to realize on-chip antenna front ends [48].

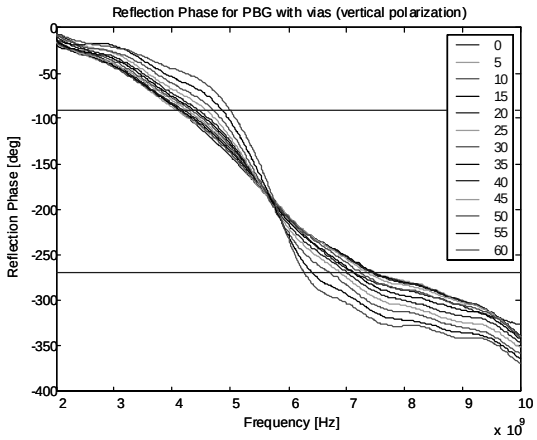

Figure 5a. The measured reflection phase versus the angle of incidence for a metallo-dielectric EBG design (see [27]) with vias, for vertical polarization.

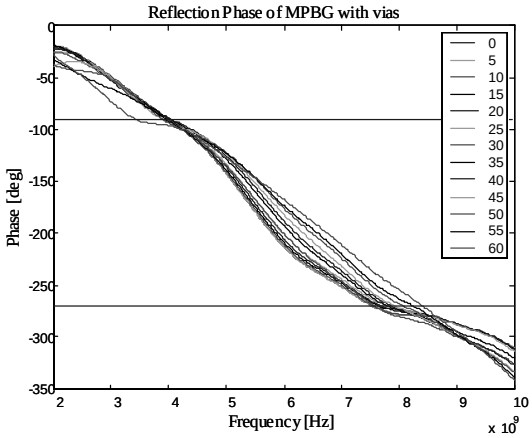

Figure 5b. The measured reflection phase versus the angle of incidence for a metallo-dielectric EBG design (see [27]) with vias for horizontal polarization.

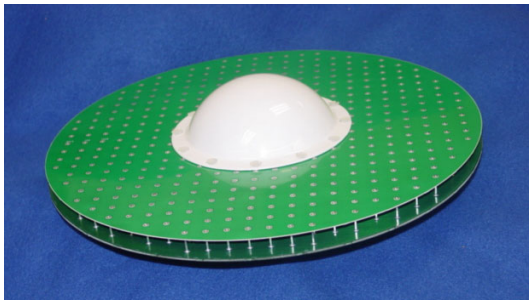

Figure 6. (a) A metallo-dielectric EBG antenna for GPS applications. (reproduced with the kind permission of Will Mc Kinzie).

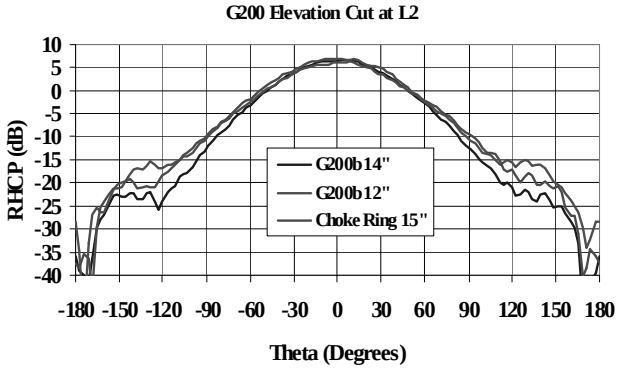

Figure 6. (b) The measured patterns for 12 inch and 14 inch metallo-dielectric EBG antennas, and for a choked version. The pattern roll-off of the 14 inch antenna is better than that of the choke-ring antenna by 2 dB to 3 dB at the horizon (reproduced with the kind permission of Will Mc Kinzie).

Very good performance has been obtained with these metallo-dielectric EBGs for next-generation GPS applications [16]. Figure 6 shows a comparison between the performance of a choked and a metallo-dielectric EBG antenna. Not only did the use of the metallo-dielectric EBG in the antenna reduce the weight by a factor of 10, the height by a factor of four, and was cheaper to manufacture, but it also outperformed the choked horn by several dBs at the horizon.

5. Tunable Electromagnetic-Bandgap Antennas and Components

Ideally, an EBG component would be fully dynamic, reconfigurable, and multifunctional. Such a concept is evidently clearly visionary, but investigations into the basic tuning capabilities that electromagnetic crystals may provide is essential in evaluating their future role. To that end, a proof-of-concept and technological demonstration of tuning capability is essential.

Because the properties of EBG components rely on the contrast between the dielectric constant of the materials involved, any variation of the dielectric constant of at least one of the involved materials will lead to sensitive tuning of the properties of the EBG component. Some alternatives exist to attain tuning of the dielectric constant of the materials used for the EBG components:

- Optically inducing a change of dielectric properties by photo-exciting additional charge carriers
- Electrically inducing a change of dielectric properties by injecting additional charge carriers
- Micromechanically modifying the device geometry and/or the dielectric loading
- Electrically modifying the device geometry and/or the dielectric loading.

The first two approaches are closely related, since the presence of additional charge carriers modifies the dielectric constant. Optically induced tunable devices are a useful approach for being able to quickly analyze the fundamental properties of charge-carrier modulations to accomplish tuning capability in a device. Laser beams (both CW and pulsed) can be used to photo-excite charge carriers at certain locations inside the electromagnetic bandgap. Tunable components can be developed (switches, tunable filters, switchable directional couplers, etc. [49]; see Figure 7) with a good degree of tuning capability [50]. The

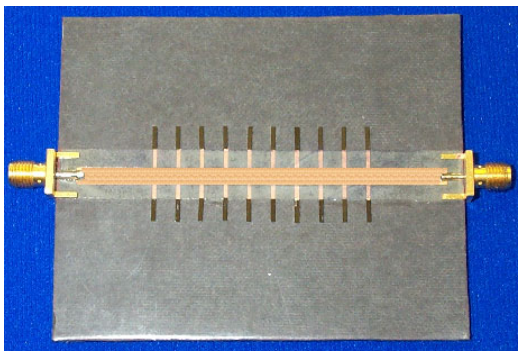

Figure 7. (a) A photograph of a tunable EBG prototype. High-resistivity silicon strips can be seen at the dipole ends.

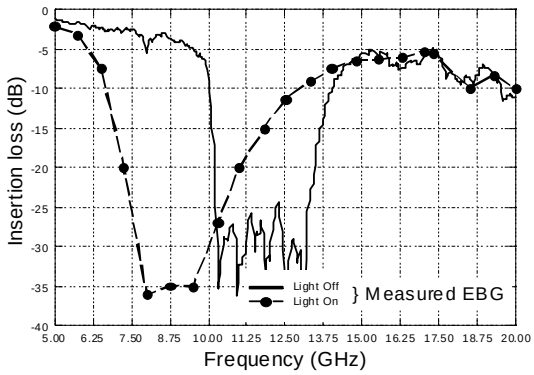

Figure 7. (b) The measured results of EBG tuning using optical injection of carriers.

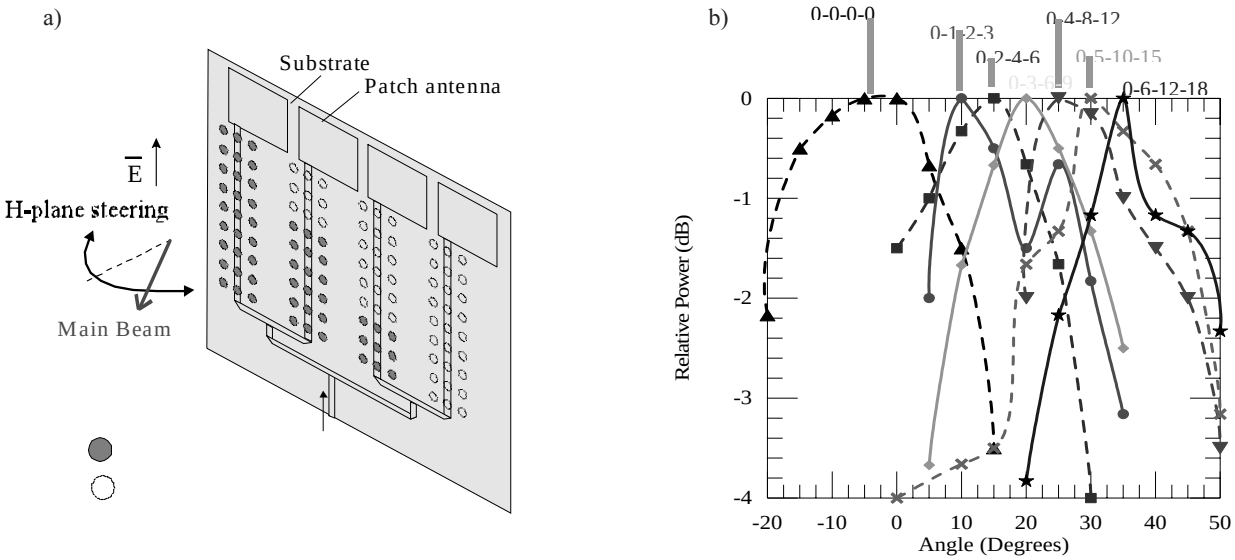

Figure 8. (a) A four-element patch array with the EBG holes on the ground plane. Only nine EBG periods are shown here. (b) The measured beam patterns for the different ground-plane configurations. The array steered in increments of approximately 6°. Only the peaks of the steered pattern are shown (reproduced with the kind permission of Jung-Chih Chiao).

effect of switching the defect on and off could produce a shift of the band edge (the lower cutoff frequency at the −10 dB level) by about 90% and 100%, driving the LEDs using 0.6 amps and 3 amps, respectively. Measurements revealed an increase of more than 30% in the depth of the band stop when the defects were switched on. Overall, this type of defect mainly affects the falling edge of the bandgap.

The last two approaches are also closely related. The third method is based on micro-electro-mechanical system (MEMS) fabrication technologies, where one can electrically modify the position of membranes and/or switches, and modulate the local properties of the EBG components ([51, 52]; see Figure 8). Entire arrays of MEMS and EBGs are also already being manufactured [53; see Figure 9].

An example of the fourth category is given in [54], where PIN diodes were inserted along the wires of a two-dimensional metallic structure.

6. (Sub) Millimeter-Wave Electromagnetic-Bandgap Antennas

A new generation of scientific space-borne instruments, included in both Earth observation and scientific missions, is under consideration at millimeter and sub-millimeter wavelengths. As the frequency increases, a planar structure that integrates the antenna, mixer, local oscillator, and all peripheral circuitry onto one single substrate becomes an attractive option. While conceptually simple, in practice it is challenging to develop and test an integrated planar antenna on a semiconductor substrate that has good radiation efficiency and can be easily integrated with the active circuit. One of the problems encountered is that planar antennas on high-dielectric-constant substrates couple a significant fraction of the input power into substrate

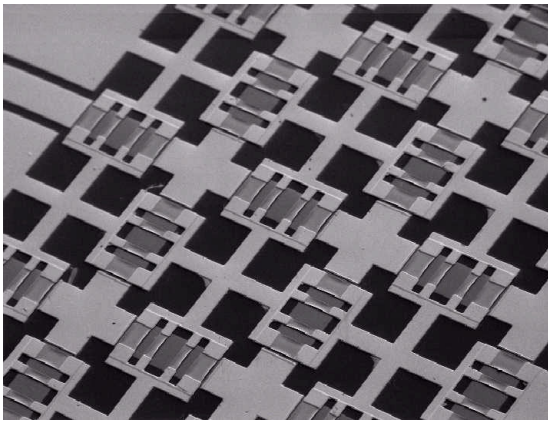

Figure 9. A MEMS matrix to tune both the normal and parallel refractive index and the direction of the energy flow (reproduced with the kind permission of Marc Thevenot and Pierre Blondy).

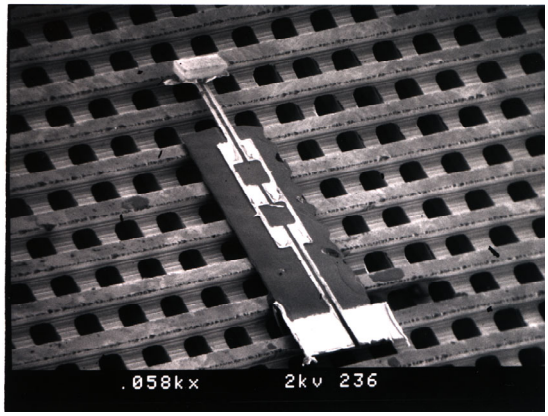

Figure 10a. An electron-microscope photograph of a 500 GHz dipole antenna on top of a "woodpile."

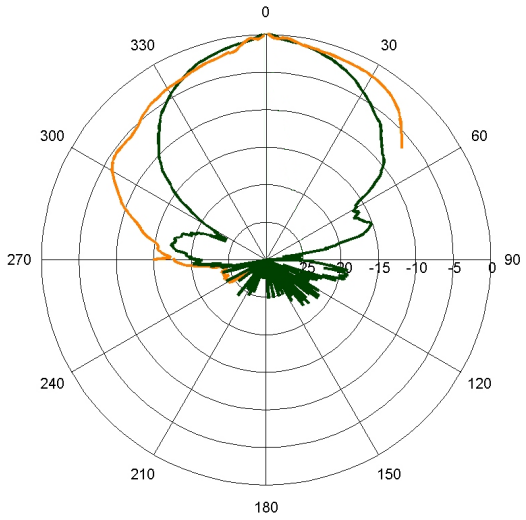

Figure 10b. The measured radiation pattern for the E and H planes for the antenna of Figure 10a (the black line is the E plane and the red line is the H plane).

modes. Since these do not contribute to the primary radiation pattern, substrate-mode coupling is generally considered to be a loss mechanism. The problem can be overcome by removing the possible existence of substrate modes by using an EBG substrate, providing an example of the application of EBG materials. The radiation pattern of an integrated antenna system at 500 GHz [23] is shown in Figure 10. The EBG crystal used was the so-called layer-by-layer or woodpile structure [55].

A significant technological push has been achieved in this domain by the StarTiger concept from the European Space Agency. A sub-millimeter-wave EBG mixer, with good performance at room temperature, and several EBG components have been realized ([56]; see Figure 11).

A quasi-optical EBG structure for spatial-filtering applications has been fabricated (using the DRIE process) to operate at 80 GHz, 140 GHz, and 350 GHz. The filter comprises two plates ([57]; see Figure 12), each having two monolithic orthogonal layers of rods and internal mounting lugs. The device is tuned by shifting the two plates laterally with respect to each other. A tuning range of 7 GHz was achieved by 240 μm of translation. The prototype devices were characterized using free-space measurements.

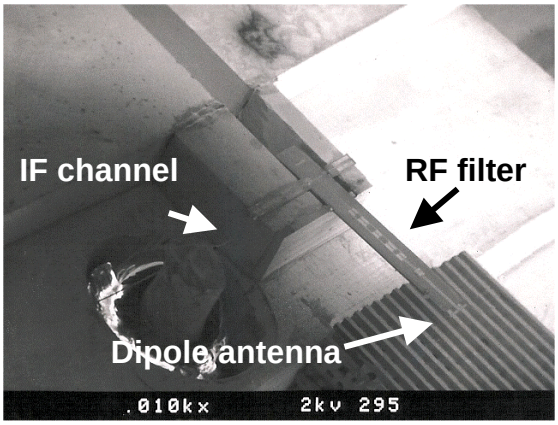

Figure 11a. An EBG heterodyne mixer at 250 GHz.

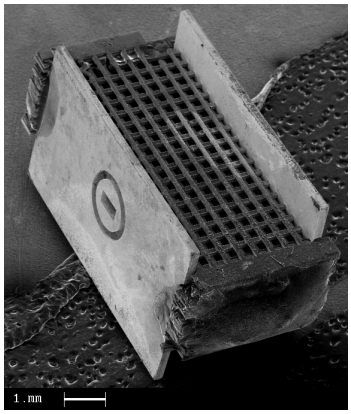

Figure 11b. A sub-millimeter-wave waveguide and the transition to a normal waveguide.

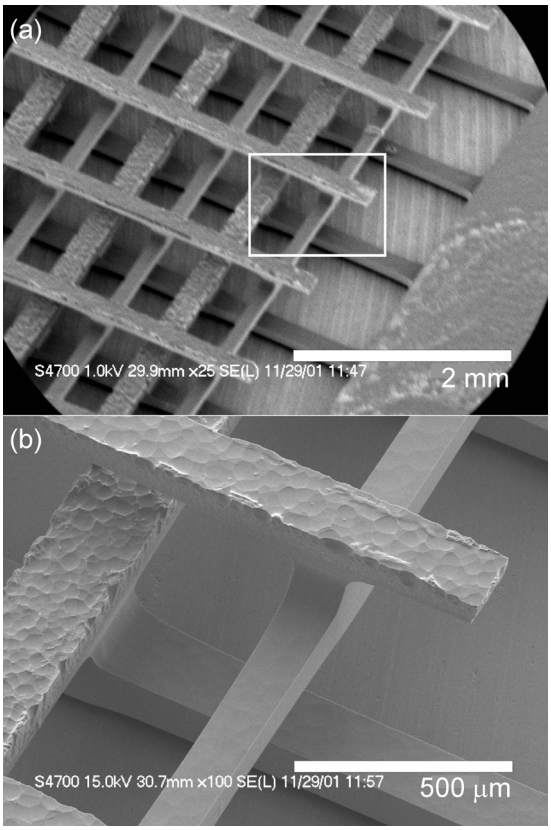

Figure 12. Scanning electron micrographs of (a) two plates interlocking and (b) a close-up of them. The micrographs were taken before the plates were coated with gold. The two rough surfaces are the original unpolished wafer surface (reproduced with the kind permission of Tim Drysdale, University of Glasgow).

7. EBG Defects and Waveguiding

An ideal EBG crystal is constructed by the infinite repetition of identical structural units in space. Considerable effort in theoretical, experimental, and material fabrication

research has predicted and demonstrated many of the properties of these ideal crystals. Introducing some disorder by placing a "defect unit" within an otherwise-perfect EBG crystal can create localized transmission peaks within the forbidden bandgap of the structure. Some of the work was based on a single-mode air waveguide, created within a square lattice of dielectric pillars. Even bends, couplers, and add-drop multiplexers have been proposed in this technology [58, 59]. However, air-waveguiding solutions in two dimensions lack confinement in the third vertical direction. Furthermore, they require infinitely deep structures, which can be readily analyzed but are more challenging to fabricate. A more pragmatic solution would be based on a dielectric waveguide and uses the inverse geometry, i.e., air holes in a dielectric host. Conversely, dielectric-channel guidance does have the added benefit that guiding is maintained within the periodic plane by total internal reflection, which is not the case for guides made from air.

Recently, an alternative to the linear-defect waveguide has attracted considerable attention. This alternative makes use of a periodic chain of localized defects that have been either completely or partially in-filled. The introduction of several localized defects within coupling distance of each other opens up a mini-band of allowed transmission [22, 60]. Chains or cascades of localized defects form a mechanism for waveguiding commonly referred to as coupled-cavity waveguides: CCWs. Experimental verification of two-dimensional CCWs has been performed in the microwave regime. It has frequently been assumed that bends can be introduced into the waveguide's path by taking advantage of the crystal's inherent lattice symmetry without consequential bend-reflection loss. However, it can be shown theoretically that the mini-pass band created by coupled-cavity waveguide bends may reach 100% transmission only for a strict set of criteria [22].

Another interesting application of defects is terahertz local oscillator generation. It is well known that a defect mode within a electromagnetic bandgap is localized. This suggests that a high-Q and lossless cavity for an electromagnetic wave can be realized, and that it should be possible to make an efficient and compact oscillator. It has been shown that it is possible to generate THz radiation using a nonlinear ZnTe material as the defect material [61].

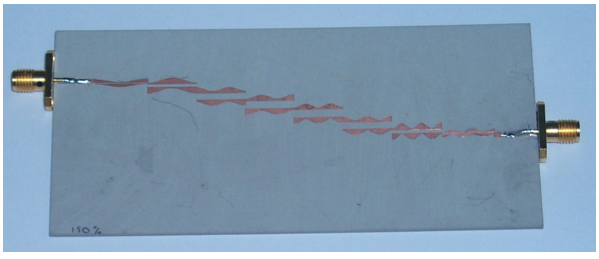

Figure 13a. A picture of a wiggly-line filter resulting from applying the strip-width perturbation to the classical coupled-line order-seven Butterworth bandpass microstrip filter centered at 2.5 GHz with a 10% fractional bandwidth (reproduced with the kind permission of Mario Sorolla).

8. EBG Resonators and Filters

Resonators based on two-dimensional EBG technology have been recently proposed as an alternative to current planar technologies [62-65]. Resonator structures can be fabricated on soft or organic substrates by using inexpensive standard printed-circuit board (PCB) processing techniques, and they can be readily incorporated in commercial products. The dimensions of the cavities can be reconfigured, as in [50-51], by switching the metallic posts on and off electrically or mechanically to achieve a different resonant frequency.

EBG resonators are commonly used to design different types of filters, i.e., two-, four-, or six-pole Tchebyshev filters [62]. In general, EBG technology allows the production of high-Q filters [62, 63] with high isolation [64] and low insertion losses [64, 65] relative to what could be obtained in other planar architectures. Furthermore, EBG resonator fabrication makes these filters amenable to planar circuit integration. The use of high-k ceramics (mainly, TiO_2) to fabricate this EBG resonator has led to Q factors above 1000, without suffering surface-wave losses due to the nature of the EBG technology [64, 65].

The use of EBG circuits for filter applications ([66-70]) in planar microwave technology has been proposed in different ways. One approach is by means of a honeycomb-lattice of holes drilled in a microstrip substrate in order to achieve harmonic tuning in power amplifiers, but the rejection level and bandwidth obtained were modest. To overcome the last problem, it has been proposed to realize the EBG by etching a two-dimensional structure of holes in the ground plane of the microstrip circuit [66].

Another way to produce compact designs is the "uni-planar compact EBG structure," where the slow-wave effect produced by a distributed two-dimensional LC structure allows a considerable size reduction in the circuit. A spurious-free bandpass filter and a high-performance low pass filter were obtained by using a coupled microstrip line in a slow-wave substrate [67].

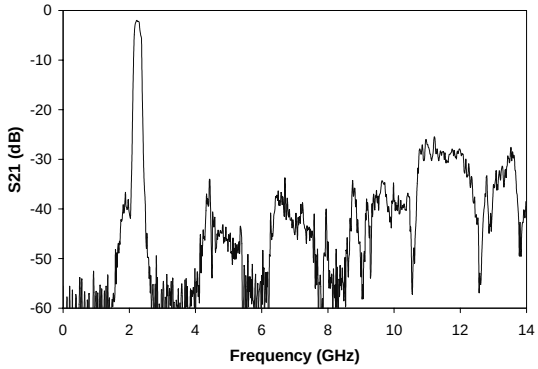

Figure 13b. The measured S_{21} parameter for the wiggly-line filter of Figure 13a (reproduced with the kind permission of Mario Sorolla).

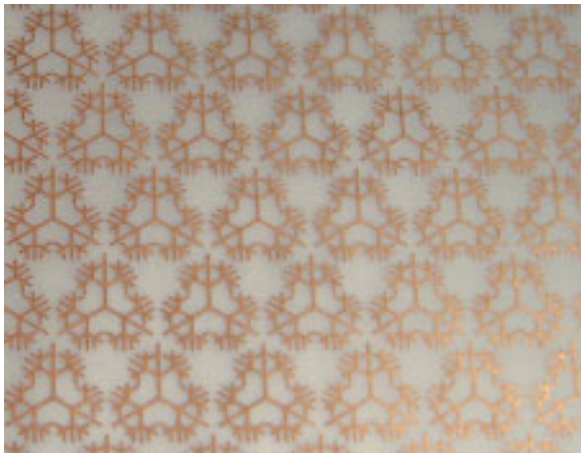

Figure 14. (a) A fractal-type tripole array.

Figure 14. (b) An interdigital tripole array.

The last approach consists of producing the EBG structure in the upper strip of the microstrip line, to solve the fabrication problem of the defected ground-plane structures. Even spurious-free bandpass filters are possible, maintaining the desired band response by using a continuous periodic-strip modulation of the coupled lines' width ([68]; see Figure 13).

9. Miniaturization

Miniaturization of microwave components and antennas has become increasingly important in recent years. Modern wireless communication systems require small microwave elements that are pertinent to high-level integration into compact lightweight systems. Miniaturization can be achieved by reducing the resonant frequency of a dipole element while maintaining its length (unit-cell dimensions), i.e., by fitting a longer effective electrical length in a fixed physical space [71, 72, 73]. It is well known that at certain frequencies outside the bandgap, periodic structures support waves – commonly termed slow waves – with phase velocity and guided wavelength significantly reduced with respect to those of a wave propagating in a comparable homogeneous medium. This property can be exploited for the miniaturization of microwave elements such as tripole array elements [74]. An approach to this is to examine elements with periodic

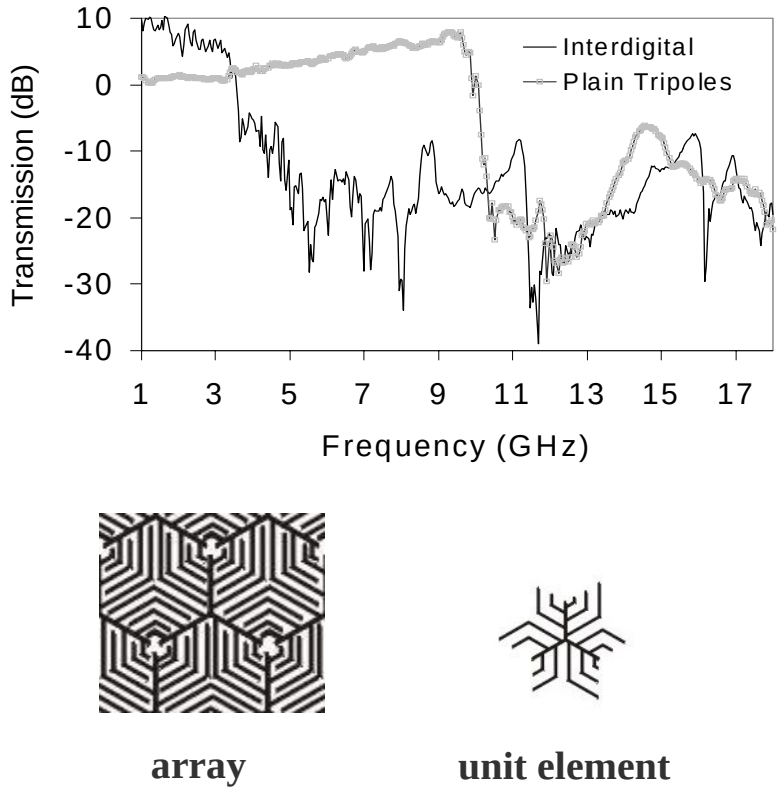

Figure 15. The measured transmission response of the interdigital tripole array. Schematic drawings of the array and its unit element are shown

loading. Multiple-order periodic loading of basic elements possesses a good degree of flexibility in the design [74, 75]. Fractal-type structures are subsequently produced using second-order loading (Figure 14a). This can also be used for multi-band artificial magnetic conductor designs (see Section 4, [44]). Another way of increasing the length of the loading stubs without increasing the unit cell and, at the same time, increasing the capacitive coupling between successive elements is the interdigital topology. This topology is shown in Figure 14b. The loadings of successive dipoles are shifted so that they can extend to the full length allowed by the array geometry. Figure 15 shows the transmission coefficient for dipoles loaded with eight stubs, each 8.5 mm long end-to-end. Measured results were in good agreement with theory for these configurations. The interdigital topology allows for maximum loading length, leading to further reduction of the bandgap frequency. Furthermore, the increased coupling between successive elements increases the fractional bandwidth of the bandgap.

10. Conclusion

Currently, there is a need for wide, multi-band device functionality, and for multifunctional devices. As long as the market generates a technology pull, the development of novel components and subsystems will always be in demand. Ideally, these components and subsystems will be required to be dynamic, reconfigurable, and multifunctional.

The technological potential of electromagnetic crystals for developing such novel components and subsystems offers a very promising alternative, which could potentially overcome the limitations of current technology. EBG technology is a breakthrough, mainly due to its ability to guide and efficiently control electromagnetic waves. We will need to identify component feature(s) of electromagnetic-bandgap structures that give added value over and above current approaches in order to drive this technology towards the marketplace. This paper has presented several applications where EBG technology could play a major role. Several antenna, waveguide, and filter configurations have been discussed. It was also shown that tunable EBG devices can be made. As long as primary EBG components emerge with functional efficiency, the realization of a complete system will become a distinct possibility.

11. Acknowledgements

The authors wish to thank all the people that contributed to this paper: in particular, Inigo Ederra and Mario Sorrolla from Universidad Publica de Navarra; Gerard Tayeb from Institut Fresnel; Bernard Jecko from IRCOM; Jung-Chih Chiao from the University of Texas-Arlington; Yang Hao and Clive Parini from Queen Mary University; Pekka Salonen from Tampere University of Technology; Richard Ziolkowski from the University of Arizona; William McKinzie from Etenna; Andrew Reynolds from Nortel Networks; and R. Lee, R. Seager, Alex Feresidis, George Gousetis, and Alford Charaya from Loughborough University.

This paper includes portions of P. de Maagt, R. Gonzalo, Y. C. Vardaxoglou, and J.-M. Baracco, "Electromagnetic Bandgap Antennas and Components for Microwave and (Sub)millimeter Wave Applications," *IEEE Transactions on Antennas and Propagation*, **AP-51**, 10, October 2003, pp. 2667-2677. Those portions are copyright 2003 by the Institute of Electrical and Electronics Engineers, and are used with permission.

12. References

1. E. Yablonovitch, "Inhibited Spontaneous Emission in Solid State Physics and Electronics," *Physical Review Letters*, **58**, 1987, pp. 2059-2062.

2. A. A. Oliner, "Periodic Structures and Photonic Band-Gap Terminology: Historical Perspectives," *Proceedings of the 29th European Microwave Conference*, **3**, Munich, Germany, October 1999, pp. 295-298.

3. J. Arriaga, A. J. Ward, and J. B. Pendry, "Order-N Photonic Band Structures for Metals and Other Dispersive Materials," *Physical Review*, **B59**, 1999, pp. 1874-1877.

4. Gyeong-il Kweon and N. M. Lawandy. "Quantum Electrodynamics in Photonic Crystals," *Optics Communications*, 15 July 1995, pp. 388-411.

5. H. S. Sozuer and J. W. Haus, "Photonic Bands: Convergence Problems with the Plane-Wave Method," *Physical Review B*, **45**, 24, 15 June, 1992, pp. 13962-13972.

6. N. Stefanou, V. Karathanos, and A. Modinos, "Scattering of Electromagnetic Waves by Periodic Structures," *J. Phys. Condens. Matter*, **4**, 1992, pp. 7389-7400.

7. P. M. Bell, J. B. Pendry, L. Martin Moreno, and A. J. Ward, "A Program for Calculating Photonic Band Structures and Transmission Coefficients of Complex Structures," *Comp. Phys. Commun.*, **85**, 1995, pp. 307-322.

8. Fan Yang and Y. Rahmat-Samii, "Microstrip Antennas Integrated with Electromagnetic Band-Gap (EBG) Structures: A Low Mutual Coupling Design For Array Applications," *IEEE Transactions on Antennas and Propagation*, **AP-51**, October 2003, pp. 2936-2946.

9. N. Farahat and R. Mittra, "Analysis of Frequency Selective Surfaces Using the Finite Difference Time Domain (FDTD) Method," IEEE International Symposium on Antennas and Propagation *Digest*, **2**, 16-21 June 2002, pp. 568-571.

10. H. Mosallaei and Y. Rahmat-Samii, "Grand Challenges in Analyzing EM Band-Gap Structures: An FDTD/Prony Technique Based on the Split-Field Approach," IEEE International Symposium on Antennas and Propagation *Digest*, **2**, 8-13 July 2001, pp. 47-50.

11. J. A. Roden, S. D. Gedney, M. P. Kesler, J. G. Maloney, and P. H. Harms, "Time-Domain Analysis of Periodic Structures at Oblique Incidence: Orthogonal and Nonorthogonal FDTD

Implementations," *IEEE Transactions on Microwave Theory and Techniques*, **MTT-46**, April 1998, pp. 420-427.

12. S. Sudhakaran, Y. Hao, and C. G. Parini, "An Enhanced Prediction of Negative Refraction from EBG-Like Structures," to appear in *Microwave and Optical Technology Letters*, May 20, 2004.

13. A. L. Reynolds and J. M. Arnold, "Interleaving Two-Dimensional Lattices to Create Three-Dimensional Photonic Bandgap Structures," *IEE Proceedings on Optoelectronics*, **145**, December 1998, pp. 436-440.

14. R. Gonzalo, P. de Maagt, and M. Sorolla, "Enhanced Patch Antenna Performance by Suppressing Surface Waves Using Photonic Band-Gap Structures," *IEEE Transactions on Microwave Theory and Techniques*, **MTT-47**, 11, November 1999, pp. 2131-2138.

15. P. K. Kelly, L. Diaz, M. Piket-May, and L. Rumsey, "Scan Blindness Mitigation Using Photonic Bandgap Structure in Phased Arrays," *Proc. SPIE*, **3464**, July 1998, pp. 239-248.

16. R. Hurtado, W. Klimczak, W. E. McKinzie, and A. Humen, "Artificial Magnetic Conductor Technology Reduces Weight and Size for Precision GPS Antennas," Navigational National Technical Meeting, San Diego, CA, January 28-30, 2002.

17. R. Remski, "Modeling Photonic Bandgap (PBG) Structures Using Ansoft HFSS7 and Optimetrics," Ansoft International Roadshow (lecture series), August-October 2000, slides 36-40.

18. R. F. Jimenez Broas, D. F. Sievenpiper, and E. Yablonovitch, "A High-Impedance Ground Plane Applied to Cellphone Handset Geometry," *IEEE Transactions on Microwave Theory and Techniques*, **MTT-49**, 7, July 2002, pp. 1262-1265.

19. P. Salonen, M. Keskilammi, and L. Sydanheimo, "A Low-Cost 2.45 GHz Photonic Band-Gap Patch Antenna for Wearable Systems," *Proceedings of the 11th International Conference on Antennas and Propagation, ICAP 2001*, 17-20 April 2001, Manchester, UK, pp. 719-724.

20. T. Lopetegi, M. A. G. Laso, R. Gonzalo, M. J. Erro, F. Falcone, D. Benito, M. J. Garde, P. de Maagt, and M. Sorolla, "Electromagnetic Crystals in Microstrip Technology," *Optical and Quantum Electronics*, **34**, 1/3, January/March 2002, pp. 279-295.

21. F.-R. Yang, K.-P. Ma, Y. Qian, and T. Itoh, "A Novel TEM Waveguide Using Uniplanar Compact Photonic-Bandgap (UC-PBG) Structure," *IEEE Transactions on Microwave Theory and Techniques*, **MTT-47**, 11, November 1999, pp. 2092-2098.

22. U. Peschel, A. Reynolds, B. Arredondo, F. Lederer, P. Roberts, T. Krauss, and P. de Maagt, "Transmission and Reflection Analysis of Functional Coupled Cavity Components," *IEEE Journal of Quantum Electronics*, **38**, 7, June 2002, pp. 830-837.

23. R. Gonzalo, I. Ederra, C. Mann, and P. de Maagt, "Radiation Properties of Terahertz Dipole Antenna Mounted on Photonic Crystal," *Electronics Letters*, **37**, 10, 10 May 2001, pp. 613-614.

24. M. M. Sigalas, R. Biswas, Q. Li, D. Crounch, W. Lleung, R. Jacobs-Woodbury, B. Lough, S. Nielsen, S. McCalmont, G. Tuttle, and K. M. Ho, "Dipole Antennas on Photonic Band-Gap Crystals – Experiment and Simulation," *Microwave and Optical Technology Letters*, **15**, 3, June 20, 1997, pp. 153-158.

25. I. Ederra, J. J. Sanz, B. Martinez, R. Gonzalo, and P. de Maagt, "Slot Antenna Configuration Using PBG Technology," *Proceedings JINA, Volume 2*, 12-14 November, 2002, Nice, France, pp. 169-172.

26. K. Agi, J. Malloy, E. Schamiloglu, M. Mojahedi, and E. Niver, "Integration of Microstrip Patch Antenna with a Two-dimensional Photonic Crystal Substrate," *Electromagnetics*, **19**, 3, May-June 1999, pp. 277-290.

27. J. S. Colburn and Y. Rahmat-Samii, "Patch Antennas on Externally Perforated High Dielectric Constant Substrates," *IEEE Transactions on Antennas and Propagation*, **AP-47**, 12, December 1999, pp. 1785-1794.

28. R. Coccioli, F. Yang, K. Ma, and T. Itoh, "Aperture-Coupled Patch Antenna on UC-PBG Substrate," *IEEE Transactions on Microwave Theory and Techniques*, **MTT-47**, 11, November 1999, pp. 2123-2130.

29. A. S. Andrenko, Y. Ikeda, and O. Ishida, "Application of PBG Microstrip Circuits for Enhancing the Performance of High-Density Substrate Patch Antennas," *Microwave and Optical Technology Letters*, **32**, 5, March 2002, pp. 340-344.

30. E. R. Brown, C. D. Parker, and E. Yablonovith, "Radiation Properties of a Planar Antenna on a Photonic-Crystal Substrate," *Journal of the Optical Society of America B*, **10**, 2, February 1993, pp. 404-407.

31. T. H. Liu, W. X. Zhang, and M. Zhang, "A Spiral Antenna Backed on Photonic Bandgap Material," *Proceedings of the International Symposium on Antennas and Propagation*, 21-25 August, Fukuoka, Japan.

32. J. M. Baracco and P. de Maagt, "Radiating Element on a Photonic Bandgap Structure for Phased Array Applications," *Proceedings JINA Volume 2*, 12-14 November, 2002, Nice, France, pp. 169-172.

33. F. Yang and Y. Rahmat-Samii, "A Low Profile Circularly Polarized Curl Antenna Over an Electromagnetic Bandgap (EBG) Surface," *Microwave and Optical Technology Letters*, **31**, 4, 2001, pp. 264-267.

34. M. Thevenot, C. Cheype, A. Reineix, and B. Jecko, "Directive Photonic-Bandgap Antennas," *IEEE Transactions on Microwave Theory and Techniques*, **MTT-47**, 11, November 1999, pp. 2115-2122.

35. C. Cheype, C. Serier, M. Thevenot, T. Monediere, A. Reineix, and B. Jecko, "An Electromagnetic Bandgap Resonator Antenna," *IEEE Transactions on Antennas and Propagation*, **AP-50**, 9, September 2002, pp. 1285-1290.

36. B. Temelkuran, E. Ozbay, J-P. Kavanaugh, G. Tuttle, and K-M. Ho, "Resonant Cavity Enhanced Detectors Embedded in Photonic Crystals," *Applied Physics Letters*, **72**, 19, May 11, 1998, pp. 2376-2378.

37. M. Thevenot, A. Reineix, and B. Jecko, "A Dielectric Photonic Parabolic Reflector," *Microwave and Optical Technology Letters*, **21**, 6 June 20, 1999, pp. 411-414.

38. Min Qiu and Sailing He, "High-Directivity Patch Antenna with Both Photonic Bandgap Substrate and Photonic Cover," *Microwave and Optical Technology Letters*, **30**, 1 July, 2001, pp. 41-44.

39. R. Gonzalo, G. Nagore, I. Ederra, B. Martinez, H. Pellemans, P. Haring Bolivar, and P. de Maagt, "Coupling Between Patch Antennas on Photonic Crystals," *Proceedings 24th ESTEC Antenna Workshop on Innovative Periodic Antennas: Photonic Bandgap, Fractal and Frequency Selective Structures*, 30 May-1 June 2001, Noordwijk, The Netherlands, pp. 17-22.

40. S. Enoch, G. Tayeb, P. Sabouroux, N. Gurin, and P. Vincent, "A Metamaterial for Directive Emission," *Phys. Rev. Lett.*, **89**, 2002, p. 213902.

41. D. Sievenpiper, L. Zhang, R. F. J. Broas, N. G. Alexopolous, and E. Yablonovitch, "High-Impedance Electromagnetic Surfaces with a Forbidden Frequency Band," *IEEE Transactions on Microwave Theory and Techniques*, **MTT-47**, 11, November 1999, pp. 2059-2075.

42. Y. R. Lee, A. Chauraya, D. S. Lockyer, and J. C. Vardaxoglou, "Dipole and Tripole Metallodielectric Photonic Bandgap (MPBG) Structures for Microwave Filter and Antenna Applications," *IEE Proc. Optoelectron.*, **127**, 6, December 2000, pp. 395-400.

43. F. Yang and Y. Rahmat-Samii, "Reflection Phase Characterizations of the EBG Ground Plane for Low Profile Wire Antenna Applications," *IEEE Transactions on Antennas and Propagation*, **AP-51**, 10, October 2003, pp. 2691-2703.

44. A. P. Feresidis, A. Chauraya, G. Goussetis, J. C. Vardaxoglou, and P. de Maagt, "Multiband Artificial Magnetic Conductor Surfaces," *Proceedings IEE Seminar on Metamaterials for Microwave and (Sub)Millimetre Wave Applications*, 24 November 2003, London, UK, pp. 2/1-2/4.

45. C. R. Simovski, P. de Maagt, S. A. Tretyakov, M. Paquay, and A. A. Sochava, "Angular Stabilization of the Resonant Frequency of Artificial Magnetic Conductors for TE-Incidence," accepted for publication in *Electronics Letters*.

46. A. Monorchio, G. Manara, and L. Lanuzza, "Synthesis of Artificial Magnetic Conductors by Using Multilayered Frequency Selective Surfaces," *IEEE Antennas and Wireless Propagation Letters*, **1**, 2002, pp. 196-199.

47. S. A. Tretyakov and S. I. Maslovski, "Thin Absorbing Structure for All Incidence Angles Based on the Use of High-Impedance Surfaces," *Microwave and Optical Technology Letters*, **38**, 3, August 5 2003, pp. 175-178.

48. Y. Hao and C. Parini, "Isolation Enhancement of PBG Microstrip Diplexer Patch Antenna," *Proceedings 11th International Conference on Antennas and Propagation ICAP 2001*, 17-20 April 2001, Manchester, UK, pp. 86-89.

49. J. C. Vardaxoglou, D. S. Lockyer, Y. L. R. Lee, and A. Chauraya, "Photonic Bandgap and Bandpass Characteristics from Metallodielectric Periodic Array Structures," *Proceedings 24th ESTEC Antenna Workshop on Innovative Periodic Antennas: Photonic Bandgap, Fractal and Frequency Selective Structures*, 30 May-1 June 2001, Noordwijk, The Netherlands, pp. 213-217.

50. J. C. Vardaxoglou, A. Chauraya, A. P. Feresidis, and P. de Maagt, "Tunable Metallodielectric Electromagnetic Band Gap (MEBG) Structures with Defects," *Proceedings of International Conference on Electromagnetics in Advanced Applications (ICEAA)*, Torino, Italy, September 2003, pp. 667-670.

51. M. J. Hill, R. W. Ziolkowski, and J. Papapolymerou, "A High-Reconfigurable Planar EBG Cavity Resonator," IEEE Microwave and Wireless Components Letters, 11, 6, June 2001, pp. 255-257.

52. B. Elamaran, I-M Chio, L-Y Chen, and H-C Chiao, "A Beam-Steerer Using a Reconfigurable PBG Ground Plane," IEEE International Microwave Symposium, 11-16 June 2000, Boston, Massachusetts, USA.

53. L. Mercier, M. Thevenot, P. Blonby, and B. Jecko, "Design and Characterization of a Smart Periodic Material Including MEMS," *Proceedings 27th ESA Antenna Technology Workshop on Innovative Periodic Antennas: Electromagnetic Bandgap, Left-Handed Materials, Fractal and Frequency Selective Surfaces*, 9-11 March 2004, Santiago de Compostela, Spain.

54. A. Delustrac, F. Gadot, E. Akmansoy, and T. Brillat, "High-Directivity Planar Antenna Using Controllable Photonic Bandgap Material at Microwave Frequencies," *Applied Physics Letters*, **78**, 2002, p. 4196.

55. R. Gonzalo, B. Martinez, C. Mann, H. Pellemans, P. Haring Bolivar, and P. de Maagt, "A Low Cost Fabrication Technique for Symmetrical and Asymmetrical Layer-by-Layer Photonic Crystals at Sub-Millimeter Wave Frequencies," *IEEE Transactions on Microwave Theory and Techniques*, **MTT-50**, 10, October 2002, pp. 2384-2392.

56. I. Ederra, F. van de Water, A. Laisne, C. M. Mann, P. de Maagt, G. McBride, D. Castiglione, A. McCalden, L. Deias, J. P. O'Neill, J. Teniente Vallinas, D. Haskett, D. Jenkins, A. Zinn, M. Ferlet, and R. Edeson, "EBG Millimetre-Wave Components Design," *3rd ESA Workshop on Millimetre Wave Technology and Applications: Circuits, Systems, and Measurement Techniques*, Espoo, Finland, May 21-23, 2003.

57. T. Drysdale, R. Blaikie, and D. Cumming, "Calculated and Measured Transmittance of a Tunable Metallic Photonic Crystal Filter for Terahertz Frequencies, *Applied Physics Letters*, **83**, 26, 29 December 2003, pp. 5362-5364.

58. S. Fan, P. R. Villeneuve, J. D. Joannopoulos, and H. A. Hauss, "Channel Drop Filters in Photonic Crystals," *Optics Express*, **3**, 1, April 1998, pp. 4-11.

59. A. Mekis, J. C. Chen, I. Kurland, S. Fan, P. R. Villeneuve, and J. D. Joannopoulos, "High Transmission Through Sharp Bends in Photonic Crystal Waveguides," *Physics Review Letters*, **77**, 18, October 1996, pp. 3787-3790.

60. A. Reynolds, U. Peschel, F. Lederer, P. Roberts, T. Kraus, and P. de Maagt, "Coupled Defects in Photonic Crystals," *IEEE Transactions on Microwave Theory and Techniques*, **MTT-49**, 10, October 2001, pp. 1860-1867.

61. M. Tani, P. Gu, K. Sakai, H. Kitahara, M. Suenaga, and M. W. Takeda, "THz Wave Generation by Difference Frequency Mixing in Photonic Crystal Cavity," *Proceedings 8th International Conference on Terahertz Electronics*, 28-29 September 2000, Darmstadt, Germany, pp. 301-304.

62. T. Euler and J. Papapolymerou, "Silicon Micromachined EBG Resonator and Two-Pole Filter with Improved Performance Characteristics" *IEEE Microwave and Wireless Components Letters*, **13**, 9, September 2003, pp. 373-375.

63. Hsiuan-ju Hsu, M. J. Hill, R. W. Ziolkowski, and J. Papapolymerou, "A Duroid-Based Planar EBG Cavity Resonator Filter with Improved Quality Factor," *IEEE Antennas and Wireless Propagation Letters*, **1**, 2002, pp. 67-70.

64. William J. Chappell, Matthew P. Little, and Linda P. B. Katehi, "High Isolation Planar Filters Using EBG Substrates," *IEEE Microwave and Wireless Components Letters*, **11**, 6, June 2001, pp. 246-248.

65. W. J. Chappell and Xun Gong, "Wide Bandgap Composite EBG Substrates," *IEEE Transactions on Antennas and Propagation*, **AP-51**, 10, October 2003.

66. V. Radisic, Y. Qian, R. Coccioli, and T. Itoh, "Novel 2-D Photonic Bandgap Structure for Microstrip Lines," *IEEE Microwave and Guided Wave Letters*, **8**, February 1998, pp. 69-71.

67. F. R. Yang, K. P. Ma, Y. Qian, and T. Itoh, "A Uniplanar Compact Photonic Bandgap (UC-PBG) Structure and Its Applications for Microwave Circuits," *IEEE Transactions on Microwave Theory and Techniques*, **MTT-47**, August 1999, pp. 1509-1514.

68. T. Lopetegi, M. A. G. Laso, J. Hernandez, M. Bacaicoa, D. Benito, M. J. Garde, M. Sorolla, and M. Guglielmi, "New Microstrip 'Wiggly-Line' Filters with Spurious Passband Suppression," *IEEE Transactions on Microwave Theory and Techniques*, **MTT-49**, 9, September 2001, pp. 1593-1598.

69. D. Nesic, "A New Type of Slow-Wave 1-D PBG Microstrip Structure Without Etching in the Ground Plane for Filter and Other Applications," *Microwave and Optical Technology Letters*, **33**, 6, June 20 2002, pp. 440-443.

70. D. Nesic, "A New Type of Slow-Wave 1-D PBG Microstrip Band-Pass Filter," *Microwave and Optical Technology Letters*, **37**, 3, May 5 2003, pp. 201-203.

71. S. Rogers, W. McKinzie, and G. Mendolia, "AMCs Comprised of Interdigital Capacitor FSS Layers Enable Lower Cost Applications," IEEE International Symposium on Antennas and Propagation, Columbus, OH, June 21-27, 2003.

72. S. Tse, B. Sanz Izquierdo, J. C. Batchelor, and R. J. Langley, "Reduced Sized Cells for Electromagnetic Bandgap Structures," *Electronics Letters*, **39**, 24, 27 November 2003.

73. A. P. Feresidis, G. Apostolopoulos, N. Serfas, and J. C. Vardaxoglou, "Closely Coupled Metallodielectric Electromagnetic Band Gap (CCMEBG) Structures Formed by Double Layer Dipole and Tripole Arrays," accepted for publication in *IEEE Transactions on Antennas and Propagation*.

74. A. P. Feresidis, G. Apostolopoulos and J. C. Vardaxoglou, "Miniaturised Metallodielectric EBG Structures," *Proceedings of the International Conference on Electromagnetics in Advanced Applications (ICEAA)*, Torino, Italy, September 2003, pp. 671-674.

75. G. Goussetis, A. P. Feresidis, and J. C. Vardaxoglou, "Performance of Metallodielectric EBG Structures with Periodic Loaded Elements," *Proceedings of the IEE Seminar on Metamaterials for Microwave and (Sub)Millimetre Wave Applications*, 24 Nov. 2003, London, UK, pp. 7/1-7/5.

Techniques for the Compensation for Chromatic-Dispersion Effects in Fiber-Wireless Systems

D. Hervé, J.L. Corral
J.M. Fuster, J. Herrera,
A. Martinez, V. Polo
F. Ramos, E. Vourc'h
J. Marti

1. Introduction

Fibre-wireless systems have been extensively studied over the past years with a view towards the development of broadband-access solutions [1-3]. In such networks, base stations can be made simple and compact when the radio-frequency (RF) signals are generated in the central stations, but severe constraints are thus imposed on the fiber links. One of the major problems encountered is the dispersion-induced RF power fading, which is also known as the carrier-suppression effect [4]. When using conventional intensity modulation of an optical source (Figure 1), the resulting signal consists of an optical carrier and two sidebands. The three spectral components of such an optical double-sideband (ODSB) signal experience different propagation speeds in the fiber. As the photo-detected RF signal results from the combination of the beating of each sideband with the optical carrier, destructive interference may cause cancellation of the power, P_{RF} :

$$P_{RF} \propto \cos^2\left(\frac{\pi L D \lambda^2 f_m^2}{c}\right), \qquad (1)$$

where D (ps/(nm km)) is the dispersion parameter, L is the fiber length, f_m is the RF carrier frequency, λ is the optical carrier wavelength, and c is the speed of light in a vacuum.

From the mid-1990s, various techniques – such as the use of chirped fiber-Bragg gratings (FBG) [5, 6] – have been proposed in order to compensate for, or to mitigate, this transmission penalty. It is also possible to take advantage of the optical single-sideband (OSSB) format, the chirp effect in optical modulators, or optical phase conjugation (OPC). This paper reviews most of these techniques involving schemes based on external optical modulators, optical filtering, and nonlinear effects.

2. Single-Sideband Transmission Schemes

The generation of an optical single-sideband signal with carrier (OSSB+C) – instead of the conventional optical double-sideband signal – eliminates the power-fading phenomenon, since the detected RF power results from only one beat signal. Eliminating one of the two sidebands

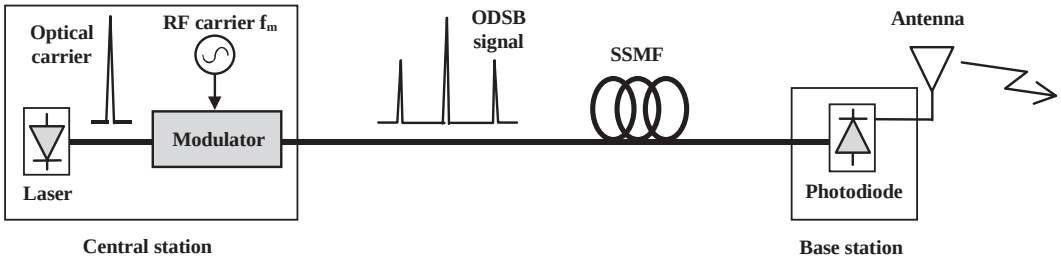

Figure 1. A fiber-radio link implementing conventional intensity-modulation and direct photo detection. Such a transmission scheme may be confronted with severe penalties due to the chromatic-dispersion effect undergone by the optical double-sideband (ODSB) signal in the standard single-mode fiber.

D. Hervé and E. Vourc'h are with the Laboratoire d'Electronique et des Systèmes de Télécommunications, UMR CNRS 6165, GET / ENST Bretagne, Technopôle Brest-Iroise, CS83818, 29238 BREST Cedex 3, France; E-mail: didier.herve@enst-bretagne.fr.
J. L. Corral, J. M. Fuster, J. Herrera, A. Martínez, V. Polo, F. Ramos, and J. Martí are with the Fibre-Radio Group, Nanophotonics Technology Centre, Universidad Politécnica de Valencia, Campus del Camino de Vera, s/n 46022 Valencia, Spain; E-mail: vpolor@upvnet.upv.es.

Editors Note: This is one of the invited *Reviews of Radio Science*, from Commission D.

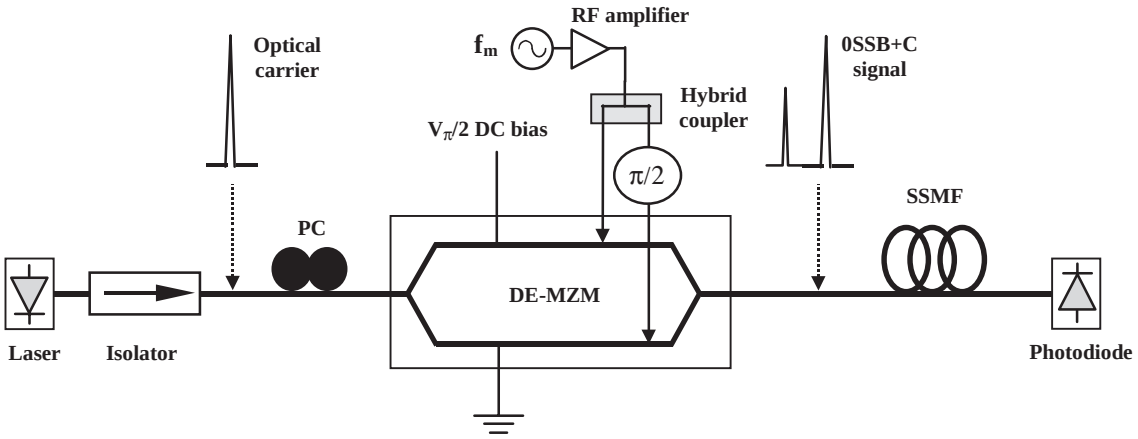

Figure 2. The experimental setup of the optical single-sideband-with-carrier (OSSB+C) source, based on a dual-electrode Mach-Zehnder modulator (DE-MZM).

of the optical spectrum can be obtained by optical filtering [7-10], or by implementing the Hilbert transform in the optical domain. Several schemes involve a dual-electrode Mach-Zehnder modulator (DE-MZM) [11], two electro-absorption modulators (EAM) in tandem configurations [12], or two cascaded phase modulators and intensity modulators [13]. Other proposed arrangements consist in incorporating a dual-electrode Mach-Zehnder modulator within a Sagnac interferometer [14, 15], implementing optical SSB modulation with suppressed carrier (OSSB+SC). Unlike other dispersion-compensation principles, the optical single-sideband signal with carrier format is independent of the fiber length and of its dispersion parameter.

In this section, four types of optical single-sideband techniques are described, showing the experimental setups that include either special external modulation arrangements or optical filtering.

2.1 OSSB+C Source Based on a Dual-Electrode Mach-Zehnder Modulator

In the source proposed by Smith et al. [11], a distributed-feedback (DFB) laser feeds a dual-electrode Mach-Zehnder modulator, biased at half its V_π switching voltage, which is also known as the quadrature-bias (QB) point. The RF signal is first divided into two parts, one of which is phase shifted by 90°, and applied to the electrodes (Figure 2). This work has shown a 1.5 dB maximum RF power degradation as a function of the applied RF signal in the 0-20 GHz range after optical single-sideband signal with carrier transmission through 79.6 km of standard single-mode fiber (SSMF). In addition, Smith et al. validated their technique by a dispersion-compensated broadband millimeter-wave (38 GHz) fiber-wireless transmission system [16]. Using this technique, the carrier suppression effect is completely overcome, but non-linear effects must be carefully considered [17].

A modification of the arrangement shown in Figure 2 has been recently proposed [18] that makes it possible to transmit the same information simultaneously at baseband or intermediate frequency (IF) and modulated onto an RF carrier, for instance at 40 GHz [19]. This scheme is dispersion tolerant and it has a remote local oscillator (LO) signal, thus alleviating the hardware requirements at the base station [22].

2.2 Integrated Lightwave Millimetric OSSB+C Source

Vergnol et al. proposed an indium phosphide (InP) integrated alternative [12] to the previous hybrid optical single-sideband signal with carrier source using a dual-electrode Mach-Zehnder modulator. It is to be noted that the integrated configuration is different from the hybrid configuration, since it comprises a distributed-feedback laser, two 40 GHz bandwidth electro-absorption modulators, a semiconductor optical amplifier (SOA), and two multimode interferometer (MMI) couplers (Figure 3). The laser provides an optical carrier that is divided into two signals of equal amplitudes, but optically phase shifted $\pi/2$ by means of a two-by-two multimode-interferometer coupler. Each output arm of the coupler feeds a high-speed electro-absorption modulator (EAM). These modulators are driven by electrical signals that originate from the same RF source, but are phase shifted by $\pi/2$. Finally, a two-by-one multimode-interferometer coupler combines the two modulated optical signals, giving an optical single sideband with carrier signal. Experimental validation of this device has shown fading-free transmission of a 38 GHz RF signal through a 50 km standard single-mode fiber link. The ripple of the photo-detected power level along the fiber proved to be as low as 2 dB. Compared with a hybrid source, the main advantage of the InP integrated device is its compactness.

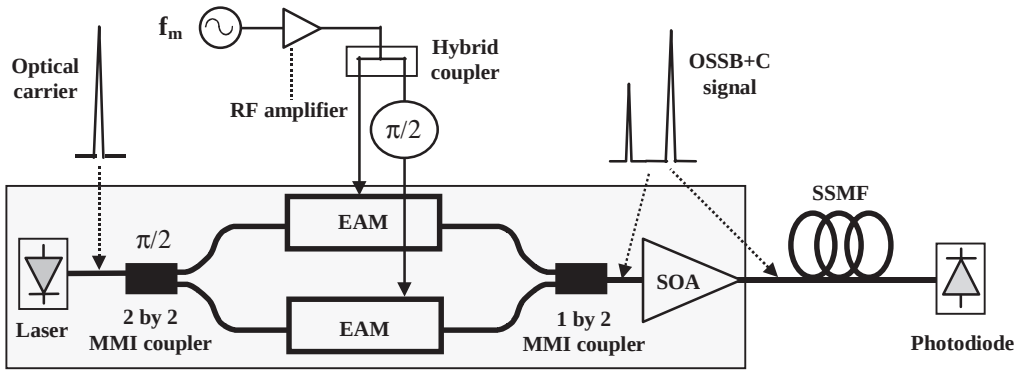

Figure 3. The experimental setup of the integrated optical single-sideband-with-carrier (OSSB+C) source

2.3 OSSB Signal Generation Implementing a Bragg Grating

The simplest way to generate an optical single sideband with carrier signal relies on the suppression of one of the sidebands of an optical double sideband signal by means of an optical filter. Such filtering was first applied to baseband digital transmission with a view toward compensating for chromatic dispersion in long-distance digital transmissions [7]. Then, Park et al. extended optical single sideband filtering to fiber-radio systems, and used a fiber Bragg grating in order to filter out one sideband of an optical double-sideband signal (Figure 4) [8]. The transmission of a 25 GHz RF signal over a 51 km-long standard single-mode fiber link was carried out, leading to no fading of the photo-detected power level. Although it is very easy to implement, this filtering technique is dependant on the wavelength of the optical carrier, and it requires a narrow-bandwidth optical filter.

2.4 Wavelength-Self-Tunable Single-Sideband (WST-SSB) Filter

Iron-doped indium phosphide (InP:Fe) is primarily known as a semi-insulating substrate, but it is also a photorefractive crystal in the infrared. In such a material – which is electro-optic – an illumination can generate free carriers that diffuse and may be trapped in the forbidden band, thanks to iron centers. Thus, interference induces a periodic charge distribution by using counter-propagating illumination in such a crystal. The periodic space-charge field thus obtained generates a periodic refractive-index variation via the electro-optic effect. Equation (2) gives the period, Λ, of such a dynamic Bragg grating. In addition, according to the Bragg diffraction condition and Snell's law, the signal wavelength, λ_s, that will be diffracted by the index grating under an angle of incidence θ satisfies Equation (3).

$$\Lambda = \frac{\lambda_p}{2n_m}, \tag{2}$$

$$\lambda_s = \lambda_p \sqrt{1-\left(\frac{\sin\theta}{n_m}\right)^2}. \tag{3}$$

In the above equations, λ_p is the wavelength of the pump beam that generates the grating, and n_m is the medium average refractive index, which equals 3.17 for InP:Fe.

In a wavelength-self-tunable single-sideband (WST-SSB) filter (Figure 5), the input optical double-sideband signal is divided into a pump beam and a signal beam by means of a 3 dB coupler. Thanks to the reflection of the pump beam off a mirror placed behind the InP:Fe crystal, interference due to each λ_i ($i = 1, 2, 3$) pump line generates a dynamic Bragg grating, G_i. In addition, suitable adjustment of θ according to Equation (3) enables λ_1 and λ_2 signal lines to be diffracted by G_1 and G_3, respectively [9]. Thus, the output signal of the device is an optical double

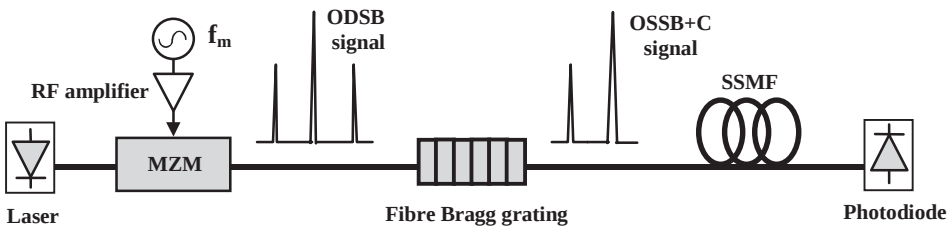

Figure 4. Optical single sideband with carrier (OSSB+C) generation implementing a fiber Bragg grating.

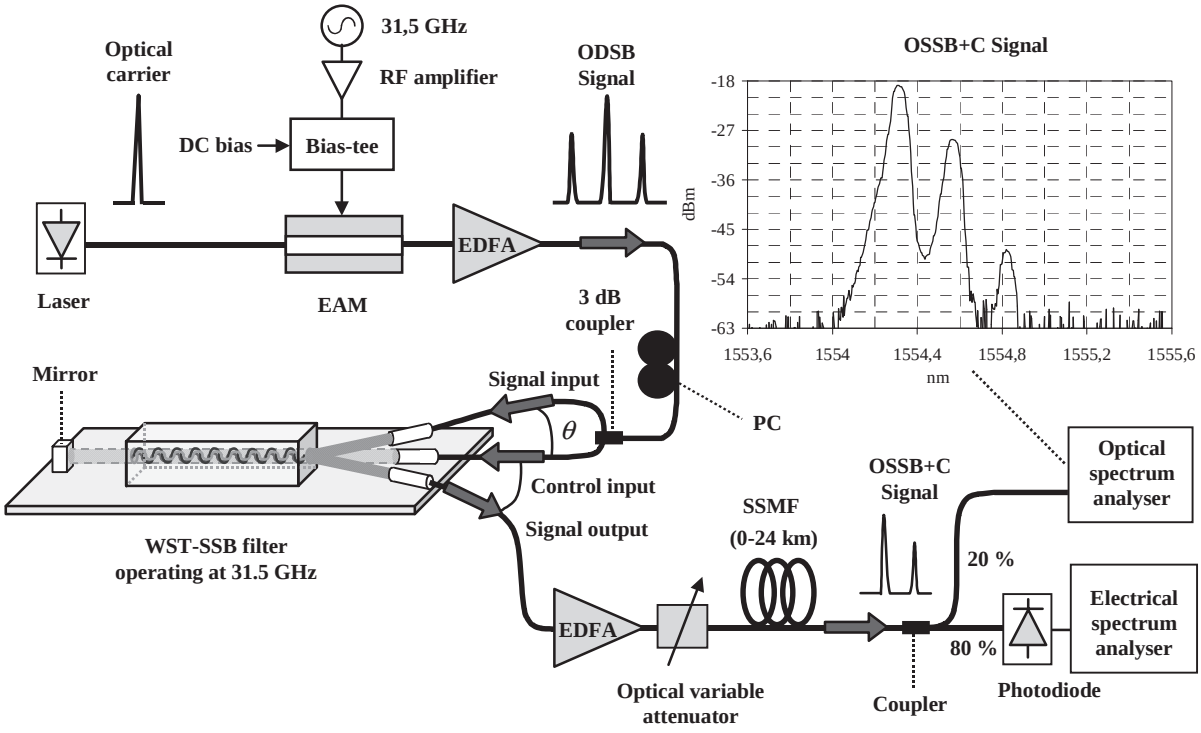

Figure 5. The experimental setup of the wavelength-self-tunable single-sideband (WST-SSB) filter and the measured output optical single sideband with carrier (OSSB+C) spectrum.

sideband with carrier (ODSB+C) signal, made up of a part of the lower sideband and carrier of the input optical double-sideband signal. Since the input signal itself generates the dynamic Bragg gratings that are responsible for its own optical single sideband with carrier diffraction, the technique has the advantage of being independent of the optical-carrier wavelength. This property makes the technique advantageous if compared to integrated optical single-sideband sources working at a given wavelength, or to optical single-sideband sources based on fixed optical filters.

Wavelength-self-tunable single-sideband filters, operating at various frequencies, were built by implementing 30 mm long photorefractive InP:Fe bulk crystals. Light was coupled into the crystal and collected at the output by means of fibered collimators. Prior to gluing all of the elements of the device onto an invar mount, micro-positioning of the collimators made it possible to adjust the θ angles so as to set the operating radio frequency of the filter.

Filters operating at 31.5 GHz RF were characterized, and the results are shown in Figure 6. In accordance with predictions, the filtered signal was actually optical single sideband with carrier. In addition, by varying the optical-carrier wavelength, the device was verified to be wavelength self-tunable. With regards to the other main characteristics of the filter, the full width at half maximum (FWHM) – which is proportional to the inverse of the grating length, L – was 1.9 GHz, the response time was of the order of a few milliseconds, and the fiber-to-fiber loss was 28 dB. The latter characteristic is imputable to the low photorefractive-effect efficiency of InP:Fe. Nevertheless, this drawback can be almost totally compensated by an erbium-doped fiber amplifier (EDFA) placed at the output of the device. Furthermore, wavelength-self-tunable single-sideband filters exhibited polarization sensitivity up to 9 dB, which is, however, not a drawback when wavelength-self-tunable single-sideband filters are transmitter devices. Finally, thanks to an extremely high upper-sideband rejection of 29 dB, the ripple of the photo-detected power level along the fiber proved to be as low as 0.8 dB.

3. Mitigation Techniques Using External Modulators

3.1 Pre-Chirping

Optical transmitters with negative chirp have been proposed to increase the frequency-length product of optical digital links, using either Mach-Zehnder electro-optical modulators (MZM) [21, 22] or electro-absorption modulators [23, 24]. In the framework of analog fiber-optic links, the interplay between the frequency chirp of the externally modulated transmitter and the fiber chromatic dispersion induces a displacement of the frequency notches of the dispersion-induced RF penalty [25] to higher frequencies, therefore increasing the −3 dB bandwidth of the link. This approach has been demonstrated employing an optical transmitter based on an electro-absorption modulator [26, 27], as shown in Figure 7. The electro-absorption modulator chirp parameter has a strong dependence on the bias voltage, and it is therefore possible

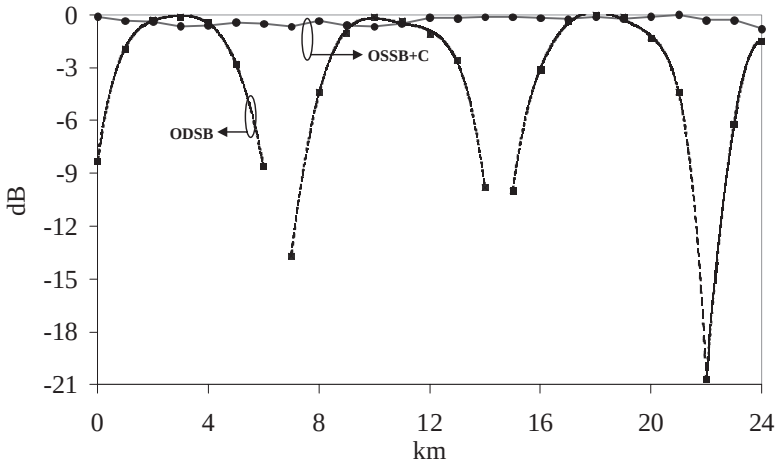

Figure 6. The relative photo-detected power level as a function of fiber length for optical double sideband (ODSB) and optical single sideband with carrier (OSSB+C) signals (modulation frequency 31.5 GHz).

to obtain negative values of this parameter for high reverse bias voltages. The photo-detected current at the output of an externally modulated analog link can be obtained as [25]

$$I_{RF} \propto \sqrt{1+\alpha^2}\cos\left[\frac{\pi LD\lambda^2}{c} f_{RF}^2 + \arctan(\alpha)\right], \quad (4)$$

where α is the chirp parameter of the transmitter, L is the link length, D is the fiber-dispersion parameter, λ is the optical wavelength, c is the speed of light in a vacuum, and f_{RF} is the frequency of the modulating signal. Figure 8 shows the experimental results obtained using the setup depicted in Figure 7, in which a continuous-wave laser was externally modulated using an electro-absorption modulator (BT Labs AT2036D2 41). The dispersion-induced RF power fading after transmission through a coil of standard single-mode fiber was measured using a light-wave component analyzer (LCA). It was demonstrated that the dispersion-induced RF power penalty frequency notches were up-shifted to higher frequencies when the electro-absorption modulator was biased at certain points of its transfer curve, resulting in negative α parameters. The theoretical results (dashed lines) agreed very well with experiments carried out for two fiber spans ($L = 25$ km and $L = 75$ km) and two electro-absorption modulator chirp parameters, $\alpha = -0.52$ and $\alpha = +1.2$, corresponding to bias points of $V_{bias} = -4$ V and $V_{bias} == 0.5$ V, respectively.

3.2 Nonlinear Optical Modulation with Suppressed Optical Carrier

The use of cascaded Mach-Zehnder modulators to implement frequency up-conversion schemes was proposed to generate and transmit millimeter-wave signals with a sharp reduction of the dispersion-induced RF power penalty [28-30]. The Mach-Zehnder modulator was biased at non-linear points of its optical transfer curve: either at the minimum-transmission bias (MITB) point or at the maximum-transmission bias (MATB) point [31, 32]. This method is limited by the high electrical power local-oscillator signal required to achieve efficient transmissions [32, 33].

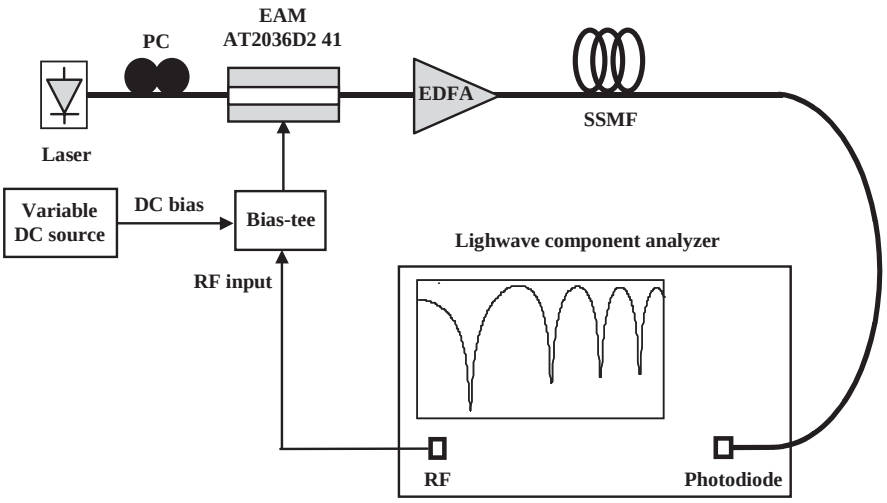

Figure 7. The experimental arrangement of an electro-absorption modulator (EAM) -based optical transmitter with adjustable chirp parameter.

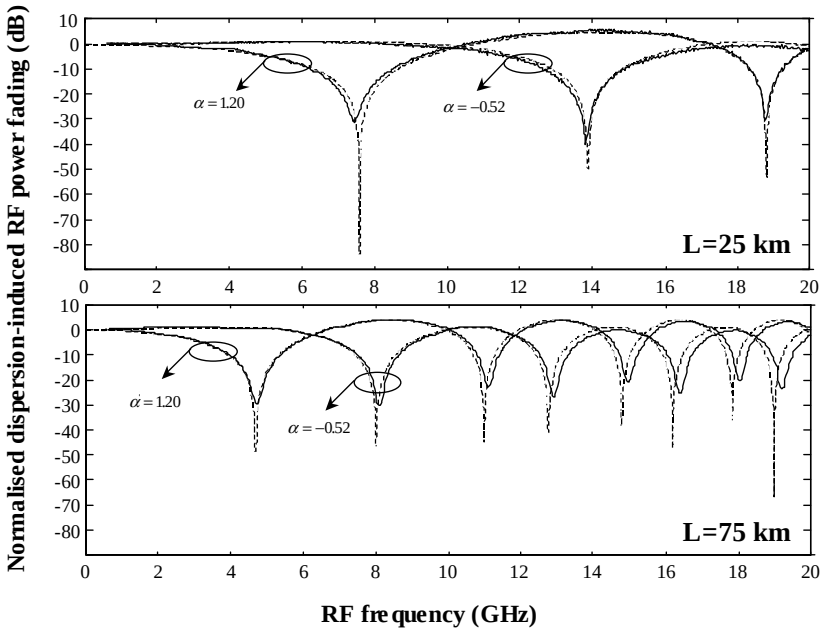

Figure 8. The theoretical (dashed) and experimental (solid) normalized dispersion-induced RF power penalty for two lengths of fiber (L = 25 km and L = 75 km) and for different chirp parameters of the electro-absorption modulator EAM (α= –0.52 and α = 1.2).

Figure 9 depicts the schematic of a photonic up-converter using two cascaded external optical modulators (EOM). The first one is used to modulate the information signal at an intermediate frequency (f_{IF}) that will be up-converted to RF using a harmonic of the local-oscillator signal. After transmission through a standard single-mode fiber, the signal at $f_{RF} = nf_{LO} + f_{IF}$ is photo detected and radiated by the base-station antenna. Depending on the chosen bias point of the local-oscillator external optical modulator, dispersion-tolerant behavior is obtained at different harmonics of the local-oscillator frequency. The right orders are $n = 2 + 4k$ for the minimum-transmission bias case, and $n = 4 + 4k$ for the maximum-transmission bias case ($k = 0,1,2,...$). Figure 10 shows the experimental verification of dispersion-tolerant transmission through a 50 km fiber-optic link of 100 MHz and 1 GHz IF tones, up-converted to frequencies of up to 12 GHz using a second harmonic of the local-oscillator signal (minimum-transmission bias case, $k = 0$). It may be observed how the carrier-suppression effect was overcome when the local-oscillator external optical modulator was biased at the minimum-transmission bias point. Similar results were obtained for the maximum-transmission bias case [31].

4. Techniques Based on Nonlinear Effects

4.1 Optical Phase Conjugation Based on Four-Wave Mixing

The feasibility of using optical phase conjugation (OPC) to compensate for the fiber-induced nonlinear distortion in cable television (CATV) networks and microwave analog systems was previously outlined in [34, 35]. Optical phase conjugation has also been demonstrated to be a powerful technique for compensating for the carrier-suppression effect that appears in optical microwave/millimeter-wave radio-over-fiber links [36-38]. The advantage of this technique with respect to others is that it also reduces the effect of fiber-induced self-phase modulation (SPM) [39], and does not impose as stringent conditions on the modulating signal as does the optical single-sideband format. The optical phase conjugation technique consists of placing an optical phase conjugator approximately at the mid-span of the optical link. Under several design constraints [39-40], the combined effects of

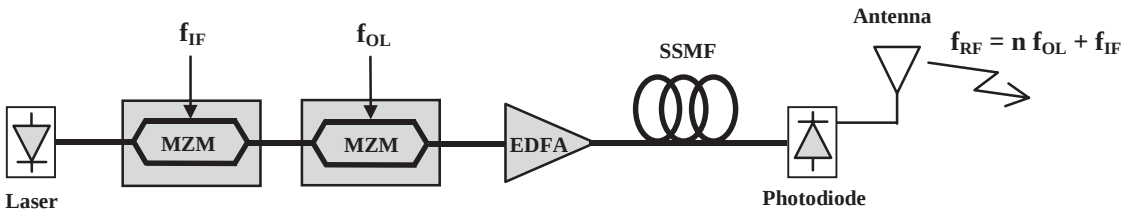

Figure 9. A schematic diagram of the photonic up-converter using two external modulators in series.

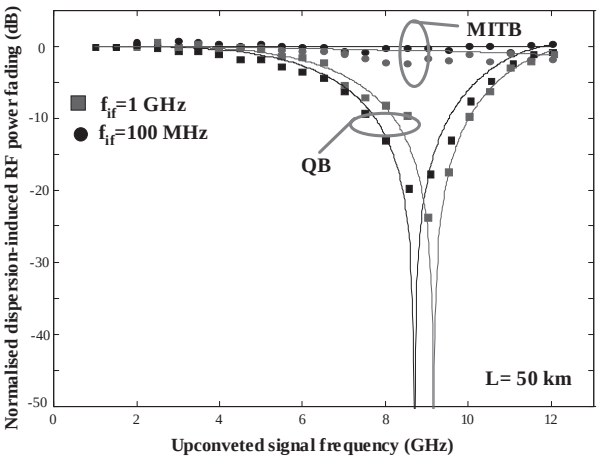

Figure 10. The dispersion-induced RF power penalty as a function of the RF frequency for the transmission of IF tones through a 50 km standard single-mode fiber fiber-optic link. The experimental results (symbols) agree very well with theory (solid lines).

chromatic dispersion and self-phase modulation, introduced by the first fiber span, may be compensated for by the following optical phase conjugation and by subsequent propagation through the second fiber span with similar characteristics.

The most common way of producing the phase-conjugated signal is by means of four-wave mixing (FWM) in a semiconductor optical amplifier (SOA) or in a dispersion-shifted fiber (DSF). Experimental results of fading-free fiber-optic transport of a millimeter-wave signal at 60 GHz, employing a semiconductor optical amplifier-based optical phase conjugation, were presented in [36]. Although the semiconductor optical amplifier-based conjugator provides a larger conversion efficiency, the dispersion-shifted-fiber based conjugator makes it possible to produce a larger input signal power without distortion, and a higher signal-to-noise ratio (SNR) may therefore be achieved [41].

The experimental arrangement used to demonstrate the compensation for the carrier-suppression effect by means of four-wave mixing in a dispersion-shifted fiber is depicted in Figure 11. A tunable laser, operating at 1551 nm, provides the optical carrier. The Mach-Zehnder modulator (MZM) output, with an optical power of 0 dBm, is launched into 25 km of standard single-mode fiber. To compensate for the chromatic dispersion effects of the first 25 km standard single-mode fiber span, a dispersion-shifted fiber-based optical phase conjugation is placed at the mid-span of the optical fiber link. The optical phase conjugation converts the input signal into a phase-conjugated replica by means of four-wave mixing through 12.7 km of dispersion-shifted fiber. The pump laser has an optical power of +3 dBm and is tuned to the zero-dispersion wavelength of the dispersion-shifted fiber (1550 nm). The pump wave and the transmitted wave are combined and amplified to induce nonlinear effects in the dispersion-shifted fiber. The same polarization state is obtained for the two waves by using a polarization controller (PC). The phase-conjugation efficiency is inversely proportional to the pump power, and is also dependent on the dispersion-shifted fiber's length, having an optimum at a fiber length of about 17.4 km [42] (slightly longer than our 12.7 km-length dispersion-shifted fiber). The conjugated signal at the output of the dispersion-shifted fiber is now filtered and amplified up to 0 dBm to be further transmitted through the second 25 km standard single-mode fiber span. The propagation through this second fiber span compensates for the chromatic dispersion

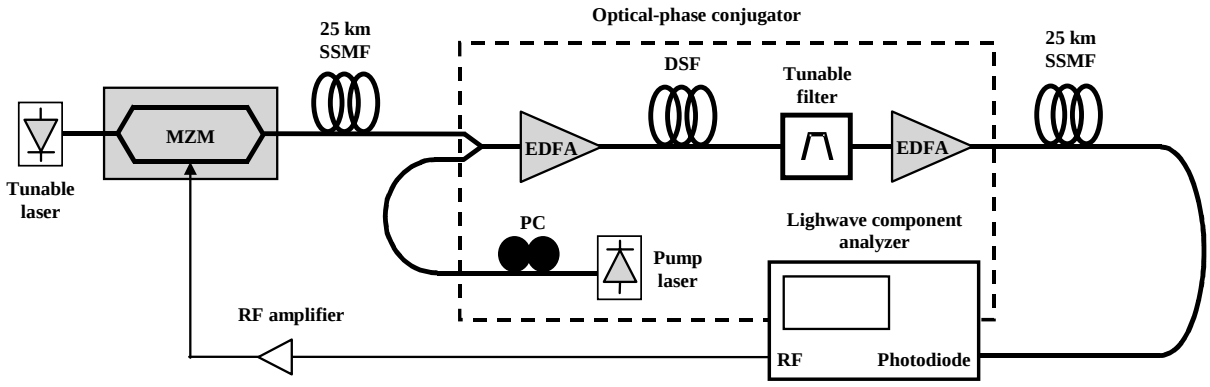

Figure 11. The experimental setup of the dispersion-shifted fiber (DSF) -based optical phase conjugation (OPC) compensation system.

accumulated at the output of the first fiber span [39]. Finally, the output of the optical fiber is photo detected, and the overall system frequency response is measured.

The simulation results of the normalized RF detected power for 50 km of standard single-mode fiber were obtained using the system model described in [35]. Figure 12 shows the cases with four-wave mixing (solid line) and without four-wave mixing (dashed line). The experimental results obtained with four-wave mixing (black circles) and without four-wave mixing (white circles) are also depicted in Figure 12, showing excellent agreement with the simulation results. The dispersion-induced power penalty was almost fully mitigated when employing dispersion-shifted-fiber-based four-wave mixing. The frequency response with four-wave mixing was nearly flat, with a variation of less than ±2 dB. This ripple was attributed to the effect of harmonics generated by the Mach-Zehnder modulator, due to the high modulation index used in the experiment (the electrical power at the RF port of the Mach-Zehnder modulator was +10 dBm). The nonlinear transfer function of the modulator and the distortion introduced by the electrical amplifier generated measured second- and third-order harmonic levels at the output of the Mach-Zehnder modulator of −30 dBc and −43 dBc, respectively, for a half-wave dc voltage of the modulator of 9 V and a modulating frequency of 2 GHz.

4.2 SOA Boosters

The use of semiconductor optical amplifiers as transmitting boosters was recently proposed to reduce the chromatic dispersion effects that occur during the fiber propagation of light in conventional microwave-optical transmissions operating near 1550 nm. It was found that the chirp introduced by the semiconductor optical amplifier under saturation conditions may be useful to mitigate the dispersion-induced effects in both digital [43] and analog [44] optical transmissions. According to a theoretical study [45], the carrier-suppression effect in conventional microwave optical links may be considerably alleviated by adjusting the semiconductor optical amplifier's input power.

The propagation of an RF externally modulated optical wave through a dispersive and nonlinear single-mode fiber in the presence of a chirp at the optical transmitter may be modeled by the frequency transfer function of a microwave optical link [46]:

$$H(z,\omega) = C_{IM-IM}(z,\omega) + \frac{1}{2} H_{PM}(\omega) C_{PM-IM}(z,\omega), \quad (5)$$

where z is the fiber distance, ω is the angular frequency, C_{IM-IM} and C_{PM-IM} are the conversion functions between intensity modulation (IM) and phase modulation (PM) in the optical fiber, and H_{PM} is the optical transmitter phase-modulation response. Furthermore, it is well known that a semiconductor optical amplifier operating under gain saturation exhibits phase modulation at its output, which may be controlled by means of the semiconductor optical amplifier's input power [43]. Therefore, it is here considered that a semiconductor optical amplifier booster be placed at the output of the optical transmitter, in order both to amplify the optical signal and to control its chirp.

In order to characterize the effect of the semiconductor optical amplifier chirp during the propagation through the single-mode fiber, the traveling-wave equations of the semiconductor optical amplifier, as given in [47], have been considered. From these equations, and assuming a small-signal approach [48], the optical-transmitter phase-modulation response may be finally expressed as [45]

$$H_{PM}(\omega) = -\alpha_N (G_0 - G)(1 + P_0/P_{sat} + j\omega\tau_c)^{-1}, \quad (6)$$

where α_N is the semiconductor optical amplifier's linewidth enhancement factor, τ_c is the carrier lifetime, P_0 is the power launched into the semiconductor optical amplifier, G stands for the saturated semiconductor optical amplifier's gain expressed in nepers, and G_0 is the unsaturated gain. The frequency transfer function of the microwave optical link may be finally obtained from Equation (5) and Equation (6).

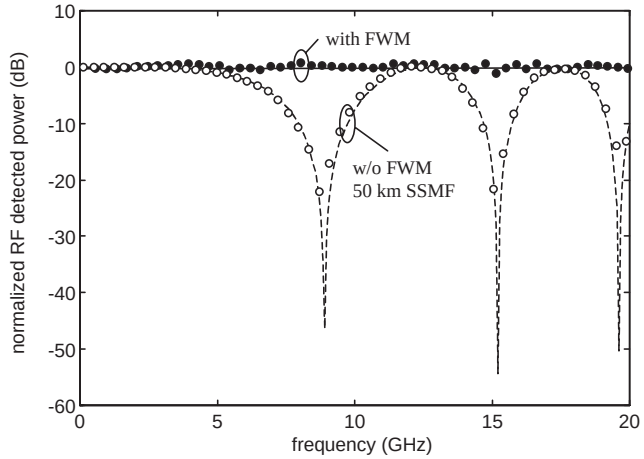

Figure 12. The simulation (lines) and experimental (symbols) results of the normalized RF detected power for a 50 km optical standard single-mode fiber (SSMF) span with four-wave mixing (FWM) (solid line and black circles) and without four-wave mixing (dashed line and white circles).

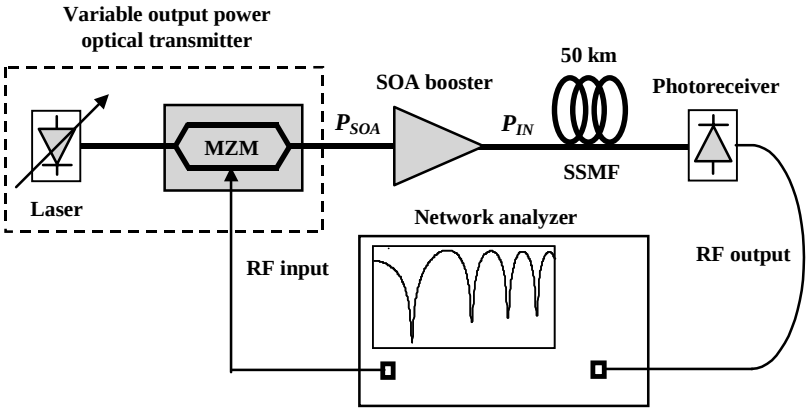

Figure 13. The experimental setup for demonstrating the reduction of chromatic dispersion effects employing a semiconductor optical amplifier (SOA) booster.

The experimental arrangement used to measure the frequency transfer function of the microwave-optical link employing a semiconductor optical amplifier booster at the optical transmitter is shown in Figure 13. An optical carrier at 1550 nm from a laser diode with variable output power was externally modulated with an RF signal, employing a chirp-free Mach-Zehnder modulator, and then amplified by the semiconductor optical amplifier booster (Philips CQF871). The variable optical power at the output of the laser, and therefore at the input of the semiconductor optical amplifier, was used to control the phase modulation and chirp at its output. The semiconductor optical amplifier output was then launched into a standard single-mode fiber of 50 km length, and finally photo detected, in order to recover the RF signal. The experimental measurements of the normalized frequency transfer function of the optical link are shown in Figure 14, up to an RF frequency of 12 GHz, under different conditions. The RF response, when no semiconductor optical amplifier was employed, exhibited deep notches. Furthermore, these notches were shifted to higher frequencies as the optical power at the standard single-mode fiber's input, P_{IN}, increased, which was due to the self-phase modulation effect [46].

On the other hand, the dispersion-induced RF carrier-suppression effect can be significantly alleviated by increasing the optical power at the semiconductor optical amplifier input, P_{SOA}, as shown in Figure 14. These RF responses were flatter for higher semiconductor optical amplifier input powers. It is to be noted that this flattening effect saturated for $P_{SOA} = +10$ dBm. The RF responses with the semiconductor optical amplifier were obtained by keeping the semiconductor optical amplifier's bias current fixed at 300 mA. As the semiconductor optical amplifier's bias current was kept constant during the measurements, the semiconductor optical amplifier experienced gain saturation when the optical power at its input was increased. The optical powers at the output of the semiconductor optical amplifier (the standard single-mode fiber input) for each measurement are also shown in Figure 14.

The measurements, which were compared with the frequency transfer function from Equation (5), are also given in Figure 14 (dashed line), and good agreement is shown. It may be may concluded that the chirp introduced by the semiconductor optical amplifier booster is useful for reducing the carrier-suppression effect and for increasing the dynamic range of analog optical links [44].

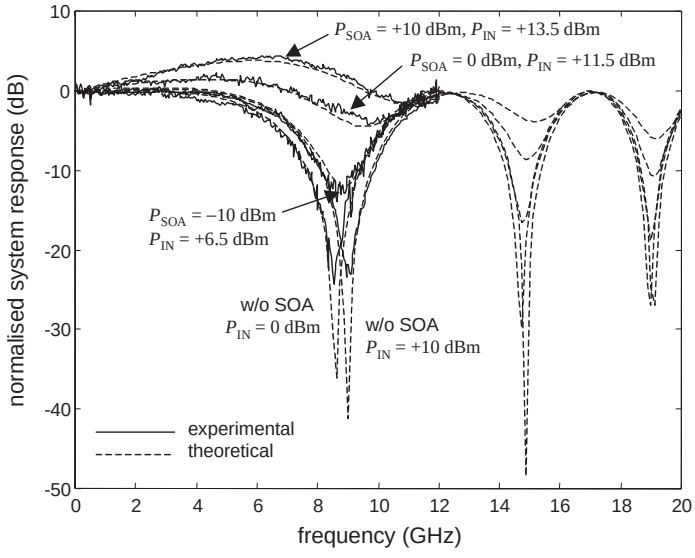

Figure 14. The normalized frequency response of the analog optical link under different conditions.

Finally, the nonlinear distortion (NLD) arising from the semiconductor-optical-amplifier-based transmitter was also measured, using both single-tone (harmonic distortion) and two-tone (third-order intermodulation distortion) driving signals at the RF port of the Mach-Zehnder modulator. For single-tone nonlinear distortion measurements, an RF tone of 6 GHz was used in the experiment. For the two-tone nonlinear distortion measurement, two RF tones of 1.9 GHz and 2.1 GHz were employed. Figure 15 shows second-order (HD2) and third-order (HD3) harmonic distortion levels as a function of the semiconductor optical amplifier's input power. The nonlinear distortion-level floor imposed by the Mach-Zehnder modulator is also depicted in Figure 15. For second-order harmonic distortion (HD2), an increase of nearly 10 dB (at +10 dBm semiconductor optical amplifier input power) was observed, owing to the semiconductor optical amplifier's nonlinear response. However, the third-order harmonic distortion (HD3) increase could be up to 15 dB, even though it was not relevant, due to the relatively high values of the second-order harmonic distortion. A third-order intermodulation distortion ($2f_2 - f_1$) level of about -52 dBc was also obtained for a semiconductor optical amplifier input power of $+10$ dBm. Therefore, the semiconductor optical amplifier's input power must be carefully controlled in order to achieve both equalization and linearity.

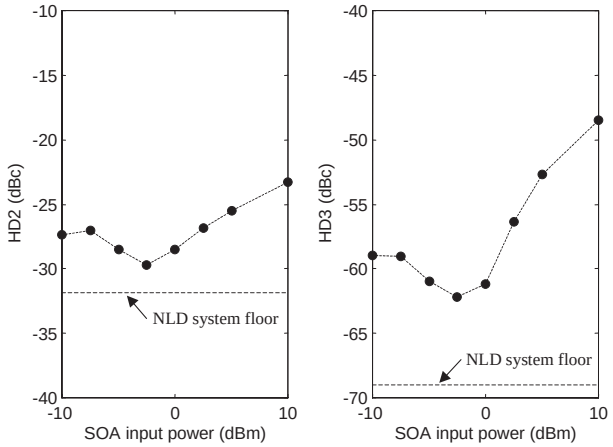

Figure 15. The harmonic distortions generated by the semiconductor optical amplifier (SOA) -based transmitter. The nonlinear distortion (NLD) system floor is shown.

5. Discussion

Several techniques to compensate for the dispersion-induced carrier-suppression effect in fiber-wireless systems have been investigated. These techniques are based on single-sideband transmission schemes, pre-chirping effects in external modulators or semiconductor optical amplifier boosters, electro-optic modulators biased at non-linear points, and optical phase conjugators. The experimental results show a good reduction – or even perfect mitigation – of the frequency notches appearing in the system's frequency response.

Numerous optical single sideband with carrier sources have been studied and reported over the past years. The technique based on a dual-electrode Mach-Zehnder modulator has the advantage of robustness and commercial availability. On the other hand, the integrated configuration is more compact, but it requires a more complex technology. Regarding the use of optical filters to remove one of the sidebands from an optical double-sideband signal, it is to be noted that such an alternative may be wavelength dependent. The impact of insertion loss and stability also has to be considered for any of the proposed configurations.

Other techniques, implementing external modulators, have been proposed. Among them, pre-chirping is a very simple approach, but the compensation is not perfect and is dependent on the link length. Chromatic dispersion effects are mitigated using the approach of nonlinear optical modulation with a suppressed carrier, enabling broad-bandwidth operation with the important advantage of harmonic generation. Nevertheless, the latter solution requires high electrical local-oscillator powers, which increase the cost and complexity of the system.

Furthermore, the use of semiconductor optical amplifier boosters significantly reduces the frequency notches (up to 20 dB), when the optical power at the semiconductor optical amplifier input is correctly adjusted to slightly saturate the semiconductor optical amplifier and control its frequency chirp. Finally, the optical phase conjugation technique makes it possible to perfectly compensate for the carrier-suppression effect, even in the presence of self-phase modulation, provided that the optical phase conjugator is correctly configured and placed at the mid-span of the fiber-optic link.

6. Conclusion

In this paper, techniques for compensating for the dispersion-induced RF power penalty that occurs in fiber-wireless transmissions have been reviewed. Many techniques have been proposed, based either on the single-sideband format, the use of external modulators, or the generation of nonlinear effects. Experimental results have demonstrated compensation for the carrier-suppression effect for frequencies well into the millimeter-wave band. This ensures the applicability of fiber-wireless techniques to next-generation broadband wireless access and transport networks.

7. List of Abbreviations

- CATV cable television
- DFB distributed feedback
- DE-MZM dual-electrode Mach-Zehnder modulator
- DSF dispersion-shifted fiber
- EAM electro-absorption modulator
- EDFA erbium-doped fiber amplifier

- EOM external optical modulator
- FWHM full width at half maximum
- FWM four-wave mixing
- HD2 2nd-order harmonic distortion
- HD3 3rd-order harmonic distortion
- IF intermediate frequency
- IM intensity modulation
- InP:Fe iron-doped indium phosphide
- LCA lightwave component analyzer
- LO local oscillator
- MZM Mach-Zehnder modulator
- MATB maximum transmission bias
- MITB minimum transmission bias
- MMI multimode interferometer
- NLD nonlinear distortion
- ODSB optical double sideband
- OPC optical phase conjugation
- OSSB optical single sideband
- OSSB+C optical single sideband with carrier
- OSSB+SC optical single sideband with suppressed carrier
- PC polarization controller
- PM phase modulation
- QB quadrature-bias
- RF radio frequency
- SNR signal-to-noise ratio
- SOA semiconductor optical amplifier
- SPM self-phase modulation
- SSMF standard single mode fiber
- WST-SSB wavelength-self-tunable single-sideband

8. References

1. D. Wake, I. C. Smith, N. G. Walker, I. D. Henning, and R. D Carver, "Video Transmission Over a 40 GHz Radio-Fibre Link," *Electronics Letters*, **28**, 21, 1992, pp. 2024-2025.

2. A. J. Seeds, "Broadband Fibre-Radio Access Networks," in *Proceedings of the International Topical Meeting on Microwave Photonics*, Princeton, USA, 1998, pp. 1-4.

3. A. Nirmalathas, C. Lim, D. Novak, and R. B. Waterhouse, "Progress in Millimetre-Wave Fiber-Radio Access Networks," *Annals of Telecommunications*, **56**, 1-2, 2001, pp. 27-38.

4. H. Schmuck, "Comparison of Optical Millimetre-Wave System Concepts with Regard to Chromatic Dispersion," *Electronics Letters*, **31**, 21, 1995, pp. 1848-1849.

5. J. Marti, J. M. Fuster, and R. I. Laming, "Experimental Reduction of Chromatic Dispersion Effects in Lightwave Microwave/Millimetre-Wave Transmissions Using Tapered Linearly Chirped Fibre Gratings," *Electronics Letters*, **33**, 13, 1997, pp. 1170-1171.

6. S. A. Havstad, A. B. Sahin, O. H. Adamczyk, Y. Xie and A. E. Willner, "Distance-Independent Microwave and Millimeter-Wave Power Fading Compensation Using a Phase Diversity configuration," *IEEE Photonics Technology Letters*, **12**, 8, 2000, pp. 1052-1054.

7. K. Yonenaga and N. Takachio, "A Fiber Chromatic Dispersion Compensation Technique with an Optical SSB Transmission in Optical Homodyne Detection Systems," *IEEE Photonics Technology Letters*, **5**, 8, 1993, pp. 949-951.

8. J. Park, W. V. Sorin, and K. Y. Lau, "Elimination of the Fibre-Chromatic Dispersion Penalty on 1550 nm Millimetre-Wave Optical Transmission," *Electronics Letters*, **33**, 6, 1997, pp. 512-513.

9. E. Vourc'h, D. Le Berre, and D. Hervé, "Lightwave Single Side-Band Wavelength Self-Tunable Filter Using an InP:Fe Crystal for Fiber-Wireless Systems," *IEEE Photonics Technology Letters*, **14**, 2, 2002, pp. 194-196.

10. J. Capmany, D. Pastor, P. Munoz, B. Ortega, S. Sales, and A Martinez, "**Multiwavelength Optical SSB Generation for Dispersion Mitigation in WDM Fibre Radio Systems Using AWG Multiplexer,"** *Electronics Letters*, **38**, 20, 2002, pp. 1194-1196.

11. G. H. Smith, D. Novak, and Z. Ahmed, "Overcoming Chromatic-Dispersion Effects in Fiber-Wireless Systems Incorporating External Modulators," *IEEE Transactions on Microwave Theory and Techniques*, **MTT-45**, 8, 1997, pp. 1410-1415.

12. E. Vergnol, F. Devaud, D. Tanguy, and E. Pénard, "Integrated Lightwave Millimetric Single Sideband Source: Design and Issues," *IEEE Journal of Lightwave Technology*, **16**, 7, 1998, pp. 1276-1284.

13. B. Davies and J. Conradi, "Hybrid Modulator Structures for Subcarrier Optical Single Sideband," *IEEE Photonics Technology Letters*, **10**, 4, 1998, pp. 600-602.

14. M. Y. Frankel and R. D. Esman, "Optical Single-Sideband Suppressed-Carrier Modulator for Wide-Band Signal Processing," *IEEE Journal of Lightwave Technology*, **16**, 5, 1998, pp. 859-863.

15. A. Loayssa, D. Benito, and M. J. Garde, "Single-Sideband Suppressed-Carrier Modulation Using a Single-Electrode Electrooptic Modulator," *IEEE Photonics Technology Letters*, **13**, 8, 2001, pp. 869-871.

16. G. H. Smith and D. Novak, "Broadband Millimeter-Wave (38 GHz) Fibre-Radio System Using Electrical and Optical SSB Modulation to Overcome Dispersion Effects," *IEEE Photonics Technology Letters*, **10**, 1, 1998, pp. 141-143.

17. F. Ramos and J. Marti, "Comparison of Optical Single-Sideband Modulation and Chirped Fiber Gratings as Dispersion Mitigating Techniques in Optical Millimeter-Wave Multichannel Systems," *IEEE Photonics Technology Letters*, **11**, 11, 1999, pp. 1479-1481.

18. V. Polo, A. Martinez, J. Marti, F. Ramos, A. Griol, and R. Llorente, "Simultaneous Baseband and RF Modulation Scheme in GBit/s Millimetre-Wave Wireless Fibre Networks," *Proceedings of the International Topical Meeting on Microwave Photonics*, Oxford, UK, 2000, pp. 168-171.

19. A. Martinez, V. Polo, J. L. Corral, and J. Marti, "**Experimental Demonstration of Dispersion-Tolerant 155-Mb/s BPSK Data Transmission at 40 GHz using an Optical Coherent Harmonic Generation Technique**," *IEEE Photonics Technology Letters*, **15**, 5, 2003, pp. 772-774.

20. A. Martinez, V. Polo, and J. Marti, "Simultaneous Baseband and RF Optical Modulation Scheme for Feeding Wireless and Wireline Access Networks*," IEEE Transactions on Microwave Theory and Techniques*, **MTT-49**, 10, 2001, pp. 2018-2024.

21. A. H. Gnauck, S. K. Korotky, J. J. Veselka, J. Nagel, C. T. Kemmerer, W. J. Minford, and D. T. Moser, "Dispersion Penalty Reduction Using an Optical Modulator with Adjust-

able Chirp," *IEEE Photonics Technology Letters*, **3**, 10, 1991, pp. 916-918.

22. J. C. Cartledge and R. G. McKay, "Performance of 10 Gb/s Lightwave Systems Using an Adjustable Chirp Optical Modulator and Linear Equalization," *IEEE Photonics Technology Letters*, **4**, 12, 1992, pp. 1394-1396.

23. J. A. J. Fells, M. A. Gibbon, I. H. White, G. H. B. Thompson, R. V. Penty, C. J. Armistead, E. M. Kimber, D. J. Moule, and E. J. Thrush, "Transmission Beyond the Dispersion Limit Using a Negative Chirp Electroabsorption Modulator," *Electronics Letters*, **30**, 14, 1994, pp. 1168-1169.

24. J. C. Cartledge and B. Christensen, "**Optimum Operating Points for Electroabsorption Modulators in 10 Gb/s Transmission Systems Using Nondispersion Shifted Fiber,"** *IEEE Journal of Lightwave Technology*, **16**, 3, 1998, pp. 349-357.

25. F. Devaux, "Optimum Prechirping Conditions of Externally Modulated Lasers for Transmission on Standard Fibre," *IEE Proceedings-Optoelectronics*, **141**, 6, 1994, pp. 363-366.

26. V. Polo, J. Marti, F. Ramos, and D. Moodie, "Mitigation of Chromatic Dispersion Effects Employing Electroabsorption Modulator-Based Transmitters," *IEEE Photonics Technology Letters*, **11**, 7, 1999, pp. 883-885.

27. A. Stöhr, K. Kitayama, and T. Kuri, "Fiber-Length Extension in an Optical 60-GHz Transmission System Using an EA-Modulator with Negative Chirp," *IEEE Photonics Technology Letters*, **11**, 6, 1999, pp. 739-741.

28. J. O'Reilly and P. M. Lane, "Remote Delivery of Video Services Using mm-Waves and Optics," *IEEE Journal of Lightwave Technology*, **12**, 2, 1994, pp. 369-375.

29. R. Hofstetter, H. Schmuck, and R. Heidemann, "Dispersion Effects in Optical Millimeter-Wave Systems Using Self-Heterodyne Method for Transport and Generation," *IEEE Transactions on Microwave Theory and Techniques*, **MTT-43**, 9, 1995, pp. 2262-2269.

30. J. M. Fuster, J. Marti, J. L. Corral, V. Polo, and F. Ramos, "Chromatic Dispersion Effects in Electro-Optical Up-Converted Millimetre-Wave Fibre-Optic Links," *Electronics Letters*, **33**, 23, 1997, pp. 1969-1970.

31. J. M. Fuster, J. Marti, J. L. Corral, V. Polo, and F. Ramos, "Mitigation of Dispersion-Induced Power Penalty in Millimetre-Wave Fibre-Optic Links," *Electronics Letters*, **34**, 19, 1998, pp. 1869-1870.

32. J. M. Fuster, J. Marti, J. L. Corral, V. Polo, and F. Ramos, "Generalized Study of Dispersion-Induced Power Penalty Mitigation Techniques in Millimeter-wave Fiber-Optic Links," *IEEE Journal of Lightwave Technology*, **18**, 7, 2000, pp. 933-940.

33. J. L. Corral, J. Marti, and J. M. Fuster, "**General Expressions for IM/DD Dispersive Analog Optical Links with External Modulation or Optical Up-Conversion in a Mach-Zehnder Electrooptical Modulator,"** *IEEE Transactions on Microwave Theory and Techniques*, **MTT-49**, 10, 2001, pp. 1968-1976.

34. J. Marti and F. Ramos, "Compensation for Dispersion-Induced Nonlinear Distortion in Subcarrier Systems Using Optical-Phase Conjugation," *Electronics Letters*, **33**, 9, 1997, pp. 792-794.

35. F. Ramos and J. Marti, "Compensation for Fiber-Induced Composite Second-Order Distortion in Externally Modulated Lightwave AM-SCM Systems Using Optical-Phase Conjugation," *IEEE Journal of Lightwave Technology*, **16**, 8, 1998, pp. 1387-1392.

36. K. Kitayama and H. Sotobayashi, "Fading-Free Fiber-Optic Transport of 60 GHz-Optical DSB Signal by Using In-Line Phase Conjugator," *Proceedings of the Optical Fiber Communication Conference*, San Diego, USA, 1999, pp. 64-66.

37. F. Ramos, J. Marti, and V. Polo, "Compensation of Chromatic Dispersion Effects in Microwave/Millimeter-Wave Optical Systems Using Four-Wave Mixing Induced in Dispersion-Shifted Fibers," *IEEE Photonics Technology Letters*, **11**, 9, 1999, pp. 1171-1173.

38. H. Sotobayashi, and K. Kitayama, "Cancellation of the Signal Fading for 60 GHz Subcarrier Multiplexed Optical DSB Signal Transmission in Nondispersion Shifted Fiber Using Midway Optical Phase Conjugation," *IEEE Journal of Lightwave Technology*, **17**, 12, 1999, pp. 2488-2497.

39. S. Watanabe and M. Shirasaki, "Exact Compensation for Both Chromatic Dispersion and Kerr Effect in a Transmission Fiber Using Optical Phase Conjugation," *IEEE Journal of Lightwave Technology*, **14**, 3, 1996, pp. 243-248.

40. S. Watanabe, G. Ishikawa, T. Naito, and T. Chikama, "Generation of Optical Phase-Conjugate Waves and Compensation for Pulse Shape Distortion in a Single-Mode Fiber," *IEEE Journal of Lightwave Technology*, **12**, 12, 1994, pp. 2139-2146.

41. H. Geiger, S. Y. Set, R. I. Laming, M. J. Cole, and L. Reekie, "Comparison of DSF- and SOA-Based Phase Conjugators Employing Noise-Suppressing Fiber," *Proceedings of the Optical Fiber Communication Conference*, Dallas, USA, 1997, pp. 150-151.

42. W. Wu, P. Yeh, and S. Chi, "Phase Conjugation by Four-Wave Mixing in Single-Mode Fibers," *IEEE Photonics Technology Letters*, **6**, 12, 1994, pp. 1448-1450.

43. T. Watanabe, N. Sakaida, H. Yasaka, F. Kano, and M. Koga, "Transmission Performance of Chirp-Controlled Signal by Using Semiconductor Optical Amplifier," *IEEE Journal of Lightwave Technology*, **18**, 8, 2000, pp. 1069-1077.

44. J. Marti, F. Ramos, and J. Herrera, "Experimental Reduction of Dispersion-Induced Effects in Microwave Optical Links Employing SOA Boosters," *IEEE Photonics Technology Letters*, **13**, 9, 2001, pp. 999-1001.

45. J. Herrera, F. Ramos, and J. Marti, "Frequency Response of Analogue Optical Links Employing SOA-Boosters," *Electronics Letters*, **38**, 19, 2002, pp. 1115-1116.

46. F. Ramos and J. Marti, "Frequency Transfer Function of Dispersive and Nonlinear Single-Mode Optical Fibers in Microwave Optical Systems," *IEEE Photonics Technology Letters*, **12**, 5, 2000, pp. 549-551.

47. A. A. M. Saleh, "Nonlinear Models of Travelling-Wave Optical Amplifiers," *Electronics Letters*, **24**, 14, 1988, pp. 835-837.

48. K. Oberman, S. Kindt, D. Breuer, and K. Petermann, "Performance Analysis of Wavelength Converters Based on Cross-Gain Modulation in Semiconductor-Optical Amplifiers," *IEEE Journal of Lightwave Technology*, **16**, 1, 1998, pp. 78-85.

The Lower Ionosphere: Abandoned by Communication, to be Re-Discovered for Aeronomy

M. Friedrich

Abstract

The point is made that research on the lower ionosphere is still of importance, despite the decline in interest for communication. Today, the emphasis must be on the space weather aspect, and on the fact that ionospheric research provides important supporting information for atmospheric science, including global change investigations. Examples of ionospheric evidence are presented that are of potential interest to atmospheric scientists, who may not aware of such data.

1. Introduction

Ionospheric research is the oldest field of atmospheric physics to extend beyond altitudes accessible by balloons. The need to understand the reflecting and absorbing layer surrounding the Earth was obviously of great importance for the communication community. With the advent of satellites as relays for frequencies high enough to be virtually unaffected by the ionosphere, interest in the ionized atmosphere resided with scientists, as opposed to communication engineers. So often, military needs stimulated investigations and encouraged scientists to attempt to understand the behavior of the ionosphere. After World War II, much of the knowledge gathered by both Germany and the Allies was pooled, and the endeavor of the International Reference Ionosphere (IRI) constituted a civilian/scientific spin-off. There are essentially three areas where the ionosphere is important for wave propagation: (1) the total electron content (TEC) determines the group velocity of satellite navigation signals; (2) the maximum electron density, usually found in the F region (f_0F_2), determines the highest frequency reflected by the ionosphere; and, finally, (3) the product of the collision frequency and the electron density – which is a maximum in the D region – determines the absorption of a signal traversing the ionosphere. The largest absorption occurs under very disturbed conditions in the auroral zone or the polar cap, and amounts to perhaps 10 dB at 30 MHz; hence, at 10 GHz (a typical frequency used today for satellite communication), we can expect the loss caused by the ionosphere to be much smaller than, for example, that due to humidity on the feed of the satellite antenna. The IRI does include the D region, starting at an altitude of 60 or 80 km. However, functions used to describe and/or predict the ionosphere higher up do not seem to be adequate for the lower ionosphere. Dedicated models of the lower ionosphere are therefore required in order to realistically describe the part of the ionosphere that is more closely related to the neutral atmosphere than to other regions of the ionosphere. Measurements in the lower ionosphere have been used to monitor processes in the neutral middle atmosphere. Anthropogenic changes, such as the greenhouse effect, can be detected in that part of the ionosphere.

2. Theoretical Behavior

For convenience, the lower ionosphere will be defined here as the height region where the lifetime of free electrons is short enough that one can safely assume steady state. Hence, transport of plasma or a hysteresis between sunrise and sunset can generally be ignored; this simplification is probably acceptable up to 150 km. On the other hand, this height region, notably the D region, is characterized by a large dependence on the composition of the neutral background atmosphere. To illustrate this argument, Figure 1 shows typical ionization processes of the daytime non-auroral lower ionosphere [1]. For these specific conditions, the dominating source of free electrons is the ionization of nitric oxide (NO) by solar Lyman-α in the range from 65 to 95 km. Above this height, solar extreme ultraviolet (EUV) and X-rays dominate, and below, galactic cosmic rays dominate. The figure demonstrates the importance of the trace gas NO and its variability for the formation of the daytime ionosphere.

M. Friedrich is with the Department of Communications and Wave Propagation, Technical University Graz, Inffeldgasse 12, A-8010 Graz, Austria; Tel: +43-316-673-7441; Fax: +43-316-463697;
E-mail: friedrich@inw.tu-graz.ac.at

Editors note: This is one of the invited *Reviews of Radio Science*, from Commission G.

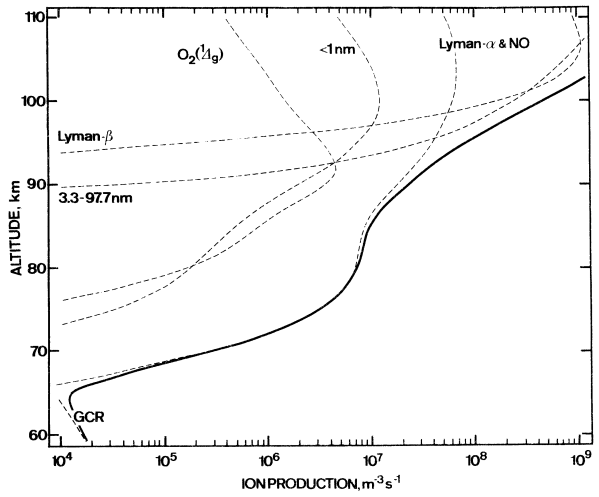

Figure 1. Ionization processes for non-auroral daytime conditions and high solar activity [1].

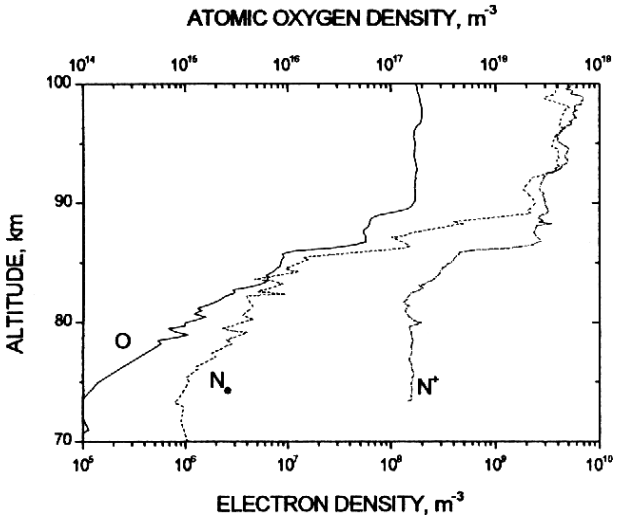

Figure 3. The densities of atomic oxygen, positive ions, and electrons measured aboard the same sounding rocket (NLTE-2, ESRANGE, March 6, 1998, solar zenith angle 116°; [2]).

The reaction competing with ionization is the recombination of electrons with positive ions. In reality, this is not the only process in which free electrons are lost, and one therefore uses the term "effective electron recombination rate" or "electron loss rate." Figure 2 shows a very simplified scheme, which is, however, sufficient to qualitatively explain the general behavior. The features relevant for arguing that the neutral composition is important are the chemical reactions containing atomic oxygen (O). Indicated are two paths with O that both lead to a reduced effective recombination rate, and, hence, to a positive correlation of electron density, N_e, with [O]. Atomic oxygen inhibits the formation of cluster ions (which have very large recombination rates), and provides a reverse reaction to the attachment of electrons to neutrals (negative ions, X^-), i.e., another electron-loss process. Figure 3 shows possibly the only case where the densities of electrons, positive ions, and atomic oxygen were measured aboard the same rocket payload. The clear correlation of the electron-density ledge at 86 km and the structural details at 80 km are not unexpected, yet this provides striking evidence that O indeed decisively impacts on electron densities in the lower ionosphere [2].

Another good example, demonstrating the impact that the nature of the positive ions has on the concentration of electrons, is given in Figure 4. The partial ion densities of a rocket-borne mass spectrometer showed that molecular ions dominated above 77.3 km, whereas below that height, the positive species were mainly cluster ions of the type $NO^+(H_2O)_n$ and $H^+(H_2O)_n$, which have significantly larger recombination rates [3]. In the right panel, the effective recombination rate, $\psi = q/N_e^2$, is plotted from data obtained by the same rocket [4]. Clearly, at heights where clusters dominate, ψ reaches much larger values.

Early theoretical steady-state models of the lower ionosphere were established, for example, by [5], who only considered six charged species and a given neutral atmosphere. A similar approach was taken by [6], however calculating more species (17) and testing the model extensively against a variety of ionospheric data. The conclusion at the time – which probably still largely holds – was that realistic inputs (solar fluxes, minor species) were more important than a more-refined chemistry. Examples of models that calculate both the neutral and ionized atmosphere in a time-dependent computation are, for

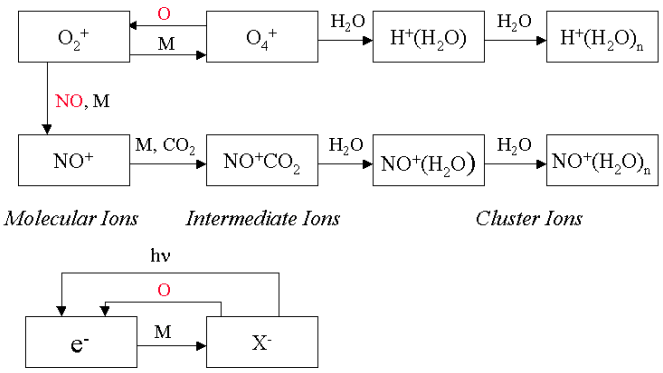

Figure 2. A simple scheme of the chemistry governing the loss of free electrons. The primarily produced ions are O_2^+ and NO^+, X^- are all negative ions, and M is the neutral number density.

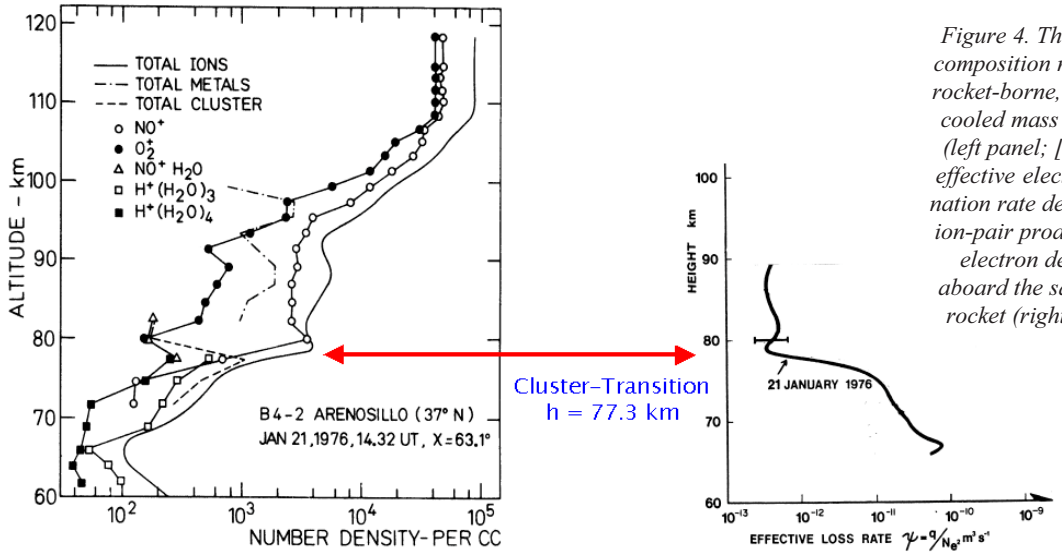

Figure 4. The positive ion composition measured by a rocket-borne, cryogenically cooled mass spectrometer (left panel; [14]), and the effective electron-recombination rate determined from ion-pair production, q, and electron density, N_e, aboard the same sounding rocket (right panel; [4]).

example, those by the Boulder group [7] and the perhaps most recent model, UBAIM [8]. Ultimately, results of theoretical and empirical models should converge: that this is not (yet) the case is demonstrated by the comparison in Figure 5. Corresponding results of the empirical model FIRI [9] and of the theoretical model UBAIM are shown for the same geophysical conditions, i.e., mid-winter, 15° N, and low solar activity ($F_{10.7}$ = 67 Jy). The altitude range of 70 km to 120 km was chosen because FIRI was optimized for that region, but both models start at 60 km, and FIRI extends to 140 km, whereas UBAIM has the upper limit shown in the figure. There are several noteworthy differences. The night-time E-region densities are modeled much lower than the data suggests, and the night-time "valley" – well known from ionosonde observations – is not reproduced by UBAIM. On the other hand, the twilight bulge at 70 km in FIRI is primarily due to rocket-borne probe measurements, calibrated by wave propagation data at higher altitudes, and furthermore mostly originate from one institution (University of Illinois) and one rocket range (Wallops Island, VA). A systematic instrumental artifact of these measurements – crucial for the establishment of FIRI at twilight conditions – can therefore not be ruled out. Partial-reflection measurements have also shown similar bulges [10], but generally this technique has its limitations for electron-density measurements, and seems to have fallen out of favor with the ionospheric community because of difficulties in the interpretation [11].

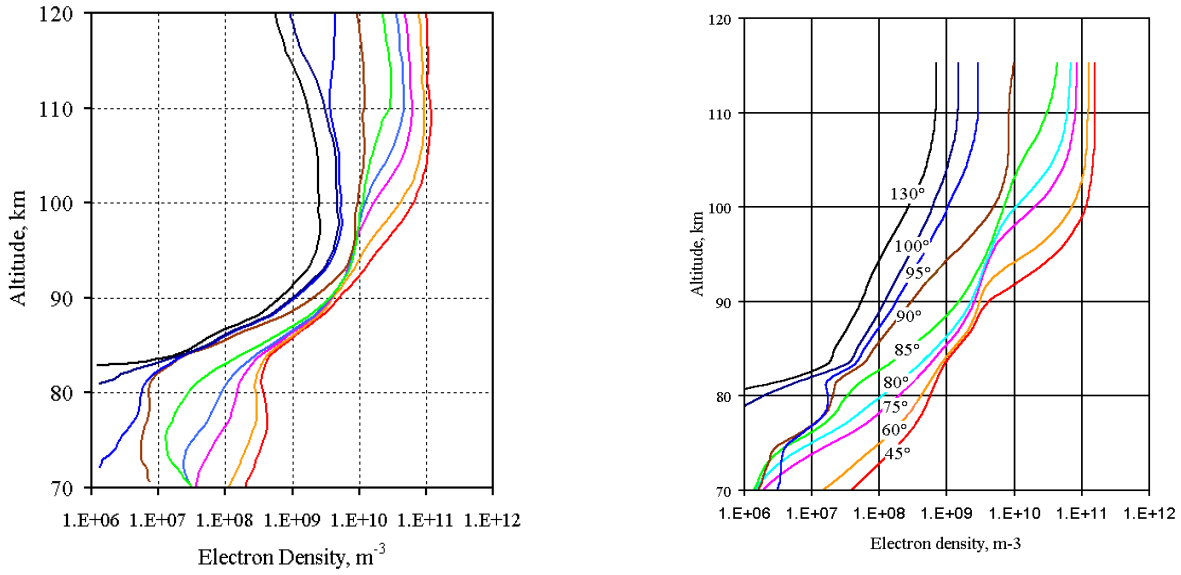

Figure 5. Electron densities for various solar zenith angles in mid-winter at 15°N and low solar activity. Left: empirical model FIRI [9]; right: theoretical model UBAIM [8] calculated for the same conditions (mean of a.m. and p.m.).

3. Supporting Data

Measurements of parameters of the mesosphere (a.k.a. the D region) are difficult to obtain remotely from satellites, or from the ground, but also by *in-situ* measurements with rockets. Sounding rockets dedicated to the study of the mesosphere will have an apogee of 100 km, and thus typical velocities of 1 km/s in the height region of the measurements. Data collection is further hampered by the large background density and the resulting aerodynamic distortion in the vicinity of the payload. Electron densities are best derived from *semi-in-situ* measurements, i.e., by transmitting HF waves from the ground to the flying payload. The most common of these methods makes use of the dual-refractive properties of the Earth's magneto-plasma by measuring the change of polarization (Faraday rotation). The method is completely immune to payload charge and aerodynamic effects, but yields only moderate height resolution (typically, 1 km). In combination with a plasma probe aboard the same payload, normalized to the wave-propagation data, one achieves the best possible accuracy and resolution [11-13]. Of such "good" profiles, only just over 300 have been established since the advent of sounding rockets. Ground-based methods to derive N_e generally have much higher density thresholds and poorer height resolutions, and are therefore better suited for studies of the E or the disturbed D regions (e.g., EISCAT).

Because of the importance of the atmospheric background for the formation of the D region, we need atmospheric data in order to verify theoretical models and to identify inadequacies in it. The nature of the ions of both polarities is vital for the understanding of N_e. From the late 1960s until the early 1990s, cryogenically cooled mass spectrometers were flown on sounding rockets, principally by only two groups: the Max-Plank-Institute for Nuclear Physics in Heidelberg, and the University of Bern. Unfortunately, no mass spectrometer has been flown since 1993, and all tests of theoretical model results with (partial) ion densities have to be made with data gathered at least a decade ago. Mass spectrometers for mesospheric research are very complex instruments, expensive and logistically difficult to launch. Also, their data require much experience in the interpretation. For instance, the size of the water-cluster ions has seemingly grown in the 1970s, not because of anthropogenic causes, but simply because these fragile ions better survived passage into the mass spectrometer in later instruments [14], and also because it was found that the telemetry signals at frequencies used in early sounding rockets (P band, 240 MHz) could break up large water-cluster ions [15]. Other pitfalls of mass-spectrometer results include spin modulation, even in centrally mounted instruments, and mass discrimination depending on the angle of attack.

As pointed out in Section 2, negative ions constitute a sink for free electrons. They are difficult to measure directly, because electrostatic probes cannot separate them from electrons. Hence, most accessible information about their abundance is based on forming the difference between the density of positive ions to electrons: because of charge neutrality, the difference must be due to negative ions. The available data are very scarce, and direct measurements by mass spectrometers are even rarer (see above). Hence, the validity of theoretical values of λ (the concentration of negative ions/concentration of electrons) is difficult to confirm. Attempts to empirically model the abundance of negative ions show large scatter and generally unsatisfactory results [16-17].

The neutral atmosphere background is very important for the understanding and modeling of the ionospheric D region. Many measurements are conducted at auroral latitudes at which – in particular – standard atmospheres seem to only poorly describe the real situation. Notably, the region around the mesopause was found to be significantly colder in summer than predicted by both MSIS and CIRA. Temperatures colder than in the standard models are required in order to allow for the formation of noctilucent clouds (NLC; [18]). However, very cold temperatures also explain the much greater height of the transition from cluster to molecular ions observed in the arctic summer. Figure 6 shows the pressure of an equal number density of cluster and molecular ions as functions of temperature (updated from [19]).

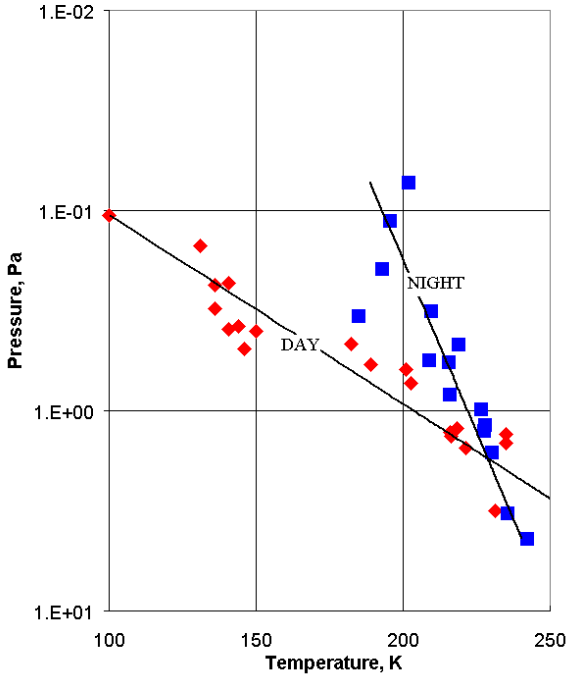

Figure 6. The pressure at the transition from cluster to molecular ions as a function of temperature. Note that for very low temperatures, the transition occurs at about the same height as under night conditions. Pressures of 10, 1, and 0.1 Pa are typically at altitudes of 65, 80, and 93 km, respectively ([19], updated).

4. The High-Latitude Situation

All parameters influencing the formation of the ionosphere at non-auroral latitudes also apply at high geomagnetic latitudes. However, in addition sporadic and essentially unpredictable fluxes of energetic charged particles, originating from the Sun, are guided by the Earth's magnetic field to the high-latitude atmosphere. In Figure 7, electron densities from the European Incoherent Scatter Radar (EISCAT), near Tromsø, Norway, and from sounding rockets are plotted as a function of solar zenith angle at a pressure typical for the E region [20]. Two features can be seen: (1) at night both the variability and the maximum densities are higher than during the day, and (2) during the day there is a distinct lower limit below which only a few (erroneous) values occur. Since this lower limit appears to follow a Chapman-type behavior (i.e., controlled by the solar zenith angle), one can form the envelope and thus establish True Quiet electron densities. These True Quiet (daytime) profiles are markedly larger than what, for example, FIRI predicts for the highest non-auroral latitude (60°). In an aeronomical interpretation, this suggests higher nitric-oxide concentrations. Nitric oxide in the thermosphere is a byproduct of the ionization of N_2, and since NO has a fairly long lifetime, its concentration will be enhanced even in otherwise quiet periods between particle events.

More often than not, the additional ionization by far dominates over all other processes that prevail at non-auroral latitudes. Hence, predicting the high-latitude ionosphere is futile, but empirical models can retrospectively describe the state of the ionosphere by data from ground-based instruments. The following parameters (beyond those that describe the non-auroral ionosphere) can be expected to characterize the high-latitude lower ionosphere:

- The index *Kp* is established from observations of the geomagnetic field by stations outside the auroral zone. Disturbances of the geomagnetic field are due to currents in the E region; hence, any magnetic index will characterize the E rather than the D region. *Kp* is a three-hourly index. Because disturbances of the high-latitude ionosphere are mostly on a much shorter time scale, *Kp* (but essentially also other magnetic indices) is only a poor descriptor of the disturbed state of the ionosphere. Using *Kp* alone to describe the degree of disturbance was most recently done by [21].

- A riometer measures the ionospheric attenuation of natural extraterrestrial radio sources in the 20 to 50 MHz range. Since radiowave absorption is proportional to N_e and collision frequency (itself proportional to pressure), this product maximizes in the D region: riometer absorption therefore reflects electron-density enhancements in the 80 to 90 km region. The earliest attempt to use riometer absorption to describe auroral electron-density profiles was by [22]. More rocket data were included and processed separately for day and night by [16], whereas [23] applied essentially that idea to EISCAT (UHF) data. Models based purely on rocket data suffer from the small number of cases; using EISCAT alone yields distorted results because of the threshold of that instrument.

- The charged particles that cause the additional ionization are guided by the Earth's magnetic field. Hence, the geometry between the solar wind and the Earth's magnetic field has an expected influence on the efficiency of capturing such particles and ultimately precipitating them into the upper atmosphere. One can therefore expect a dependence on local geomagnetic time (also known as "UT effect" [24-25]).

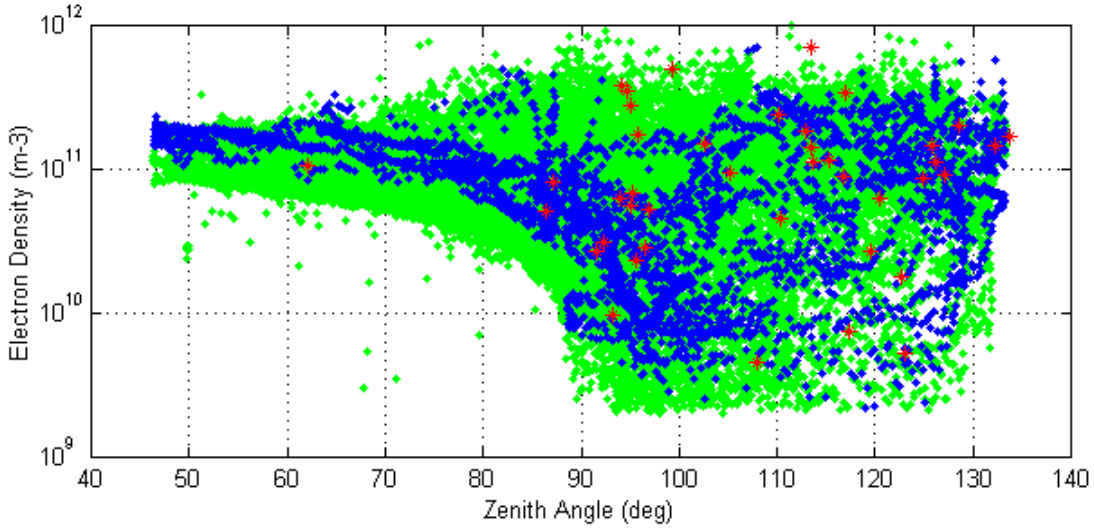

Figure 7. Auroral-zone electron densities at a pressure typical for the E region as a function of solar zenith angle. The blue dots are from high solar activity, and the red symbols are rocket data. Note the much larger variability at night and the distinct lower boundary during the day defining the True Quiet electron densities [20].

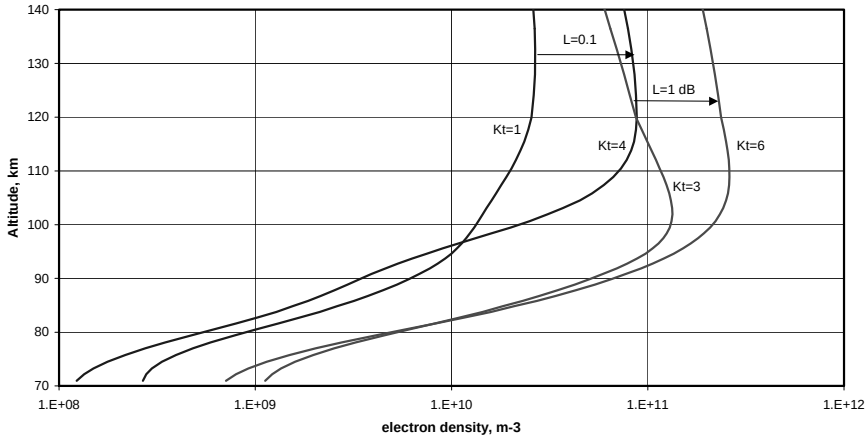

Figure 8. The dependence of auroral nighttime electron densities at different riometer absorption (0.1 dB and 1 dB) on the local K index; note that K is only significant in the E region. Results are from the neural-network-based model [26].

A very promising attempt to process both rocket and EISCAT data by applying neural networks is currently being pursued. Figure 8 shows modeled nighttime profiles for two different values of riometer absorption (0.1 dB and 1 dB), and each for low and high values of local *K* (from Tromsø). As anticipated, *K* correlates with E-region densities. The fact that the curves cross over (reverse dependence on *K* at lower altitudes) is necessary because the profiles – both for high *and* low *K* – have to lead to the same riometer absorption they are meant to represent [26-27].

5. Applications of Lower-Ionosphere Data/Models

As pointed out in the introduction, the communication community is no longer the driving force behind lower-ionosphere research, not even as a potential user. However, because of the strong dependence of electron densities on minor constituents, electron densities (or even radiowave absorption observations) can provide realistic boundaries for minor constituents, notably O and NO, but conceivably also clues concerning temperature.

Daytime electron densities in the D region reflect the corresponding densities of NO, since the ionizing flux (Lyman-α) varies only little and predictably with solar activity [28]. Hence, it is permissible to draw conclusions concerning [NO] from electron densities as exercised by [29], and more recently by [30]. In the latter paper, the applicability of [NO] derived from the instrument HALOE aboard the UARS satellite was tested with an empirical model of electron densities based on rocket soundings. HALOE data are derived from selective extinction of the solar spectrum by the Earth's limb: hence, data are available for sunrise and sunset. Because the lifetime of NO is of the order of days, one does not expect a diurnal variation. The HALOE results clearly showed larger densities for sunset and a maximum of the asymmetry at the equator and in summer. In an initial interpretation, this effect was dismissed as an unresolved problem of the retrieval procedure [31]. However, inserting sunrise and sunset [NO] in a theoretical model of the lower ionosphere resulted in electron densities very much resembling a.m./p.m. differences that had been known for decades in the ionospheric community from the measurements of radiowave absorption [32-33]. This ionospheric support of the novel satellite data eventually led theoreticians to come forth with tidal explanations of this behavior, which had not been anticipated by atmospheric scientists [34-35].

Global warming at sea level of about 0.5°C over the last 100 years is today an accepted fact, although there is still argument as to its anthropogenic origin. In the thermosphere, which contains the F region, the critical frequency, f_0F_2, and its altitude, hmF_2, have been determined for decades. An analysis of data from Sodankylä [36], and subsequently from southern high latitudes [37], showed a decrease in the height of the critical frequency, thus suggesting a cooling. Evidence for cooling was also found when observing a lowering of the reflection height near the mesopause of LF waves [38] (Figure 9). Hence, the transition from cooling to warming must be somewhere in the mesosphere, or below. [39] formed the ratio of non-auroral daytime electron densities to their respective values according to the model FIRI. Trends were produced for each kilometer as a function of time (from 1949 to 1994). With all due caution because of the paucity of data, the analysis yielded an increase of about 1% per year below 87 km, and a similar decrease above that height (Figure 10); whether these electron density trends were the results of corresponding trends in temperature is open to discussion. Trends were also found in the absorption of signals received from transmitters at frequencies from 164 kHz to 6090 kHz. However, the interpretation of the trends at the different frequencies is not yet conclusive [40]. An excellent review of temperature trends in the mesosphere was given in a recent article [41], together with assessments of the reliability of the various measurement methods.

Sprites are transient luminous events in the upper atmosphere, associated with, or triggered by, certain types of lightning flashes. They extend into the mesosphere (D region), and have only fairly recently been photographed because of their sporadic nature. However, similar to

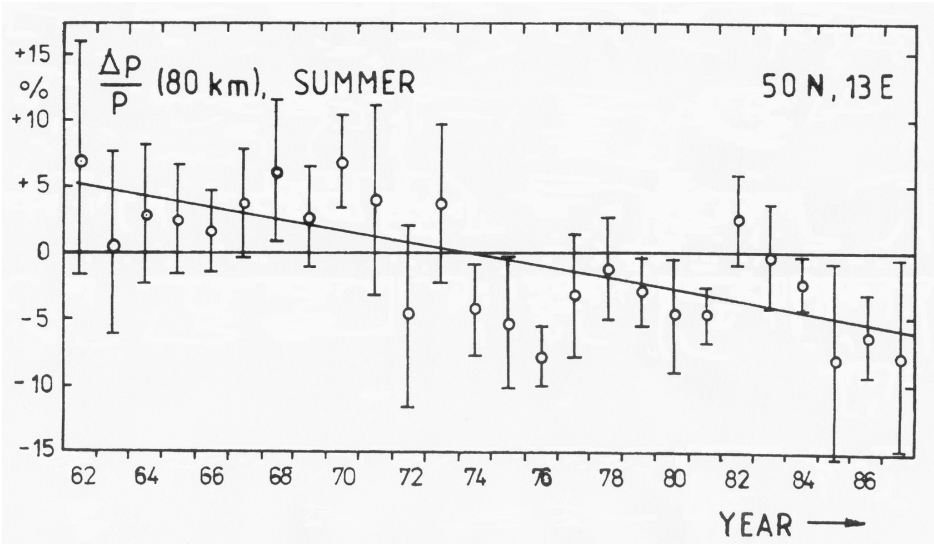

Figure 9. The relative decrease of the pressure at 80 km deduced from the reflection height of LF waves [38].

lightning in the troposphere, they produce electromagnetic signatures that can be monitored over long distances. Sprites are more common (or, at least, more often observed) in the continental United States, and a recording network in the US has already yielded interesting data on their occurrence and intensity [42]. More recently, signatures of sprites in the US were recorded in the Negev desert [43]. The localization accuracy over a 11000 km distance was a surprisingly low 180 km. These electromagnetic signatures are guided by the lowest ionosphere, and a sound knowledge of it can only help to further improve the localization accuracy.

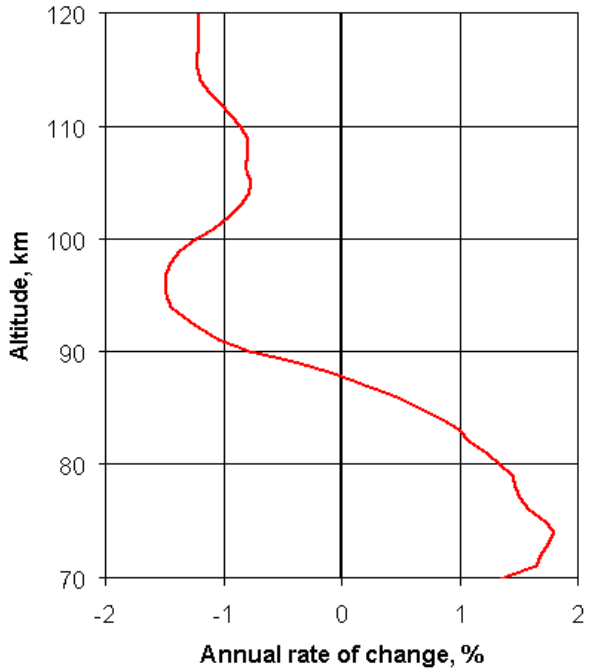

Figure 10. The annual rate of change in percent of electron densities as a function of altitude (after [39]).

As mentioned in Section 4, riometers measure the integral absorption of natural extraterrestrial radio sources. These instruments are located in the auroral zone or the polar caps because only there do electron-density enhancements occur large enough to be detectable at the relatively high frequencies. Because this additional ionization is due to fluxes of charged particles guided by the Earth's magnetic field, (chains of) riometers or imaging riometers provide an image of particles trapped in the magnetosphere. Drawing conclusions from riometer absorption related to the ionizing fluxes requires a realistic knowledge/ assumption of the effective recombination rate [44]. Very large riometer absorptions (>5 dB) are usually due to fluxes of protons (rather than electrons), and a simple correlation between the differential proton fluxes measured by a satellite and the resulting absorption is rather good [45].

A more exotic application of D-region knowledge is to simulate transmission loss of solar power satellites. It is anticipated that there will be large solar panels in orbit, and that the power thus generated will be transmitted via microwaves at about 2.5 GHz. The loss in the D region is insignificant for the link budget; however, the energy deposited in the mesosphere is quite comparable to other sources at these heights. This concept of generating power is being pursued by NASA [46], and also by the European Space Agency in a forthcoming symposium (Granada, June 2004).

6. Conclusions

Ironically, the behavior of the lower ionosphere is much better understood today than when it was of interest for communication. ELF/VLF propagation to triangulate sprites half-way around the world is today probably the only topical communications aspect of the D region. However, modern theoretical atmospheric models, such as

used for predicting climate change or the ozone hole, also yield plasma densities, albeit not as their prime outputs. Hence, the ability to predict electron densities strengthens their credibility for modeling parameters that are of more current interest. Although deducing minor constituents from ionospheric parameters may no longer be state-of-the-art these days, ionospheric data can help to identify the better of two models. Radiowave absorption beyond what one can consider to be "normal" sheds light on energy input at high latitudes, or on downward transport of nitric oxide at mid-latitudes (winter anomaly). Atomic oxygen, which participates in the odd oxygen chemistry (together with ozone), still behaves inexplicably in many respects in the mesosphere. The variability of the easily measurable nighttime ledge in N_e may help to eventually understand an anticipated similar variation of O. Parameters of the lower ionosphere appear to be useful as tracers of changes in the global climate.

7. References

1. K. M. Torkar, D. Beran, M. Friedrich, and S. Lal, "Measurement of Nitric Oxide and Related Parameters in the Equatorial Mesosphere and Lower Thermosphere," *Planet. Space Sci.*, **33**, 10, 1985, pp. 1169-1178.

2. M. Friedrich, J. Gumbel, and R. Pilgram, "Atomic Oxygen in the Mesosphere and its Relevance for the Ionosphere: A Summary of Empirical Evidence," *Proceedings of the 14th Symposium on European Rocket and Balloon Programmes and Related Research*, Potsdam, ESA **SP-437**, 1999, pp. 287-290.

3. F. Arnold and D. Krankowsky, "Ion Composition and Electron- and Ion-Loss Processes in the Earth's Atmosphere," in B. Grandal and J. A. Holtet (eds.), *Dynamical and Chemical Coupling Between the Neutral and Ionized Atmosphere*, Dordrecht, D. Reidel, 1977, pp. 93-127.

4. E. V. Thrane, B. Grandal, O. Hagen, F. Ugletveit, W. Bangert, M. Friedrich, A. Loidl, H. Schwentek, and K. M. Torkar, "Ion Production and Effective Loss Rate in the Mesosphere and Lower Thermosphere During the Western European Winter Anomaly Campaign 1975/76," *J. Atmos. Terr. Phys.*, **41**, 10-11, 1979, pp. 1097-1103.

5. A. P. Mitra and J. N. Rowe, "Ionospheric Effects of Solar Flares – IV. Changes in the D-Region Ion Chemistry," *J. Atmos. Terr. Phys.*, **34**, 5, 1972, pp. 795-806.

6. K. M. Torkar and M. Friedrich, "Tests of an Ion-Chemical Model of the *D*- and Lower *E*-Region," *J. Atmos. Terr. Phys.*, **45**, 6, 1983, pp. 369-385.

7. S. Solomon, G. C. Reid, R. G. Roble, and P. J. Crutzen, "Photochemical Coupling Between the Thermosphere and the Lower Atmosphere 2. D Region Chemistry and the Winter Anomaly," *J. Geophys. Res.*, **87**, D8, 1982, pp. 7221-7227.

8. J. Kazil, E. Kopp, S. Chabrillat, and J. Bishop, "The University of Bern Atmospheric Ion Model: Time-Dependent Ion Modeling in the Mesosphere and Lower Thermosphere," *J. Geophys. Res.*, **108**, D14, 2003, doi:10.1029/2002JDD003024.

9. M. Friedrich and K. M. Torkar, "FIRI: A Semiempirical Model of the Lower Ionosphere," *J. Geophys. Res.*, **106**, A10, 2001, pp. 21409-21418.

10. J. S. Belrose, M. J. Burke, T. N. R. Coyne, and J. E. Reed, "D-Region Measurements with Differential Absorption, Differential Phase, Partial Reflection Experiments," *J. Geophys. Res*., **77**, 25, 1972, pp. 4829-4838.

11. E. V. Thrane, "Ionospheric Profiles up to 160 km: A Review of Techniques and Profiles," in *Methods of Measurements and Results of Lower Ionosphere Structure* 1974, pp. 1-21, Berlin, Akademie Verlag, 1974, pp. 1-21.

12. T. A. Jacobsen. and M. Friedrich, "Electron Density Measurements in the Lower *D*-Region," *J. Atmos. Terr. Phys.*, **41**, 12, 1979, pp. 1195-1200.

13. L. G. Smith, "Electron Density Measurements in the Middle Atmosphere by Radio Propagation Techniques," in R. A. Goldberg (ed.), *Handbook for MAP*, **19**, 1986, pp. 173-187.

14. F. Arnold and D. Krankowsky, "Mid-Latitude Lower Ionosphere Structure and Composition Measurements During Winter," *J. Atmos. Terr. Phys*., **41**, 10-11, 1979, pp. 1127-1140.

15. F. Arnold and A. A. Viggiano, "Review of Rocket-Borne Ion Mass Spectrometry in the Middle Atmosphere," in R. A. Goldberg (ed.), *Handbook for MAP*, **19**, 1986, pp. 102-137.

16. M. Friedrich and K. M. Torkar, "High-Latitude Plasma Densities and Their Relation to Riometer Absorption," *J. Atmos. Terr. Phys*., **45**, 2-3, 1983, pp. 127-135.

17. M. Friedrich and K. M. Torkar, "An Attempt to Parameterise Negative Ions in the Ionospheric *D*-Region," *Proceedings of the 12th Symposium on European Rocket and Balloon Programmes and Related Research*, Lillehammer, ESA **SP-370**, 1995, pp. 257-261.

18. F.-J. Lübken, "Thermal Structure of the Arctic Summer Mesosphere," *J. Geophys. Res.*, **104**, D8, 1999, pp. 9135-9149.

19. M. Friedrich and K. M. Torkar, "Empirical Transition Heights of Cluster Ions," *Adv. Space Res.*, **8**, 4, 1988, pp. 235-238.

20. M. Friedrich, M. Harrich, R. J. Steiner, and F.-J. Lübken, "The Quiet Auroral Ionosphere and its Neutral Background," *Adv. Space Res*., **33**, 3, 2004, pp. 943-948.

21. A. D. Danilov, N. V. Smirnova, T. A. Blix, E. V. Thrane, and L. B. Vanina, "Some Features of Electron Density Behaviour in the High Latitude D-Region Derived from *in-situ* Measurements," *J. Atmos. Solar-Terr. Phys*., **65**, 4, 2003, pp. 417-427.

22. M. Jespersen, J. A. Kane, and B. Landmark, "Electron and Positive Ion Density Measurements During Conditions of Auroral Absorption," *J. Atmos. Terr. Phys*., **30**, 12, 1968, pp. 1955-1963.

23. S. Kirkwood and P. N. Collis, "The High Latitude Lower Ionosphere Observed by EISCAT," *Adv. Space Res.*, **11**, 10, 1991, pp. 109-112.

24. J. K. Hargreaves, A. V. Shirochkov, and A. D. Farmer, "Morning Sector Electron Precipitation Events Observed by Incoherent Scatter Radar," *J. Atmos. Terr. Phys*., **52**, 3, 1990, pp. 193-203.

25.J. K. Hargreaves and M. Friedrich, "The Estimation of *D*-Region Electron Densities from Riometer Data," *Ann. Geophysicae*, **21**, 2003, pp. 603-613.

26.L.-A. McKinnell and M. Friedrich, "Towards Neural Network Based Models for the Ionospheric *D*-Region," *Proceedings of the 16th Symposium on European Rocket and Balloon Programmes and Related Research*, St. Gallen, ESA **SP-530**, 2003, pp. 369-373.

27.L.-A. McKinnell, M. Friedrich, and R. J. Steiner, "A New Approach to Modeling the Daytime Ionospheric D-Region," *Adv. Space Res*., 2004, in press.

28.W. K. Tobiska, T. Woods, F. Eparvier, R. Viereck, L. Floyd, D. Bouwer, G. Rottman, and O. R. White, "The Solar2000 Empirical Solar Irradiance Model and Forecast Tool," *J. Atmos. Solar-Terr. Phys*., **62**, 14, 2000, pp. 1233-1250.

29.J. Taubenheim, "The Distribution of Nitric Oxide and its Variation Near the Mesopause Derived from Ionospheric Observations," *Space Res.*, **17**, 1977, pp. 271-278.

30.M. Friedrich, D. E. Siskind, and K. M. Torkar, "HALOE Nitric Oxide Measurements in View of Ionospheric Data," *J. Atmos. Solar-Terr. Phys.*, **60**, 15, 1998, pp. 1445-1457.

31.D. E. Siskind, J. T. Bacmeister, M. E. Summers, and J. M. Russell III, "Two-Dimensional Model Calculations of Nitric Oxide Transport in the Middle Atmosphere and Comparison with Halogen Occultation Experiment Data," *J. Geophys. Res.*, **102**, D3, 1997, pp. 3527-3545.

32.J. Laštovièka, "Seasonal Variation in the Asymmetry of Diurnal Variation of Absorption in the Lower Ionosphere," *J. Atmos. Terr. Phys.*, **39**, 8, 1977, pp. 891- 894.

33.J. Laštovièka, "Nitric Oxide Densities and Their Diurnal Asymmetry in the Upper Middle Atmosphere as Revealed by Ionospheric Measurements," *Atmos. Solar-Terr. Phys.*, **63**, 1, 2001, pp. 21- 28.

34.D. R. Marsh and J. M. Russell III, "A Tidal Explanation for the Sunrise/Sunset Anomaly in HALOE Low-Latitude Nitric Oxide Observations," *Geophys. Res. Lett.*, **27**, 19, 2000, pp. 3197-3200.

35.D. R. Marsh. and R. Roble, "TIME-GCM Simulations of Lower-Thermospheric Nitric Oxide Seen by the Halogen Occultation Experiment," *J. Atmos. Solar-Terr. Phys*., **64**, 8-11, 2002, pp. 889-895.

36.T. Ulich and E. Turunen, "Evidence for Long-Term Cooling of the Upper Atmosphere in Ionosonde Data," *Geophys. Res. Lett.*, **24**, 9, 1997, pp. 1103-1106.

37.M. J. Jarvis, B. Jenkins, and G. A. Rodgers, "Southern Hemisphere Observations of a Long-Term Decrease of the *F* Region Altitude and Thermospheric Wind Providing Evidence for a Global Cooling," *J. Geophys. Res*., **103**, A9, 1998, pp. 20774-20787.

38.J. Taubenheim, G. von Cossart, and G. Entzian, "Evidence of CO_2-Induced Progressive Cooling of the Middle Atmosphere Derived from Radio Observations," *Adv. Space Res*., **10**, 10, 1990, pp. 171-174.

39.M. Friedrich and K. M. Torkar, "Long-Term Trends and Other Residual Features of the Lower Ionosphere," *Proceedings of the 15th Symposium on European Rocket and Balloon Programmes and Related Research*, Biarritz, ESA **SP-471**, 2001, pp. 357-362.

40.G. Beig, P. Keckhut, R. P. Lowe, R. G. Roble, M. G. Mlynczak, J. Scheer, V. I. Formichev, D. Offermann, W. J. R. French, M. G. Shepherd, A. I. Semenov, E. E. Remsberg, C. Y. She, F. J. Lübken, J. Bremer, B. R. Clemesha, J. Stegman, F. Sigernes, and S. Fadnavis, "Review of Mesospheric Temperature Trends," *Rev. Geophysics*, **41**, 4, 2003, doi:10.1029/2002RG000121.

41. J. Laštovièka, "Long-Term Trends in the Lower Ionosphere," *Adv. Space Res.*, **28**, 7, 2001, pp. 1007- 1016.

42.U. S. Inan, A. Slingeland, and V. P. Pasko, "VLF and LF Signatures of Mesospheric/Lower Ionospheric Response to Lightening Discharge," *J. Geophys. Res*., **101**, A3, 1996, pp. 5219-5238.

43.C. Price, M. Asfur, W. Lyons, and T. Nelson, "An Improved ELF/VLF Method for Globally Geolocating Sprite-Producing Lightning," *Geophys. Res. Lett*., **29**, 3, 2002, 101029/2001GLO13519.

44.A. Osepian, S. Kirkwood, and N. Smirnova, "Variations of Electron Density and Energetic Spectra of the Precipitating Electrons During Auroral Substorms by Incoherent Scatter Data," *Cosmic Research*, **39**, 3, 2001, pp. 311-315.

45.L. Perrone, L. Alfonsi, V. Romano, and G. De Franceschi, "Polar Cap Absorption Events of November 2001 at Terra Nova Bay, Antarctica," *Ann. Geophysicae*, 2004, in press.

46."Laying the Foundation for Space Solar Power: An Assessment of NASA's Space Solar Power Investment Strategy, " The National Academies Press, 2001.

ISES Annual Report for 2003

The International Space Environment Service (ISES) encourages international monitoring and prediction of the space environment to help users reduce the impact of space weather on activities of human interest. ISES also prepares the International Geophysical Calendar each year. This calendar gives a list of 'World Days' during which scientists are encouraged to carry out their experiments. The monthly Spacewarn Bulletins, prepared on behalf of COSPAR, summarize the status of satellites in earth orbit and in interplanetary space.

The prime activities of ISES are carried out by Regional Warning Centres (RWCs) which provide space weather forecasts to the scientific and user communities primarily within their own regions. These services usually consist of forecasts or warnings of disturbances in the solar terrestrial environment. The range of the locations of RWCs results in a large diversity in the users of these forecasts. An important feature of the ISES system is that RWCs are able to construct and direct their services to the specific needs of their own customers. Users of the RWC services include: high frequency (HF) radio communicators; mineral surveyors using geophysical techniques; power line and pipeline authorities; operators of satellites and a host of commercial and scientific users. The increasing sophistication and sensitivity of modern technology has resulted in a steadily expanding range of applications where a knowledge of the solar terrestrial environment is important.

ISES assists the forecasting activities of the RWCs by facilitating the rapid exchange of space environment information. The data exchanged are highly varied in nature and in format, ranging from simple forecasts or coded information up to more complicated information such as images. A key strength of the data exchange system is that RWCs often have access to data from unique instrumentation available from the scientific community in its region. Exchange through ISES makes these data available to the wider international scientific and user community.

As well as coordinating data exchange, ISES is concerned with stimulating the exchange of knowledge about forecasting both between ISES and the wider scientific community and amongst the RWCs. In the past ISES organised a series of workshops on solar-terrestrial predictions: Boulder (1979); Meudon (1984); Sydney (1989); Ottawa (1992); and Japan (1996). At the time these were the only venues for discussing space weather forecasting and the proceedings from these meetings still represent a significant collection of papers in this area. In recent years with the new popularity of 'space weather' there have been many sessions on this topic and ISES has not wanted to create yet another one. However, we have found that many of these sessions do not deal with the practical forecasting and applications issues of concern to the ISES RWCs. ISES decided that the best way to proceed was to link to an existing series of space weather sessions; the most appropriate being the series organised by the COSPAR Panel on Space Weather. ISES has arranged with COSPAR to sponsor the special session on Space Weather Prediction: Applications and Validation at the COSPAR Scientific Assembly in Paris, July 2004.

A major new development in the communication of space weather information is the launch in October 2003 by the American Geophysical Union of the new journal: "Space Weather: The International Journal of Research and Applications". ISES is pleased to be a sponsor of this new publication devoted to space weather and its impact on technical systems, including telecommunications, electric power, and satellite navigation. Louis J. Lanzerotti is the first editor. The goal of the new journal is to be a research as well as news and information resource for space weather professionals. The journal is available on line at www.agu.org/journals/sw/. A digest of the online publication, Space Weather Quarterly (ISSN 1539-4964), is distributed four times a year free of charge through a grant from the U.S. National Science Foundation.

Within ISES, to foster greater communication of expertise between centres, we have supported visits by forecasters to other regional warning centres. RWC Australia hosted a visit by Dr Dabas from RWC India and RWC Russia hosted a visit by Dr Trichtchenko from RWC Canada. The ISES annual meetings also provide an opportunity for exchange of information between centres. ISES activities have also benefitted from the European Space Agency joining as a Collaborative Expert Center with the role to encourage and support development of space weather services; contribute expertise in space weather forecasting; and promote space weather services in centers not affiliated with ISES.

It is now over forty years since ISES was formed (originally with the name International Ursigram and World Days Service, IUWDS) by the amalgamation in 1962 of the former International World Days Service, initiated in 1959 as a part of the IGY, and the former URSI Central Committee of URSIgrams which initiated rapid international data interchange services in 1928. In 2003 we lost two people who had been very heavily involved in ISES activities for much of this time. Virginia Lincoln was the IUWDS Secretary for World Days for many years and one of the pioneers of the ISES organization. She was very active during the IGY years and helped set up the World Data Center system. Gary Heckman was IUWDS secretary for many years. As well as his noted work at NOAA's Space

Environment Center, Gary was very influential in the development of ISES up to recent times. They will both be missed.

Organisation

ISES Regional Warning Centres are located in China (Beijing), USA (Boulder), Russia (Moscow), India (New Delhi), Canada (Ottawa), Czech Republic (Prague), Japan (Tokyo), Australia (Sydney), Sweden (Lund), Belgium (Brussels), and Poland (Warsaw) with an associate warning center in France (Toulouse). The RWC in Boulder plays a special role as 'World Warning Agency (WWA)', acting as a central hub for data exchange and forecasts. Also the European Space Agency (Noordwijk) acts as an ISES collaborative expert center.

Each RWC collects data available in its own geographic area, concerning the state of the sun-earth environment, both from its own observatories and from regional scientific institutes and universities. These data and reports are distributed daily, on request to users and to other RWCs. Information transmitted through the ISES network is analyzed by Regional Warning Centers which produce a number of summary reports and forecasts. The Geoalert, a forecast of solar-geophysical conditions for the next few days, is a particularly important one of these reports. Geoalerts prepared by RWCs are sent to the WWA in Boulder each day. The WWA then issues a Geoalert which is distributed worldwide each day at 0300 UT through the ISES network.

The annual meeting of the ISES Directing Board was held in Boulder on May 18, 2003. Reports were received about the activities of each Regional Warning Center and about the International Geophysical Calendar and SpaceWarn Bulletin. On request from the International Standards Organisation (ISO), ISES agreed to review and seek opinions on a proposed standard for space environment indices. There were also discussions of how best to coordinate with new international programs such as International Living with a Star (ILWS) and Climate and Weather of the Sun Earth System (CAWSES). The next annual meeting will be held in Paris on July 18, 2004.

Publications

The International Geophysical Calendar (IGC) is prepared and distributed by the Secretary for World Days. The IGC can be accessed on the ISES Home Page and is also printed annually in many international journals. 1800 copies of IGC 2003 were printed and distributed in December, 2002.

The World Warning Agency for Satellites issues the Spacewarn Bulletin every month on behalf of COSPAR. The Spacewarn Bulletin provides a listing of launches and brief details of each launch. The WWA for Satellites is operated by the World Data Center-A for Rockets and Satellites, NASA/GSFC.

The ISES Website contains information about ISES and its Warning Centers, copies of the ISES code book, and links to the home pages of ISES centers. The URLs for ISES activities are given below.

- ISES Home Page: http://www.ises-spaceweather.org/
- International Geophysical Calendar: http://www.ises-spaceweather.org/geo_calender/
- Spacewarn Bulletins: http://nssdc.gsfc.nasa.gov/spacewarn

ISES Directing Board Membership

The present list of ISES officers and representatives is as follows:

- ISES Director: D. H. Boteler (dboteler@NRCan.gc.ca)
- ISES Deputy Director: H. Lundstedt (henrik@lund.irf.se)
- ISES Secretary for Space Weather: J. Kunches (Joseph.Kunches@noaa.gov)
- ISES Secretary for World Days: H. Coffey (Helen.E.Coffey@noaa.gov)
- RWC Australia (Sydney) delegate: R. Thompson (richard@ips.gov.au)
- RWC Belgium (Brussels) delegate: D. Berghmans (David.Berghmans@oma.be)
- ARWC France (Toulouse) delegate: A. Blusson (Annick.Blusson@cls.fr)
- RWC Canada (Ottawa) delegate: H.-L. Lam (HLam@NRCan.gc.ca)
- RWC China (Beijing) delegate: H. Wang (hnwang@bao.ac.cn)
- RWC Czech Rep. (Prague) delegate: D. Buresova (buresd@ufa.cas.cz)
- RWC India (New Delhi) delegate: R.S. Dabas (rsdabas@csnpl.ren.nic.in)
- RWC Japan (Tokyo) delegate: T. Nagatsuma (tnagatsu@crl.go.jp)
- RWC Poland (Warsaw) delegate: Z. Klos (marz@cbk.waw.pl)
- RWC Russia (Moscow) delegate: V.A. Burov (hciag@sunny.aha.ru)
- RWC Sweden (Lund) delegate: H. Lundstedt (henrik@lund.irf.se)
- WWA USA (Boulder) delegate: J. Kunches (Joseph.Kunches@noaa.gov)
- ESA (Noordwijk) delegate: A. Hilgers (Alain.Hilgers@esa.int)
- FAGS Representative: E.A. Tandberg-Hanssen (tandberger@cspar.uah.edu)
- IAU Representative: H. Coffey (Helen.E.Coffey@noaa.gov)
- IUGG Representative: H. Coffey (Helen.E.Coffey@noaa.gov)

- URSI Representatives:
  P. Wilkinson (phil@ips.gov.au)
  R. Pirjola (Risto.Pirjola@fmi.fi)
  S. Pulinets (pulse@igeofcu.unam.mx)

ISES Centres

RWC Australia
IPS Radio and Space Services
PO Box 1386
Haymarket NSW 1240
Australia
http://www.ips.gov.au/

RWC Canada
Natural Resources Canada
Geomagnetic Laboratory
7 Observatory Crescent
Ottawa Ontario K1AOY3
Canada
http://spaceweather.ca/

RWC Czech Republic
Institute of Atmospheric Physics
Academy of Sciences,
Bocni II, 141 31 Prague 4,
Czech Republic
http://rwcprague.ufa.cas.cz/

RWC Japan
Communications Research Laboratory,
4-2-1 Nukui-Kitamachi, Koganei,
Tokyo 184-8795
Japan
http://hirweb.crl.go.jp/index.html

RWC Russia
Institute of Applied Geophysics, Rostokinskaya str., 9,
129128 Moscow,
Russia
http://www.geospace.ru

World Warning Agency
NOAA Space Environment Center,
325 Broadway, Boulder, CO,
USA
http://www.sec.noaa.gov/index.html

RWC Belgium
Solar Influences Data Analysis Center (SIDC)
Royal Observatory of Belgium,
Ringlaan - 3 - Avenue Circulaire,
B-1180 Brussel,
Belgium
http://sidc.oma.be/

RWC China
National Astronomical Observatories,
Chinese Academy of Science,
20A Datun Road, Chaoyang District,
Bejing,
China
http://rwcc.bao.ac.cn/

RWC India
National Physical Laboratory,
New Delhi –110012,
India
http://npl-cgc.ernet.in

RWC Poland
Space Research Centre,
Polish Academy of Sciences,
Bartycka 18A, 00-716 Warsaw,
Poland
http://www.cbk.waw.pl/rwc/rwc.html

RWC Sweden
Swedish Institute of Space Physics,
Scheelev. 17,
SE-223 70 Lund,
Sweden
http://www.lund.irf.se/rwc

ARWC France
CLS, 8-10 rue Hermes,
31526 Ramonville Saint-Agne,
France
http://www.cls.fr/previsol

Collaborative Expert Centre
European Space Agency (ESTEC)
Keplerlaan 1, Postbus 299
2200 AG Noordwijk, The Netherlands
http://www.estec.esa.nl/wmwww/wma/spweather/

Radio-Frequency Radiation Safety and Health

James C. Lin

Current Standards and Their Bases for Safe Human Exposure to Radio-Frequency Radiation

The scenario of a persistent, publicly expressed lack of confidence in radio-frequency (RF) exposure standards pertaining to the maximum permissible exposure (MPE) level of humans exposed to RF electromagnetic radiation has been playing in many parts around the world of wireless telecommunications. Several national and international organizations are engaged in examining existing guidelines or maximum permissible exposures for humans. Each of these efforts has convened groups of interested parties to deliberate on the reasons and to decide on guidelines to deem exposure as safe, and, hopefully, to make explicit the philosophy and procedure invoked in the decision-making process.

Exposure guidelines for RF radiation have been promulgated for nearly half a century. However, our understanding of the biological effects of exposure to RF radiation is still evolving, and more so for cellular mobile telephones and wireless personal communication devices. It is expected – and mandated by some of the standards setting bodies – that any exposure criteria set forth should be evaluated periodically, and possibly revised as new information becomes available from continuing research on the subject. Likewise, rationales for the exposure criteria must be reassessed in view of new laboratory findings and human health studies.

There are two principal sets of guidelines promulgated for limiting human exposure to RF radiation worldwide. Much of the current effort is driven by the advent of cellular mobile telephony, which uses radio-frequency (RF) radiation in the range of 800 to 2500 MHz. In response, a standard was adopted by the US Federal Communications Commission (FCC) for protection against any effects of RF radiation in August, 1996 [1]. Likewise, guidelines for limiting human exposure to RF radiation from cellular mobile telephone operations have been adopted around the globe. For example, the maximum power deposition (measured in specific absorption rate of RF energy, or SAR) allowed varies between 1.6 W/kg in 1 g and 2 W/kg in any 10 g of tissue in the head, for exposure to cellular telephone wireless radiation. However, the popularity and ubiquity of cellular mobile telephones have posed new questions regarding the adequacy of the existing knowledge of biological effects of RF electromagnetic fields and of the protection afforded the public from any harmful effects of these fields.

In fact, the numbers used for the guidelines are not new, in that they were derived from then-existing (and currently promulgated) exposure guidelines for RF radiation. There is the sense that a cellular mobile telephone, putting a radiating RF source next to the user's head, is a new phenomenon that has no precedence. There has been palpable concern about the adequacy of existing scientific knowledge and uncertainties, even among the users. It is of interest to examine the scientific basis used for establishing these exposure guidelines. (For this discussion, we will not address the well-known differences among the RF guidelines promulgated for limiting human exposure in countries like Russia and the former Soviet Union. It should be noted that a draft of the amended exposure standard in China appears to have recommendations that differ from both ANSI/IEEE and CENELEC/ICNIRP guidelines.)

The use of the dosimetric quantity SAR was initiated as a recommendation of the National Council of Radiation Protection and Measurements (NCRP) [2]. This unit-mass, time-averaged rate of RF energy absorption was adopted by the American National Standards Institute (ANSI) in 1982 [3]. The limit of 1.6 W/kg in one gram of body tissue for the general public or the uncontrolled environment was recommended by the IEEE in 1992 [4]. (Note that since 1990, the development and revision of the ANSI standards

James C. Lin is with the University of Illinois at Chicago
851 South Morgan Street (M/C 154),
Chicago, Illinois 60607-7053 USA;
Tel: +1 (312) 413-1052 (direct); +1 (312) 996-3423 (main office); Fax: +1 (312) 996-6465;
E-mail: lin@uic.edu

have came under the sponsorship of the IEEE Standards Association.). The latter had followed considerations by NCRP that – for exposure criteria based on whole-body-averaged SAR – a number of studies have demonstrated that the maximum SAR in small regions inside the body may be as much as 10 to 20 times higher [5].

The ANSI/IEEE standard relied on the careful interpretation of a list of papers selected from the peer-reviewed literature that were deemed to have biological, engineering, and scientific validity. In the frequency region of interest (100 kHz to 6 GHz), a SAR value of 4 W/kg, temporally and spatially averaged over the whole body mass, was adopted as the working threshold for adverse biological effects in humans. Above this threshold, disruption of work schedules in trained rodents and primates, and other adverse biological effects, have been demonstrated. Moreover, it was noted that a metabolic heat-production rate of 4 W/kg falls well within the normal range of human thermoregulatory capacity. Recognizing that there are scientific uncertainties and also biological variability in the human population, a safety margin of 50 was incorporated into the standard, to limit exposure of the general population to 0.08 W/kg in one gram of tissue, as averaged over the entire body, for periods of 15 to 30 minutes. Clearly, the ANSI/IEEE C95.1-1992 Standard provides recommendations to prevent adverse thermal effects on the functioning of the human body, although the assessment criteria for reports of biological effects were without regard to mechanisms of interaction.

Since for a given exposure the SAR distribution inside the human body varies from point to point, a partial-body limit was recognized for all parts of the body. It was generally accepted then that the maximum localized SAR could be as high as 20 times the whole-body-averaged SAR. Therefore, for localized exposures of smaller regions in the human body, a relaxation of the maximum permissible exposure limit to 1.6 W/kg in any 1 gram of tissue was introduced for partial-body exposures.

Studies using animals in the near field have shown that the minimum cataractogenic SAR (the minimum SAR required to produce a lens cataract) is about 100 to 150 W/kg for up to 100 minutes in the vitreous body of the eye [6]. Moreover, available numerical and experimental investigations indicated that a retrolental temperature (the temperature behind the lens) of 41°C was necessary for production of posterior lens opacities in rabbits. The temperature rise was induced by a peak SAR in the eye that occurred right behind the lens for the exposure conditions investigated (2450 MHz in rabbits). If the retrolental temperature was kept from exceeding 41°C by means of whole-body hypothermia, potentially cataractogenic microwave exposure did not produce any opacity in the lenses of exposed animals. These findings supported the notion of a thermal mechanism for microwave cataractogenesis.

Indeed, the sensitivity of the visual organ to RF electromagnetic energy-induced heat formed the basis for CENELEC in its effort to promulgate the limit of 2 W/kg averaged over 10 g of tissue for partial-body exposures [7]. Clearly, the motivation was to limit temperature rises inside the eye to prevent formation of lens opacity: cataracts. Specifically, a safety factor of 10 was applied to reduce the SAR threshold of 100 W/kg to 10 W/kg. To provide for an additional margin of safety for the general public, an extra factor of five was introduced to arrive at 2 W/kg over 10 g of contiguous tissue, including the eye. This exposure limit is about 50 times below the SAR reported (inside the eye) for formation of lens cataracts. It became the accepted SAR safety limit in the head of a user for cellular mobile telephones in most European countries until 1999.

The European Union (EU) Health Council, with the support of the UK government agreed in 1999 on a recommendation for limiting exposure to RF electromagnetic fields, thereby establishing EU-wide safety standards for cellular mobile telephone emissions. The recommendation was based on the exposure limits recommended by the International Commission on Non-Ionizing Radiation Protection (ICNIRP), with its headquarters located near Munich, Germany.

In fact, the ICNIRP guidelines stipulate the same maximum SAR of 2 W/kg in any 10 g of tissue in the head and trunk up to 10 GHz over 6 minutes [8]. However, slightly different scientific bases appear to have been used in their development of the basic exposure restriction. While the restriction on SAR is intended to prevent excessive localized tissue heating, such as in the eyes and testes, considerations were given to SAR and tissue damage resulting from either partial-body or whole-body exposures that produce temperature rises on the order of 1°C in humans and laboratory animals. But the ICNIRP document did not clearly articulate the biological endpoint(s) upon which the rationale was drawn in supporting its choice of localized SAR values for the head and trunk. The guidelines were presented with the simple explanation of a desire to prevent excessive localized tissue heating. Thus, for all intents and purposes, the ICNIRP guidelines are essentially the same as the European (CENELEC) Pre-standard for partial body exposure.

It is worthy of note that – aside from the quantitative difference between the exposure standards (1.6 or 2 W/kg) – the tissue mass used to define the SARs in these standards (1 g for 1.6 W/kg or 10 g for 2 W/kg) can have a profound influence on the actual quantity of microwave energy allowed to be deposited in tissue by these exposure standards. It is well known that the distribution of absorbed microwave energy varies greatly from point to point inside a body, or inside the user's head from the RF radiation of a cellular telephone. An averaging volume that is as large as 10 g would tend to artificially smooth out the SAR distribution whether it is computed or measured. It also tends to lower

the numerical value of SAR by a factor of two or more. Thus, a 10 g SAR at 2 W/kg could be equivalent to 1 g SARs of 4 W/kg or higher. Simply put, the absorbed energy averaged over a defined tissue volume of 10 g is inherently low compared to a 1 g SAR.

The 1 g SAR is a more precise representation of localized microwave energy absorption, and a more biologically significant measure of SAR distribution inside the body or head. For example, the spherically-shaped human eye has a total mass of about 10 g. The use of an averaging volume as large as 10 g does not recognize any distinctions among tissues in the eye, and completely ignores the wide variation of SAR distribution throughout the eyeball. Also, it diminishes the safety margin of the 2 W/kg level in the eye. Likewise, the pinna or external ear has a mass that averages a little over 10 g. The adoption of 2 W/kg over 10 g of contiguous tissue grossly neglects the anatomic details of the ear and the nonuniform SAR distribution in the pinna. It could permit the deposition of RF energy in different parts of the pinna that exceeds the maximally permissible SAR by a large margin, while keeping the SAR for the entire pinna below 2 W/kg. Moreover, inside the human brain, the types and populations of cells and neurons are notably different, even in 1 g of tissue. There may be millions more cells, neurons, and aggregates impacted in a 10 g volume as compared to a 1 g averaging volume.

The quantitative values of SAR may be obtained by a detailed numerical computation, or from direct experimental measurements. The accuracy and reliability of computed results are sensitive to the models used to represent the user-handset combination, and to the parameters assumed for the head or user. Present computational schemes and resources can provide accurate induced electric field values with a spatial resolution on the order of a 1 mm in dimensions. The sensitivity and resolution of measurement instruments – such as implantable electric field probes or temperature sensors – are slightly larger, but of the same order of magnitude (a few mm).

It is important to recall that SAR is a localized quantity, and its value varies from one tiny location to another. The utility, resolution, and sensitivity of a given SAR value depend on the averaging volume or mass. The larger the averaging volume or mass, the lower the resolution and sensitivity of SAR, and the less useful it is as a metric for quantifying localized exposure and biological response.

The setting of guidelines or standards for maximum permissible levels of exposure to RF and microwave radiation is a valid approach to managing the risk of such exposures. The existing guidelines, however, are based on results obtained from acute, short-term studies that are atypical of the RF exposures associated with the handsets of cellular mobile telephones. For the first time in human history, a source of RF radiation is located right next to the head of millions of cellular mobile telephone users. Biological effects following repeated, prolonged, or lifelong exposure to RF energy emitted by these low-power wireless telecommunication devices have been investigated only during the past few years. The existing scientific results are equivocal and arguable in many respects. Consequently, there remains a widespread public concern about the adequacy of existing guidelines in safeguarding the general population against the possible harm of RF radiation from cellular mobile telephones.

References

1. FCC, *Guidelines for Evaluating the Environmental Effects of Radiofrequency Radiation*, FCC 96-326, Washington, DC, 1996.

2. NCRP, "Radiofrequency Electromagnetic Fields, Properties, Quantities and Units, Biophysical Interactions, and Measurements," NCRP Report No. 67, National Council on Radiation Protection and Measurements, Bethesda, MD, 1982.

3. ANSI, *American National Standard for Safety Levels with Respect to Human Exposure to Radio Frequency Electromagnetic Fields, 300 kHz to 300 GHz*, ANSI C95.1-1982, Institute of Electrical and Electronics Engineers, Inc., New York, 1982.

4. IEEE, *IEEE Standard for Safety Levels with Respect to Human Exposure to Radio Frequency Electromagnetic Fields, 3 kHz to 300 GHz*, IEEE C95.1-1991, Institute of Electrical and Electronics Engineers, Inc., New York, 1992.

5. NCRP, "Biological Effects and Exposure Criteria for Radiofrequency Electromagnetic Fields," NCRP Report No. 86, National Council on Radiation Protection and Measurements, Bethesda, MD, 1986.

6. J. C. Lin, "Radio-Frequency Radiation Safety and Health: Lens Opacification and Radio Frequency Electromagnetic Radiation," *URSI Radio Science Bulletin*, No. 306, 2003, pp. 45-48.

7. CENELEC, *Human Exposure to Electromagnetic Fields – High Frequency (10 kHz to 300 GHz)*, Pre-standard ENV 50166-2, European Committee for Electrotechnical Standardization (CENELEC), Brussels, 1995

8. ICNIRP, "Guidelines for Limiting Exposure to Time-Varying Electric, Magnetic, and Electromagnetic Fields (Up to 300 GHz)," *Health Physics*, **74**, 1998, pp. 494-522.

Conferences

CONFERENCE REPORT

WARS'04 CONFERENCE

Hobart, Tasmania, Australia, 18-20 February 2004

WARS04 (Workshop on the Applications of Radio Science 2004) Conference is the fifth in a series of conferences of national significance organised by the Australian National Committee for Radio Science (NCRS). It brings together Australian and International scientists and engineers conducting radio science research in areas relevant to the various URSI (International Union of Radio) Commissions.

The papers submitted to WARS04 provide an opportunity for Australian scientists and postgraduate students to present their work to their national peers and, in particular, to provide an important opportunity for cross-fertilisation of ideas between the wide range of sub-disciplines that make up radio science.

Two classes of papers were invited for WARS04:
- Research papers, refereed according to established rules,
- Information papers, where refereeing was not carried out.

The WARS conferences are normally attended by between 50 and 80 people and are residential in format. A small number of invited speakers (usually 5) set the tone of the meeting and all other papers are presented as posters. This format has been chosen to maximise wide discussion among all the attendees. In addition, the last two WARS Conferences have included a special session.

The invited talks for WARS04 covered a range of important radio science topics. Dr Andrew Parfit spoke on Fedsat, possibly one of the most sophisticated micro-satellites currently in orbit given the wide range of scientific and propagation experiments it carries. Dr David Cole spoke on space weather, commencing his talk provocatively with a picture of an atomic bomb explosion to emphasise both the harshness of the space environment and the role radiation hardening plays in electronics. Prof. Stuart Anderson spoke on sea-state scattering of radio waves, expertly surveying the processes and how they relate to target identification. Dr Ken Joyner surveyed the wide literature and current research on cancer hazards associated with mobile phones. Generally, the review demonstrated no effects have been identified and verified to date. All the invited talks stimulated productive discussions.

Prof. Ray Norris delivered a review of future radio astronomy developments and consequently how cosmology will drive technological change. This review opened a special session on these developments with several poster papers being presented on the SKA and related astronomical proposals. The poster session was followed by a successful discussion session attended by the majority of WARS attendees who enjoyed the flow of ideas.

As an experiment, at this WARS all poster presenters were invited to provide a short (90-second) talk on their papers at the beginning of the meeting. This session was well received and will be included in future WARS meetings. Prizes, some whimsical, were offered for the best deliveries. These papers covered a wide range of URSI Commission interests as can be seen in the WARS Proceedings, which is available at http://www.ips.gov.au/IPSHosted/NCRS/wars/wars2004/index.htm

A total of 68 people attended WARS04. Of these, there were a small number of overseas people from Singapore, Japan and the USA and the rest were from around Australia. The full residential registration fee was AU$500, which included all meals and accommodation. Student participation was subsidised by non-student registrations. A total of 13 students attended the meeting, which is typical of these meetings, although lower than the Committee would like. Of those who attended, 8 provided research papers and were therefore eligible for the student prize, which was won by Endawoke Yizengaw of La Trobe University.

WARS meetings are held roughly every two years and planning has already commenced for WARS06, which is likely to be held in February 2006.

17TH INTERNATIONAL WROCLAW SYMPOSIUM AND EXHIBITION ON ELECTROMAGNETIC COMPATIBILITY

Wroclaw, Poland, 29 June - 1 July 2004

The 17th International Wroclaw Symposium and Exhibition on Electromagnetic Compatibility will be held in the city of Wroclaw, Poland, from 29 June to 1 July 2004.

Since its beginning in 1972, the Wroclaw EMC Symposium, the oldest regular EMC symposium in Europe, has become one of the leading conferences in the EMC field. The Symposium is open to all bona-fide scientists and engineers throughout the world. In 2002 about 250 participants from 34 countries participated in the Symposium.

EMC is understood in a broad sense as an ability of a device, equipment, or system to function satisfactorily in its electromagnetic environment without introducing intolerable disturb-ances to anything in that environment. Spectrum management and natural EM phenomena are included.

Traditionally, plenary sessions, invited sessions, and spontaneous-paper sessions (regular and poster sessions) will constitute the core of the symposium. The panel discussions, workshops, tutorials, and exhibitions (the professional literature, and technical) will complement these.

All papers accepted for presentation will be published in English in the Proceedings paper volume and on a compact disc (CD), which will be available at the Symposium.

The EMC Symposium is organised by the The Wroclaw University of Technology, The National Institute of Telecommunications and the Office of Telecommunications and Post Regulation under the auspices of the Polish Academy of Sciences (PAN) and the Committee of Electronics and Telecommunication and is co-sponsored by the International Union of Radio Science (URSI).

The Conference Chaiman is Prof. D. J. Bem (Poland) and Vice-Chairs are Prof. A. Wierzbicki (Poland) Mr. W. Grabos (Poland).

Topics

As the technology progress and convergence pushes us towards "Information Society", the issue of electromagnetic interactions, spectrum congestion, and a rational use of spectrum resources is of increasing importance. Following the suggestions made at previous occasions, the program will address key problems related to EMC. Different kinds of papers are solicited, including research papers, lessons learned, status reports, discussion papers, etc. The ultimate goal is to build a broad and comprehensive symposium program that could match the interests and needs of different participants from industry and academia.

A non-exhaustive list of suggested topics (in alphabetic order) includes:

1. Antennas and Propagation, EMC Aspects
2. Biological Effects of EM Radiation, Technical Aspects
3. EM Environment Natural and Man-made
4. EM Hazards and EM Intended Interference Threat
5. EMC Analysis, Modelling, Prediction
6. EMC and Safety Considerations
7. EMC in Medical Electronics
8. EMC in Power Systems
9. EMC in Radio and Wire Communications
10. EMC in Telecommunication Systems
11. EMC in Transport Systems
12. EMC Measurement Techniques, Test Facilities & Instrumentation
13. EMI Reduction Techniques (Shielding, Filtering, Grounding, Signal Integrity)
14. ESD, Lightning, Transients
15. Immunity & Emissions
16. Regulatory Aspects: Directives, Standards and Specifications in EMC
17. Spectrum Congestion, Management and Monitoring

Contact

Mr. D. Wiecek
EMC Symposium
Box 2241
51-519 Wroclaw, POLAND
Tel: +4871 36 99 850
Fax: +4871 372 88 78
E-mail: d.wiecek@il.wroc.pl
Email Conference: emc@il.wroc.pl

Conference Website: www.emc.wroc.pl

VERTICAL COUPLING IN THE ATMOSPHERE/IONOSPHERE SYSTEM

Bath, United Kingdom, 12 - 15 July 2004

The Earth's atmosphere and ionosphere form a coupled system in which influences that originate at one height or region can have profound influences elsewhere in the system. Well-known examples include the wave driving of the mesosphere and lower thermosphere by gravity waves launched from the troposphere. This symposium will focus primarily on those forcing mechanisms that originate in the lower atmosphere and on their transmission into the atmosphere-ionosphere system above.

Papers are invited which address the theoretical, modelling and observational study of all aspects of these coupling processes, including studies of the different waves and tides, their generation, propagation and dissipation mechanisms. Suitable subjects include wave excitation and climatologies, heat and momentum fluxes, wave/wave and wave/mean-flow interactions, the contribution to turbulence, constituent transport and wave-driven electrodynamical processes, the role of waves in driving E- and F-region drifts, the influence of electrical processes in the lower and middle atmosphere on the electrodynamics of the ionosphere, the effects of wave transport on chemical constituents, the role of gravity waves in generating plasma instabilities and the mechanisms whereby planetary waves produce ionospheric signatures etc. The symposium will provide an excellent opportunity for the international research community to review progress to date and to suggest future directions in the investigation of all significant couplings (dynamic and electrodynamic, radiative, transport of atmospheric constituents), trigger mechanisms and feedback processes.

Review Solicited Papers

- **G. Brasseur** – Chemical structure and variability in the mesosphere and lower thermosphere: respective influences from atmospheric dynamics and solar effects
- **D.Farley** – Plasma instabilities in the ionospheric E region
- **C. Fesen** – Lower atmosphere/thermosphere/ionosphere coupling due to tides
- **D. Fritts** - Mean and Variable Forcing by Gravity Waves in the Middle Atmosphere
- **R. Garcia** – The influence of the vertically propagating waves on the dynamical and chemical structure of the mesosphere and lower thermosphere
- **J. Lastovicka** – Forcing of the ionosphere by waves from below
- **A. Richmond** – Global electrodynamic coupling of the atmosphere and ionosphere
- **M. Rycroft** – The role of electrical processes coupling the atmosphere and ionosphere
- **R. Vincent** – Wave coupling processes in the middle atmosphere and impacts on the mesosphere and lower thermosphere

Solicited Papers

- **M. Abdu** - Mesosphere- E- and F-region dynamical coupling over equatorial latitudes
- **A. Aylward** – Compositional effects due to tidal propagation in the middle and upper atmosphere: A study using CMAT
- **B. Fejer** – Lower atmospheric forcing effects in the equatorial ionosphere
- **R. Goldberg** – MaCWAVE: A program to study gravity wave forcing of the polar mesosphere during summer and winter
- **C. Haldoupis** – Tidal and planetary wave forcing of midlatitude sporadic E layers
- **Ch. Jacobi** – Quasi-two-day wave forcing and propagation in the middle atmosphere
- **R. Lieberman** – Variability of diurnal tides and their tropospheric forcing
- **E. Merzlyakov** – Some nonlinear effects in the propagation and interaction of the planetary waves in the upper atmosphere
- **N. J. Mitchell** – The planetary-wave field in the mesosphere and lower thermosphere at Arctic, middle and equatorial latitudes
- **S. Palo** – Propagation of the quasi-two-day wave into the thermosphere/ionosphere system using the NCAR TIME-GCM
- **J. Plane** – Using the meteoric metal layers to study vertical transport in the 80-120 km region
- **A. Pogoreltsev** – The role of tides and planetary wave-coupling in the middle atmosphere dynamics
- **D. Riggin** – Climatology of the 5-day wave
- **H. Rishbeth** – F-region links with the lower atmosphere?
- **M. Shepherd** - Global mesosphere lower thermosphere temperature - mean field and planetary-scale perturbations
- **A. Smith** – Short-term variability of tides and the diurnal cycles in airglow
- **J. Xiong** – Planetary waves in the mesosphere and ionosphere over Wuhan and Adelaide

Contact

Dora V. Pancheva
Department of Electr. & Electrical Engineering
University of Bath, Bath, BA2 7AY, UK
Tel: +44 (0)1225 386310, Fax: +44 (0)1225 386305
E-mail: eesdvp@bath.ac.uk
http://www.bath.ac.uk/elec-eng/IAGA2004.htm

African Regional Workshop on Radio use for Information and Communications Technology (ICT) in Rural Areas

Kenya College of Communications Technology, Nairobi, Kenya, 16 -20 August 2004

Topics

1) Digital and multimedia communications using terrestrial-based broadband radio systems
2) Trends in wireless satellite communications
3) Fixed radio access and wireless local loop
4) Intranet multimedia computer networks
5) Public switched telecommunication networks
6) Intelligent optical networks
7) The role of radio in modern information and communications technologies
8) Emerging broadband services in the LAN and WAN envirnonments
9) The impact and potential of wireless technology in education health-care, e-business, etc.
10) Computer networking using satellite radio links
11) Use of internet for economic, political and cultural integration
12) ICT as a prime mover for industrial and economic development of the rural areas
13) Spectrum utilization and management
14) Economic aspects of planning and implementation of wireless networks
15) Policy initiatives and programs for expansion and improvement of ICT in rural areas
16) The role of virtual learning centers in the changing academic environment

Contact

D.O. Oming'o
Organizing Secretary & head of the Secretariat
ICTA 2004 Workshop on Radio use for ICT
Kenya College of Communications Technology
P.O. Box 30305, 00100 GPO
NAIROBI, KENYA
Tel: +254 20 891 201
Fax: +254 20 891 949
E-mail: icta2004@kcct.ac.ke, omingod@kcct.ac.ke, ominogodo@yahoo.com

URSI CONFERENCE CALENDAR

An up-to-date version of this Conference Calendar, with links to the various conference web sites can be found at www.ursi.org : Calendar of supported meetings.
If you wish to announce your meeting in this calendar, you will find more information at www.ursi.org.

June 2004

URSI Commission F Open Symposium
Cairns, Great Barrier Reef, Australia, 1-4 June 2004
cf. announcement in RSB, March 2004, p. 63
Contact: URSI-F 2004 Conference Secretariat, c/-Unit 13, Milton Village 43 Lang Parade, Milton, Qld 4064, Australia, E-mail: registration@ursi-f2004.com (E-mail is the preferred correspondence option), Fax: +61 7 3721 6667, http://www.ursi-f2004.com

EMC'04 Sendai - 2004 International Symposium on Electromagnetic Compatibilty/Sendai
Sendai, Japan, 1-4 June 2004
Contact :Prof. R. Koga, Dept. of Communications Network Engineering, Okayama University, Japan, koga@cne.okayama-u.ac.jp, www.dev.cne.okayama-u.ac.jp

MSMW'04 - 5th International Kharkov Symposium on Physics and Engineering of Microwaves
Kharkov, Ukraine, 21-26 June 2004
cf. announcement in RSB, September 2003, p. 62-63
Contact : MSMW'04, IRE NASU 12, Ac. Proskura St., Kharkov 61085, Ukraine, Phone/Fax : +380 572-441105, E-mail: msmw04@ire.kharkov.ua, E-mail : www.ire.kharkov.ua/MSMW2004/

EMC Wroclaw '04 - 17th International Wroclaw Symposium and exhibition on Electromagnetic compatibility
Wroclaw, Poland, 29 June - 1 July 2004
cf. announcement in RSB, June 2004, p. 54
Contact: Mr. D. Wiecek, EMC Symposium, Box 2241, 51-519 Wroclaw, Poland, Tel: +4871 36 99 850, Fax: +4871 372 88 78, E-mail: d.wiecek@il.wroc.pl, http://www.emc.wroc.pl

July 2004

Vertical Coupling in the Atmosphere/Ionosphere System
Bath, UK, 12 - 15 July 2004
cf. announcement in RSB, June 2004, p. 55
Contact: Dr. Dora V. Pancheva, Department of Electronic & Electrical Engineering, Univesity of Bath, Bath, BA2 7AY UK, Tel: +44 (0)1225 386310, Fax: +44 (0)1225 386305, E-mail: eesdvp@bath.ac.uk, http://www.bath.ac.uk/elec-eng/IAGA2004

EUROEM 2004
Magdeburg, Germany, 12-16 July 2004
announcement in RSB, March 2004, p. 63
Contact: website http://www.euroem.org, E-mail: magdeburg@euroem.org

35th COSPAR Scientific Assembly an Associate Events
Paris, France, 18-25 July 2004
cf. announcement in RSB, September 2003, p. 63-64
Contact :COSPAR Secretariat, 51, bd. de Montmorency, F-75016 Paris, France, Tel: 0033-1-45250679, Fax: 0033-1-40509827, E-mail: COSPAR@COSPARHQ.org , http://www.copernicus.org/COSPAR/paris2004/useful

NATO Advanced Study Institute on Sprites, Elves and Intense Lightning Discharges
University of orsica,Corte in Corsica, 21 - 30 July 2004
Contact: Dr. Martin Füllekrug, Institutt für Geophysik, Feldbergstrasse 47, D-60323 Frankfurt am Main, Germany, Fax: +49 69 798 23959, E-mail: sprite@geophysik.uni-frankfurt.de, http://www.geophysik.uni-frankfurt.de/~fuellekr/SUMMER

August 2004

ISSSE'04 - 2004 Int. Symp. on Signals, Systems and Electronics
Linz, Austria, 10-13 August 2004
cf. announcement in RSB, December 2003, p. 65-66
Contact : Prof. Dr. Andreas Springer, Technical Program Committee Co-Chair, ISSSE'04, c/o ISSSE'04 Secretariat, Institute for Communications and Information Engineering, Johannes Kepler University of Linz, Altenbergerstrasse 69, A-4040 Linz, Austria, E-mail: issse04@icie.jku.at, http://www.icie.jku.at/issse04/

African Regional Workshop on Radio Use for Information and Communication Technology (ICT) in Rural Areas
Nairobi, Kenya, 16 - 20 August 2004
cf. announcement in RSB, June 2004, p. 56
Contact: Dr. D.O. Oming'o, Kenya College of Comm. Technology, P.O. Box 30305, 00100 GPO, Nairobi, Kenya, Tel: +254 20 891201, Fax: +254 20 891949, E-mail: omingod@kcct.ac.ke, icta2004@kcct.ac.ke

ISAP'04 - 2004 Int. Symp. on Antennas and Propagation
Sendai, Japan, 17-21 August 2004
Contact : ISAP'04, Attn. Dr. Tokio Taga, NTT DoCoMo, Inc., 3-5, Hikarino-oka, Yokosuka, 239-8536 Japan, E-mail : isap-2004@mail.ieice.org , http://www.ieice.org/cs/isap/2004

AP-RASC 2004 - 2nd Asia-Pacific Radio Science Conference
Qing, China, 24-27 August 2004
Contact : Prof. Zong Sha, China Research Institute of Radio Propagation, P.O Box 134-70, 100040 Beijing, China (CIE), Phone: +86 10 6821 2267, Fax: +86 10 6857, E-mail: z.sha@ieee.org, website http://www.cie-china.org/AP-RASC/

September 2004

Bianisotropics 2004
Ghent, Belgium, 22-24 September 2004
cf. announcement in RSB, December 2003, p. 66
Contact: Mrs. Isabelle Van Der Elstraeten, INTEC, Sint-Pietersnieuwstraat 41, B-9000 Gent, Belgium, Tel. +32 (0) 9 2643321, Fax: +32 (0)9 2643593, E-mail: isabelle.vanderelstraeten@intec.ugent.be, website: http://www.intec.ugent.be/bian04/

October 2004

Radar 2004
Toulouse, France, 19 - 21 October 2004
Contact: Société de l'Electricité, de l'Electronique et des Technologies de l'Information et de la Communication, 17, rue Hamelin, F-75783 Paris Cedex 16, France, Tel: +33 1 56 90 37 05, Fax: +33 1 56 90 37 08, E-mail: radar2004@see.asso.fr, website: http://www.radar2004.org

November 2004

JINA 2004 - 13èmes Journées Internationales de Nice sur les Antennes
Nice, France, 8-10 november 2004
cf. announcement in RSB, December 2003, p. 67
Contact: Secretariat JINA, France Telecom R&D, Fort de la Tête de Chien, F-06320 La Turbie, France, Fax: +33 4 92 10 65 19, E-mail: jina.2004@wanadoo.fr, website http://www.jina2004.com

February 2005

EMC Zurich '05 - International Zurich Symposium & Technical Exhibition on Electromagnetic Compatibility
Zurich, Switzerland, 14 - 18 February 2005
Contact: EMC Zurich 2005, Ms. M. Rafiq, ETH Zentrum,

Gloriastrasse 35, CH-8092 Zurich, Switzerland, Tel: +41 1 632 2951, Fax: +41 1 632 1198, E-mail: rafiq@emcz.ch, http://www.emc-zurich.ch

March 2005

TELECOM'2005 & JFMMA
Rabat, Morocco, 23-25 March 2005
Contact : Prof. Ahmed MAMOUNI, IEMN, Cité Scientifique, Av. Poincaré, BP. 69, 59652 Villeneuve d'Ascq, France, E-mail : Ahmed.Mamouni@iemn.univ-lille1.fr

May 2005

IES 2005 - 11th International Ionospheric Effects Symposium
Alexandria, Virginia, USA, 3 - 5 May 2005
Contact: Dr. J.M. Goodman,JMG Associates Ltd, 8310 Lilac Lane, Alexandria VA 22308, USA, Fax: +1 703 360 3954, E-mail: jm_good@cox.net, http://www.IES2005.com

August 2005

ISAP'05 - International Symposium on Antennas and Propagation
Seoul, Korea, 3 - 5 August 2005
Contact: Prof. H.J. Eom, Department of Electrical Engineering and Computer Science, Korea Advanced Institute of Science and Technology (KAIST), 373-1, Guseong-dong, Yuseong-gu Daejeon, 305-701 Korea, Tel: +82 42 869 3436, Fax: +82 42 869 8036, E-mail: hjeom@ee.kaist.ac.kr, http://www.isap05.org

ISMOT 2005 - 10th International Symposium on Microwave and Optical Technology
Fukuoka, Japan, 22-25 August 2005
Contact: Prof. Kiyotoshi Yasumoto, Department Computer Science & Communication Engineering , Kyushu University, 6-10-1, Hakozaki, Higashi-ku, Fukuoka 812-8581, Japan, Phone: +81 92 642 4045, Fax: +81 92 632 5204, E-mail: yasumoto@csce.kyushu-u.ac.jp, internet http://ismot2005.fit.ac.jp

October 2005

XXVIIIth URSI General Assembly
New Delhi, India, 23-29 October 2005
Contact: URSI Secretariat, c/o INTEC, Sint-Pietersnieuwstraat 41, B-9000 Gent, Belgium, Phone: +32 (0)9 264 3320, Fax: +32 (0)9 264 4288, E-mail: ursi@intec.rug.ac.be, internet http://www.ursi.org.

URSI cannot be held responsible for any errors contained in this list of meetings.

News from the URSI Community

BOOK PUBLISHED BY AN URSI RADIOSCIENTIST

Adaptive Antenna Arrays: Trends and Applications

Series: Signals and Communication Technology

2004, XII, 660 p. 274 illus., Hardcover, ISBN: 3-540-20199-8, Springer-Verlag, 119.95 €
by Sathish Chandran (Ed.)

The wireless industry has undergone unprecedented growth in recent time. Due to the technological developments in the field of wireless and radio technology, the world has become a place where one can communicate seamlessly without any inhibitions, at any instant of time. This brings the various communities, industries, businesses to the forefront to integrate and interact among them. As a result of this the availability of frequency bands become scarce and the service providers have to live with whatever frequency bands they have within their grasp. The limitations do not end here. In order to avoid any possible interference, the restrictions have to be imposed on the power transmitted by different service providers. Thus to make the maximum usage out of the given frequency bandwidth and to reduce the effects of any possible interferences, scientists and engineers have concentrated their works on adaptive and other antenna array techniques. Current and future markets are driving today's research. These efforts are being conducted by various regional agencies, industries, and universities.

This book *'Adaptive Antenna Arrays: Trends and Applications'* is a compilation of the works and thoughts of various scientists and engineers who are involved in this area from all over the globe. A liberal approach is adopted in here for the preparation of this book to accommodate the various beamforming techniques.

A total of 73 authors have single-handedly or jointly made their contributions of 36 chapters. These authors hail from all the five continents and from 21 countries in particular. This gives this book a global or universal outlook, in general.

In order to address, understand and rectify the various ongoing problems and activities in the area of antenna array techniques, this book is organised in the following way: The number of chapters in each sections are given in brackets.
Section 1: Overview (1)
Section 2: Adaptive Antenna Algorithms (7)
Section 3: Adaptive Antenna Applications (6)
Section 4: MIMO (2)
Section 5: Spatial Channel Modelling (7)
Section 6: Performance and Implementation issues (10)
Section 7: Experimental Results (3)

Researchers from industries, academic institutions and other research entities have contributed to various sections of this book. Various other beamforming techniques

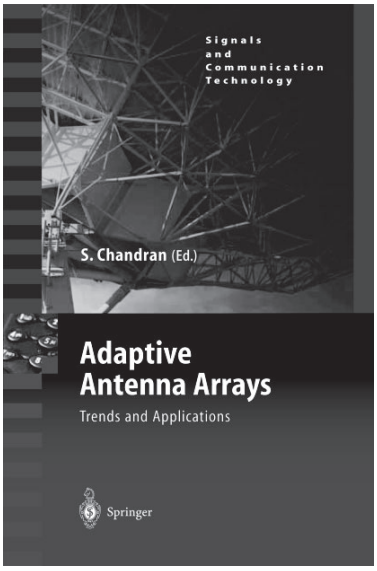

like optical beamforming, analog beamforming, various hardware and software approaches have been presented in here.

This book is useful for the engineers, researchers, final year undergraduate and postgraduate students. It is believed that this book would serve as a milestone reference for personals involved in this area of research.

Keywords associated with this book are: Adaptive Antenna, Antenna Arrays, Cellular base stations, Interference, Mobile communication, RF technology, Radiofrequency, Wireless.

Further details of this book can be found at: www.springeronline.com

URSI Website

French Translation

Since the beginning of June 2004, all topics of the URSI website have been translated into French. Our special thanks go to Professor Christian Hanuise for his expertise and dedicated help with the translations.

Records Maastricht GA

The Records of the XXVIIth General Assembly (Maastricht, The Netherlands, 2002) may be downloaded from the URSI website free of charge at http://www.ursi.org/records maastricht.pdf.
A hardcopy can also be purchased from the URSI Secretariat. The fee is 40 Euro.

http://www.ursi.org

URSI Publications

Modern Radio Science 1999

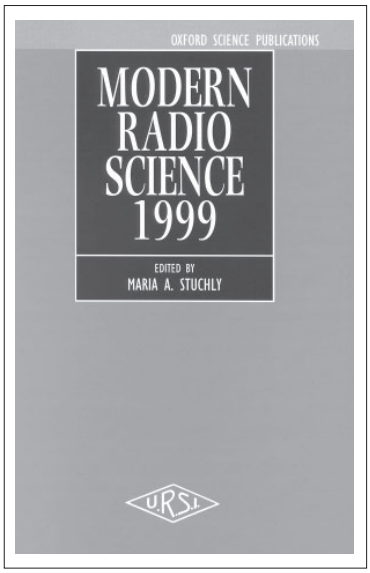

Editor: Maria Stuchly
ISBN 0-7803-6002-8
List Price : USD 49.95 Member Price : USD 45.00
IEEE Product No. PC5837

Published by Oxford University Press
in cooperation with URSI and IEEE Press
Order 24 hours a day, 7 days a week :
1-732-981 0060 (Worldwide)
1-800-678 4333 (USA & Canada)
Fax 1-732 981 9667
E-mail : customer-service@ieee.org

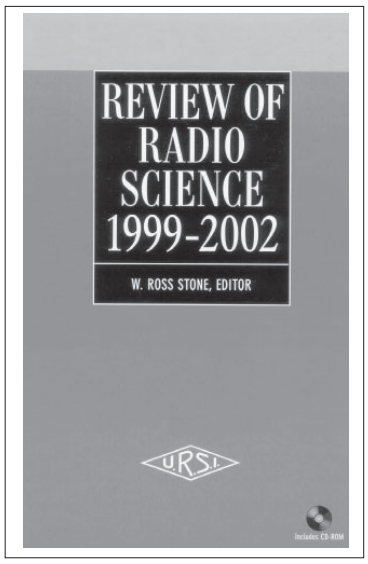

Review of Radio Science 1999-2002

Editor: W. Ross Stone
July 2002/Hardcover/977 pp
ISBN 0-471-26866-6
List Price : USD 125.00 Member Price : USD 106.25
IEEE Product No. #18493

Published by Wiley-Interscience
in cooperation with URSI and IEEE Press
Order can be sent to John Wiley & Sons, Inc.
from 8.30 a.m. to 5.30 p.m. :
1-732-469-4400 (Worldwide)
1-800-225-5945 (USA & Canada)
Fax 1-732 302-2370
E-mail : customer@wiley.com

Handbook on Radiopropagation Related to Satellite Communications in Tropical and Subtropical Countries

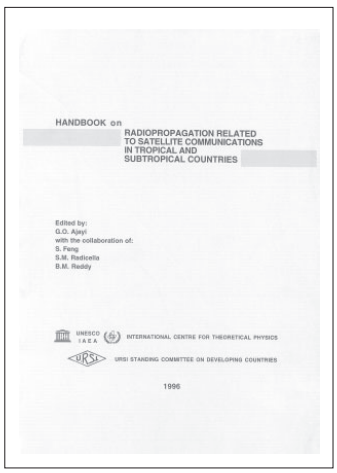

Editor: G.O. Ajayi
with the collaboration of :
S. Feng, S.M. Radicella, B.M. Reddy

Available from the URSI Secretariat
c/o Ghent University (INTEC)
Sint-Pietersnieuwstraat 41
B-9000 Gent, Belgium
tel. +32 9-264-33-20
fax +32 9-264-42-88
e-mail : ursi@intec.rug.ac.be

Wireless Networks

The journal of mobile communication, computation and information

Editor-in-Chief:
Imrich Chlamtac
Distinguished Chair in Telecommunications
Professor of Electrical Engineering
The University of Texas at Dallas
P.O. Box 830688, MS EC33
Richardson, TX 75083-0688
email: chlamtac@acm.org

Aims & Scope:
The wireless communication revolution is bringing fundamental changes to data networking, telecommunication, and is making integrated networks a reality. By freeing the user from the cord, personal communications networks, wireless LAN's, mobile radio networks and cellular systems, harbor the promise of fully distributed mobile computing and communications, any time, anywhere. Numerous wireless services are also maturing and are poised to change the way and scope of communication. WINET focuses on the networking and user aspects of this field. It provides a single common and global forum for archival value contributions documenting these fast growing areas of interest. The journal publishes refereed articles dealing with research, experience and management issues of wireless networks. Its aim is to allow the reader to benefit from experience, problems and solutions described. Regularly addressed issues include: Network architectures for Personal Communications Systems, wireless LAN's, radio , tactical and other wireless networks, design and analysis of protocols, network management and network performance, network services and service integration, nomadic computing, internetworking with cable and other wireless networks, standardization and regulatory issues, specific system descriptions, applications and user interface, and enabling technologies for wireless networks.

Wireless Networks is a joint publication of the ACM and Baltzer Science Publishers. Officially sponsored by URSI

For a complete overview on what has been and will be published in Telecommunication Systems please consult our homepage:

BALTZER SCIENCE PUBLISHERSHOMEPAGE
http://www.baltzer.nl/winet

Special Discount for URSI Radioscientists

Euro 62 / US$ 65
(including mailing and handling)

Wireless Networks ISSN 1022-0038
Contact: Mrs. Inge Heleu
Fax +32 9 264 42 88 E-mail ursi@intec.rug.ac.be
Non members/Institutions: contact Baltzer Science Publishers

BALTZER SCIENCE PUBLISHERS
P.O.Box 221, 1400 AE Bussum, The Netherlands
Tel: +31 35 6954250 Fax: +31 35 6954 258 E-mail: publish@baltzer.nl

The Journal of Atmospheric and Solar-Terrestrial Physics

SPECIAL OFFER TO URSI CORRESPONDENTS

AIMS AND SCOPE

The *Journal of Atmospheric and Terrestrial Physics* (JASTP) first appeared in print in 1951, at the very start of what is termed the "Space Age". The first papers grappled with such novel subjects as the Earth's ionosphere and photographic studies of the aurora. Since that early, seminal work, the Journal has continuously evolved and expanded its scope in concert with - and in support of - the exciting evolution of a dynamic, rapidly growing field of scientific endeavour: the Earth and Space Sciences. At its Golden Anniversary, the now re-named *Journal of Atmospheric and Solar-Terrestrial Physics* (JASTP) continues its development as the premier international journal dedicated to the physics of the Earth's atmospheric and space environment, especially the highly varied and highly variable physical phenomena that occur in this natural laboratory and the processes that couple them. The *Journal of Atmospheric and Solar-Terrestrial Physics* is an international journal concerned with the inter-disciplinary science of the Sun-Earth connection, defined very broadly. The journal referees and publishes original research papers, using rigorous standards of review, and focusing on the following: The results of experiments and their interpretations, and results of theoretical or modelling studies; Papers dealing with remote sensing carried out from the ground or space and with in situ studies made from rockets or from satellites orbiting the Earth; and, Plans for future research, often carried out within programs of international scope. The Journal also encourages papers involving: large scale collaborations, especially those with an international perspective; rapid communications; papers dealing with novel techniques or methodologies; commissioned review papers on topical subjects; and, special issues arising from chosen scientific symposia or workshops. The journal covers the physical processes operating in the troposphere, stratosphere, mesosphere, thermosphere, ionosphere, magnetosphere, the Sun, interplanetary medium, and heliosphere. Phenomena occurring in other "spheres", solar influences on climate, and supporting laboratory measurements are also considered. The journal deals especially with the coupling between the different regions. Solar flares, coronal mass ejections, and other energetic events on the Sun create interesting and important perturbations in the near-Earth space environment. The physics of this subject, now termed "space weather", is central to the Journal of Atmospheric and Solar-Terrestrial Physics and the journal welcomes papers that lead in the direction of a predictive understanding of the coupled system. Regarding the upper atmosphere, the subjects of aeronomy, geomagnetism and geoelectricity, auroral phenomena, radio wave propagation, and plasma instabilities, are examples within the broad field of solar-terrestrial physics which emphasise the energy exchange between the solar wind, the magnetospheric and ionosphericplasmas, and the neutral gas. In the lower atmosphere, topics covered range from mesoscale to global scale dynamics, to atmospheric electricity, lightning and its effects, and to anthropogenic changes. Helpful, novel schematic diagrams are encouraged. Short animations and ancillary data sets can also be accommodated. Prospective authors should review the *Instructions to Authors* at the back of each issue.

Complimentary Information about this journal:
http://www.elsevier.com/locate/JASTP?
http://earth.elsevier.com/geophysics

Audience:
Atmospheric physicists, geophysicists and astrophysicists.

Abstracted/indexed in:
CAM SCI Abstr
Curr Cont SCISEARCH Data
Curr Cont Sci Cit Ind
Curr Cont/Phys Chem & Sci
INSPEC Data
Meteoro & Geoastrophys Abstr
Res Alert

Editor-in-Chief:
T.L. Killeen, National Centre for Atmospheric Research, Boulder, Colorado, 80307 USA

Editorial Office:
P.O. Box 1930, 1000 BX Amsterdam, The Netherlands

Special Rate for URSI Radioscientists 2003:
Euro 149.00 (US$ 149.00)
Subscription Information
2002: Volume 65 (18 issues)
Subscription price: Euro 2659 (US$ 2975)
ISSN: 1364-6826

CONTENTS DIRECT:
The table of contents for this journal is now available pre-publication, via e-mail, as part of the free ContentsDirect service from Elsevier Science. Please send an e-mail message to cdhelp@elsevier.co.uk for further information about this service.

For ordering information please contact Elsevier Regional Sales Offices:

Asia & Australasia/ e-mail: asiainfo@elsevier.com
Europe, Middle East & Africa: e-mail: nlinfo-f@elsevier.com
Japan: Email: info@elsevier.co.jp
Latin America : e-mail: rsola.info@elsevier.com.br
United States & Canada : e-mail: usinfo-f@elsevier.com

Information for authors

Content

The *Radio Science Bulletin* is published four times per year by the Radio Science Press on behalf of URSI, the International Union of Radio Science. The content of the *Bulletin* falls into three categories: peer-reviewed scientific papers, correspondence items (short technical notes, letters to the editor, reports on meetings, and reviews), and general and administrative information issued by the URSI Secretariat. Scientific papers may be invited (such as papers in the *Reviews of Radio Science* series, from the Commissions of URSI) or contributed. Papers may include original contributions, but should preferably also be of a sufficiently tutorial or review nature to be of interest to a wide range of radio scientists. The *Radio Science Bulletin* is indexed and abstracted by INSPEC.

Scientific papers are subjected to peer review. The content should be original and should not duplicate information or material that has been previously published (if use is made of previously published material, this must be identified to the Editor at the time of submission). Submission of a manuscript constitutes an implicit statement by the author(s) that it has not been submitted, accepted for publication, published, or copyrighted elsewhere, unless stated differently by the author(s) at time of submission. Accepted material will not be returned unless requested by the author(s) at time of submission.

Submissions

Material submitted for publication in the scientific section of the *Bulletin* should be addressed to the Editor, whereas administrative material is handled directly with the Secretariat. Submission in electronic format according to the instructions below is preferred. There are typically no page charges for contributions following the guidelines. No free reprints are provided.

Style and Format

There are no set limits on the length of papers, but they typically range from three to 15 published pages including figures. The official languages of URSI are French and English: contributions in either language are acceptable. No specific style for the manuscript is required as the final layout of the material is done by the URSI Secretariat. Manuscripts should generally be prepared in one column for printing on one side of the paper, with as little use of automatic formatting features of word processors as possible. A complete style guide for the *Reviews of Radio Science* can be downloaded from http://www.ips.gov.au/IPSHosted/NCRS/reviews/. The style instructions in this can be followed for all other *Bulletin* contributions, as well. The name, affiliation, address, telephone and fax numbers, and e-mail address for all authors must be included with all submissions. All papers accepted for publication are subject to editing to provide uniformity of style and clarity of language. The publication schedule does not usually permit providing galleys to the author.

Figure captions should be on a separate page in proper style; see the above guide or any issue for examples. All lettering on figures must be of sufficient size to be at least 9 pt in size after reduction to column width. Each illustration should be identified on the back or at the bottom of the sheet with the figure number and name of author(s). If possible, the figures should also be provided in electronic format. TIF is preferred, although other formats are possible as well: please contact the Editor. Electronic versions of figures *must* be of sufficient resolution to permit good quality in print. As a rough guideline, when sized to column width, line art should have a minimum resolution of 300 dpi; color photographs should have a minimum resolution of 150 dpi with a color depth of 24 bits. 72 dpi images intended for the Web are generally *not* acceptable. Contact the Editor for further information.

Electronic Submission

A version of Microsoft *Word* is the preferred format for submissions. Submissions in versions of T_EX can be accepted in some circumstances: please contact the Editor before submitting. *A paper copy of all electronic submissions must be mailed to the Editor, including originals of all figures.* Please do *not* include figures in the same file as the text of a contribution. Electronic files can be send to the Editor in three ways: (1) By sending a floppy diskette or CD-R; (2) By attachment to an e-mail message to the Editor (the maximum size for attachments *after* MIME encoding is about 7 MB); (3) By e-mailing the Editor instructions for downloading the material from an ftp site.

Review Process

The review process usually requires about three months. Authors may be asked to modify the manuscript if it is not accepted in its original form. The elapsed time between receipt of a manuscript and publication is usually less than twelve months.

Copyright

Submission of a contribution to the *Radio Science Bulletin* will be interpreted as assignment and release of copyright and any and all other rights to the Radio Science Press, acting as agent and trustee for URSI. Submission for publication implicitly indicates the author(s) agreement with such assignment, and certification that publication will not violate any other copyrights or other rights associated with the submitted material.

APPLICATION FOR AN URSI RADIOSCIENTIST

I have not attended the last URSI General Assembly, and I wish to remain/become an URSI Radioscientist in the 2003-2005 triennium. Subscription to *The Radio Science Bulletin* is included in the fee.
(please type or print in BLOCK LETTERS)

Name: Prof./Dr./Mr./Mrs./Ms. _____
Family Name *First Name* *Middle Initials*

Present job title: _____

Years of professional experience: _____

Professional affiliation: _____

I request that all information, including the bulletin, be sent to my ☐ home ☐ business address, i.e.:

Company name: _____

Department: _____

Street address: _____

City and postal / zip code: _____

Province / State: _____ Country: _____

Phone: _____ ext: _____ Fax: _____

E-mail: _____

Areas of interest (please tick)

☐ A Electromagnetic Metrology
☐ B Fields and Waves
☐ C Signals and Systems
☐ D Electronics and Photonics
☐ E Electromagnetic Noise & Interference
☐ F Wave Propagation & Remote Sensing
☐ G Ionospheric Radio and Propagation
☐ H Waves in Plasmas
☐ J Radio Astronomy
☐ K Electromagnetics in Biology & Medicine

The fee is 40 Euro.
(The URSI Board of Officers will consider waiving of the fee if the case is made to them in writing)

Method of payment: VISA / MASTERCARD (we do not accept cheques)

Credit Card No ☐☐☐☐ ☐☐☐☐ ☐☐☐☐ ☐☐☐☐ Exp. date: _____

Date: _____ Signed _____

Please return this signed form to: